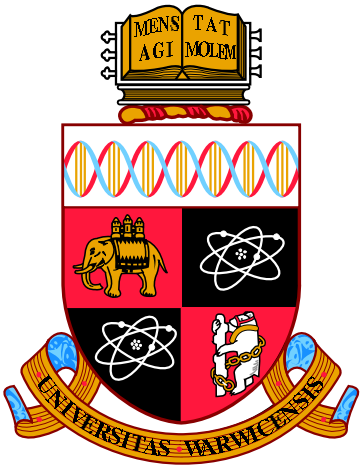

Device-to-Device Communication in Cellular Networks: Multi-Hop Path Selection and Performance

by

Hu Yuan

Thesis

Submitted to the University of Warwick in partial

fulfilment of the requirements for the degree of

Doctor of Philosophy

School of Engineering

July 2016

THE UNIVERSITY OF WARWICK

For my beloved family.

Contents

List of Tables

List of Figures

Acknowledgments

I would like to express my sincere gratitude towards my supervisors, Dr. Weisi Guo and Dr. Akeel Shah. It is my greatest fortune and pleasure to have their guidance during my Ph.D. journey.

I would also like to thank Dr. Daciana Iliescu and Dr. Zuoyin Tang for agreeing to be my Ph.D. examiners and their valuable suggestions and comments on my thesis.

I am grateful to my family who have shown their full support throughout my education life. There is no words that could express my love to them. My wife Weixian Xu, my son Tianze Yuan, my parents Ronghua Yuan, Juhua Dai, my parents-in-law Shusong Xu, Shiqin Wang, and my sister Wei Yuan and her husband Yu Rong.

My study would not have been complete without the help and the friendship of my friends, specially Xiayang Wang, he always hold a place in my happy memories of my study in the UK.

Declarations

I herewith declare that this thesis contains my own research performed under the supervision of Dr. Weisi Guo and Dr. Akeel Shah, without assistance of third parties, unless stated otherwise. No part of this thesis was submitted for a degree at any other universities.

Hu Yuan

July 2016

List of Publications

Journal

1. Y. Wu, W. Guo, H. Yuan, S. Wang, X. Chu, J. Zhang,"Device-to-device Meets LTE-Unlicensed", in *IEEE Communications Magazine*, vol. 54, no. 5, May 2016, pp. 154-159.

2. H. Yuan, W. Guo, Y. Jin, S. Wang, M. Ni, "Interference-Aware Multi-Hop Path Selection for Device-to-Device Communications in a Cellular Interference Environment" Submitted to *IET Communications*, 2017. (Accepted)

Conference (Peer Reviewed)

1. H. Yuan, W. Guo, and S. Wang, "Emergency route selection for D2D cellular communications during an urban terrorist attack", in *IEEE International Conference on Communications Workshops* (ICC), Sydney, Jun. 2014, pp. 237-242.

2. H. Yuan, W. Guo, and S. Wang, "D2D Multi-Hop Routing: Collision Probability and Routing Strategy with Limited Location Information", in *IEEE International Conference on Communications Workshops* (ICC), London, Jun. 2015, pp. 681-685.

3. H. Yuan, W. Guo, S. Wang, "Device-to-device Communications in LTE-Unlicensed Heterogeneous Network", in *IEEE International workshop on Signal Processing advances in Wireless Communications (SPAWC)*, Edinburgh, July, 2016, pp. 1-5.

Abbreviations

2G	the second generation wireless systems
3G	third generation wireless systems
4G	the fourth generation wireless systems
5G	the fifth generation wireless systems
3GPP	Third Generation Partnership Project
ACK	Acknowledgement
AP	access points
BR	broadcasting algorithm
BS	base station
CA	Collision Area
CC	conventional cellular communication
CCA	Clear Channel Assessment
CDF	cumulative distribution function
CID	connection identifier
COT	Channel Occupancy Time
C-RAN	cloud based radio access network
CSI	channel state information
CSMA	Carrier Sense Multiple Access
CTS	clean to send
D2D	Device to-device communications
DF	decode-and-forward
DPS	direct power signal

DL	downlink
EPC	evolved packet core
E-UTRAN	evolved universal terrestrial access network
fBS	femtocell base station
FFD	frequency division duplex
FLQ	FlashLinQ
FSPL	Free-space path loss
GPS	Global Positioning System
GPSR	Greedy Perimeter Stateless Routing
IAR	interference aware routing
ICS	Idle Channel Sense
ILA	interference limited area
IPE	inverse power echo
ISM	The industrial, scientific, and medical radio band
LBT	Listen Before Talk
LOS	Line-of-Sight
LTE	Long Term Evolution
LTE-A	Long Term Evolution Advanced
LTE-U	Long Term Evolution Unlicensed
MIMO	Multi-input-multi-output
MMPP	Markov modulated Poisson process
NLOS	Non-Line-of-Sight
NSPS	national security and public safety
OFDMA	Orthogonal Frequency Division Multiplexing
PCP	Poisson Cluster Process
pdf	probability density function
PL	Path loss
PLMN	public and mobile network
PP	point process

PPP	Poisson point process
PPDR	public protection and disaster relief
ProSe	Proximity-based Services
RB	resource block
RBR	restricted broadcasting algorithm
RRM	radio resource management
RTS	ready to send
SBR	Shooting and Bouncing Ray
SCAT	carrier-sensing adaptive transmission
SIC	successive interference cancellation
SINR	signal-to-interference-plus-noise-ratio
SPR	shorted path routing
TDD	Time Division Duplex
UE	user equipment
UL	uplink
UMTS	Universal Mobile Telecommunications System

List of Symbols

A	area of a 2-D space
$\mathcal{B}$	a set of Euclidean space
B	channel bandwidth
C	network capacity
$\overline{C}$	average capacity
c	the speed of light in a vacuum
f	signal frequency (in hertz)
H	fading gain
I	interference
j	Relay D2D UEs
$K_{\mathrm{SPR,IAR}}$	number of hops
m	source D2D UE
m'	destination D2D UE
N	number of points in a space
o	nearest BS
P_{BS}	BS transmission power
P_{D2D}	D2D transmission power
$\mathbb{P}_{\mathrm{CA}}$	collision probability
r_{CA}	collision area size
$Q()$	Q function
$Q(\zeta,\alpha)$	$\sqrt{\frac{\zeta}{B}-1}\arctan\left(\sqrt{\frac{\zeta}{B}-1}\right)$ for $\alpha=4$
$\mathbb{R}^d$	a d-dimensional Euclidean space
R	max. D2D trans. distance
$r_{j,j'}$	average hop distance
$r_{j,j'}^{\mathrm{SPR}}$	average hop distance for SPR

$r_{j,j'}^{\mathrm{IAR}(i)}$	average hop distance for IAR
R_{BS}	BS coverage range
Λ	density of point process
Λ_{D2D}	available D2D density
Λ'_{D2D}	co-frequency D2D density
λ	pathloss constant
$\Gamma(\cdot)$	the Gamma function
$\mathbf{1}_b\left(0, r_{\mathrm{P}}\right)\left(x_i\right)$	the indicator function of the condition $x_i \in (0, r_{\mathrm{P}})$.
μ	mean service ratio
τ	mean arrive ratio
γ	link SINR
σ^2	AWGN power
ζ	SINR threshold
Ψ	Macro-BSs coverage size

Abstract

Over the past decade, the proliferation of internet equipment and an increasing number of people moving into cities have significantly influenced mobile data demand density and intensity. To accommodate the increasing demands, the fifth generation (5G) wireless systems standards emerged in 2014. Device-to-device communications (D2D) is one of the three primary technologies to address the key performance indicators of the 5G network. D2D communications enable devices to communicate data information directly with each other without access to a fixed wireless infrastructure. The potential advantages of D2D communications include throughput enhancement, device energy saving and coverage expansion. The economic attraction to mobile operators is that significant capacity and coverage gains can be achieved without having to invest in network-side hardware upgrades or new cell deployments.

However, there are technical challenges related to D2D and conventional cellular communication (CC) in co-existence, especially their mutual interference due to spectrum sharing. A novel interference-aware-routing for multi-hop D2D is introduced for reducing the mutual interference.

The first verification scenario of interference-aware-routing is that in a real urban environment. D2D is used for relaying data across the urban terrain, in the presence of CC communications. Different wireless routing algorithms are considered, namely: shortest-path-routing, interference-aware-routing, and

broadcast-routing. In general, the interference-aware-routing achieves a better performance of reliability and there is a fundamental trade-off between D2D and CC outage performances, due to their mutual interference relationship. Then an analytical stochastic geometry framework is developed to compare the performance of shortest-path-routing and interference-aware-routing. Based on the results, the spatial operational envelopes for different D2D routing algorithms and CC transmissions based on the user equipment (UEs) physical locations are defined. There is a forbidden area of D2D because of the interference from the base stations(BSs), so the collision probability of the D2D multi-hop path hitting the defined D2D forbidden area is analysed. Depend on the result of the collision probability, a dynamic switching strategy between D2D and CC communications in order to minimise mutual interference is proposed. A blind gradient-based transmission switching strategy is developed to avoid collision within the collision area and only requires knowledge of the distances to the serving base station of the current user and the final destination user. In the final part of my research, the concept of LTE-U (Long term evolution for Unlicensed Spectrum), which suggests that LTE can operate in the unlicensed spectrum with significant modifications to its transmission protocols, is investigated. How the envisaged D2D networks can efficiently scale their capacity by utilising the unlicensed spectrum with appropriately designed LTE-Unlicensed protocols is examined.

Chapter 1

Introduction

1.1 Background

Over the past decade, two factors have significantly influenced mobile data demand density, the first of which is the proliferation of internet equipment (smart-phones, Phablets, machine-to-machine, laptops and tablets), which has led to an explosive demand for mobile multimedia services. According to the 2016 Cisco® Visual Networking Index (VNI) report, in 2015 the number of high-end devices grew from 563 million to 7.9 billion, and there will be 11.6 billion such devices by 2020. The rapidly increasing number of devices means that mobile data traffic demand is expected to grow to 30.6 exabytes per month by 2020, more than eight times that in 2015, as shown in Figure 1.1, where CAGR is Compound Annual Growth Rate.

The second factor is that an increasing number of people now live in cities [2]; for the first time in history, more than half of the human population live in cities. Whilst over 80% of the population are urban in the developed world, most of the growth will be experienced in the developing world. There-

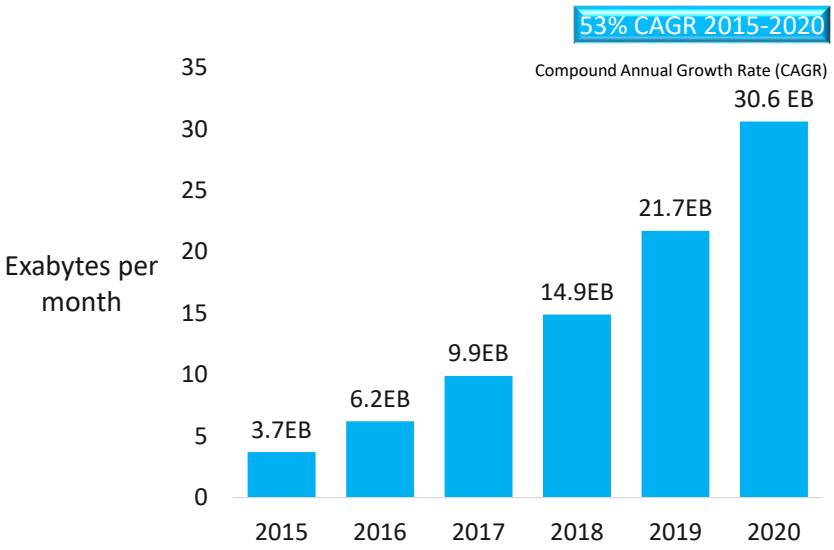

Figure 1.1: Cisco Forecasts per Month of Mobile Data Traffic by 2020 [1].

fore, not only is the mobile data demand per person (Mbits/s/user) growing, but the demand per unit area (Mbits/s/km^2) has been growing at an even greater rate in cities. Combining rapid mobile data growth and fast urbanisation trends, one can draw the conclusion that there will be an extremely high density of mobile communication devices in cities, mainly demanding multimedia services [1].

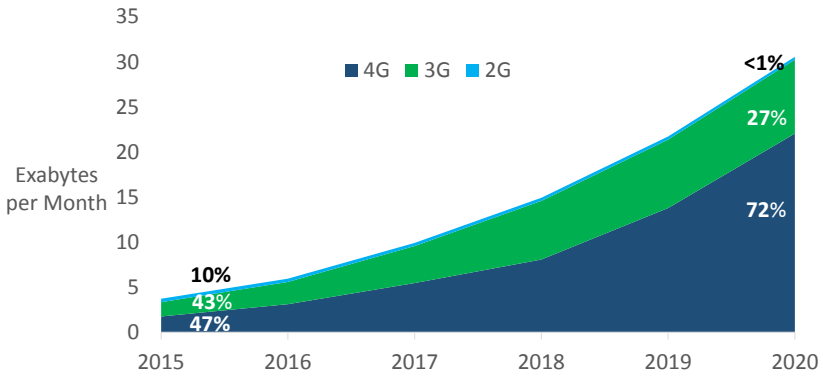

Figure 1.2: Global Mobile Traffic by Connection Type by 2020 [1].

Currently, 47% of the mobile traffic is transferred through 4G connections and the volume of traffic will grow faster than in other networks (2G, 3G) to 72% of all mobile data traffic by 2020, as shown in Figure 1.2. To accommodate increasing digital data demands, Third Generation Partnership Project (3GPP) proposed an enhanced Long Term Evolution (LTE) radio interface called LTE-Advanced (LTE-A). Its radio interface is designed with carrier aggregation [3–5], Massive Multi-input-multi-output (MIMO) [6, 7], millimeter waves and low-power nodes to provide a higher network capacity.

The fifth generation wireless systems (5G) emerged in 2014, and they aim to offer super-efficient mobile network, super-fast mobile network and converged fiber-wireless network [8]. The expectations of the 5G network would be 1,000 times higher network capacity than the 4G network and a cell data rate of 10 Gbit/s. The end to end latency is between 2 ms and 5 ms. The network densification is 1000 times higher than the 4G network and with a very high energy efficiency. The 5G network can offer lots of advanced services, such as smart city, internet of things. The primary technologies and approaches to address the key performance indicators are identified as [9]: Device-to-device communications (D2D), Massive-MIMO, millimeter wave (mm-Wave) communications technologies, energy-aware communication and energy harvesting, cloud based radio access network (C-RAN) and visualisation of wireless resources. The visions of 5G networks and the corresponding technologies are shown in Figure 1.3.

The concept of D2D communication in co-existence with cellular networks has been proposed and analyzed [10, 11]. D2D communications enable devices to communicate directly with each other with assistance by the cellular LTE network. Typically, this is achieved by utilising the high density of

Items	5G Expectations and Features	Trends/Proposal
Capacity and throughput	1000 times of throughput, cell data rate a ~10 Gb/s, signalling loads less than 100%	Spectrum reuse, different band, C-RAN, massive-MIMO, D2D
Latency	2 to 5 ms end-to-end latencies	C-RAN, D2D, and Full-duplex
Network densification	1000 times mobile data, 10000 times number of connecting	Heterogeneous networks, multi-tier network
Advanced services	smart city, service-oriented	M2M communication
Energy efficiency	10 times battery life	Wireless charging, energy harvesting

Figure 1.3: Features and trends of 5G networks.

mobile user equipment (UEs) and allowing multi-hop transmissions of delay tolerant data between UEs.

1.2 D2D in 3GPP Standardization

The 3GPP launched the first version of D2D communications in 2012 [12](3GPP Release 12). In this release, potential requirements for a Base Station (BS) controlled discovery and communications between devices that are in proximity under a Conventional Communication (CC) network coverage is identified.

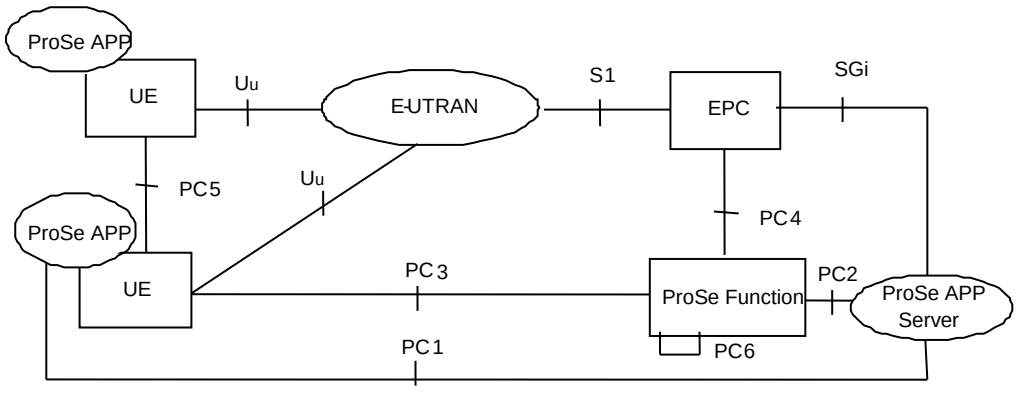

Figure 1.4: Enhancement of LTE-A network architecture with D2D communications.

1.2.1 Architecture Enhancements to Support D2D

To enable D2D Communications in a cellular network, a new architecture has been presented in [13], based on the existing LTE-A network. The supporting D2D LTE-A architecture is composed of the evolved packet core (EPC) and the evolved universal terrestrial access network (E-UTRAN), as shown in 1.4. For the network side two new functions are introduced in [14], Prose Function and Proximity-based Services (ProSe) Application Server; for the D2D UE side, a ProSe Application is enabled to support the D2D.

The ProSe Functions are: (1) providing parameters for D2D discovery and D2D communications, (2) identifying specific D2D applications and supports by the CC network, and (3) provide the network-related functions. The ProSe Application Sever is studied in [15], in which the authorization of D2D communications and discovery is handled over interface PC3 and the interface PC5 between two D2D UEs is also presented.

1.2.2 D2D Communication Scenarios

The architecture to support the ProSe is studied in [13]. The possible scenarios of direct communication without a relay are shown in in Figure 1.5. There are two main different coverage scenarios: (1) outside the public and mobile network (PLMN) coverage, and (2) within the PLMN coverage. For a UE acting as a relay, it can be UE-to-network relay or UE-to-UE relay.

The security of D2D communications is addressed by 3GPP in [16], which contains a study of all potential security risk of D2D and an evaluation of possible technical solutions needed to support such services. These requirements include a list of general requirements on ProSe security, authorization

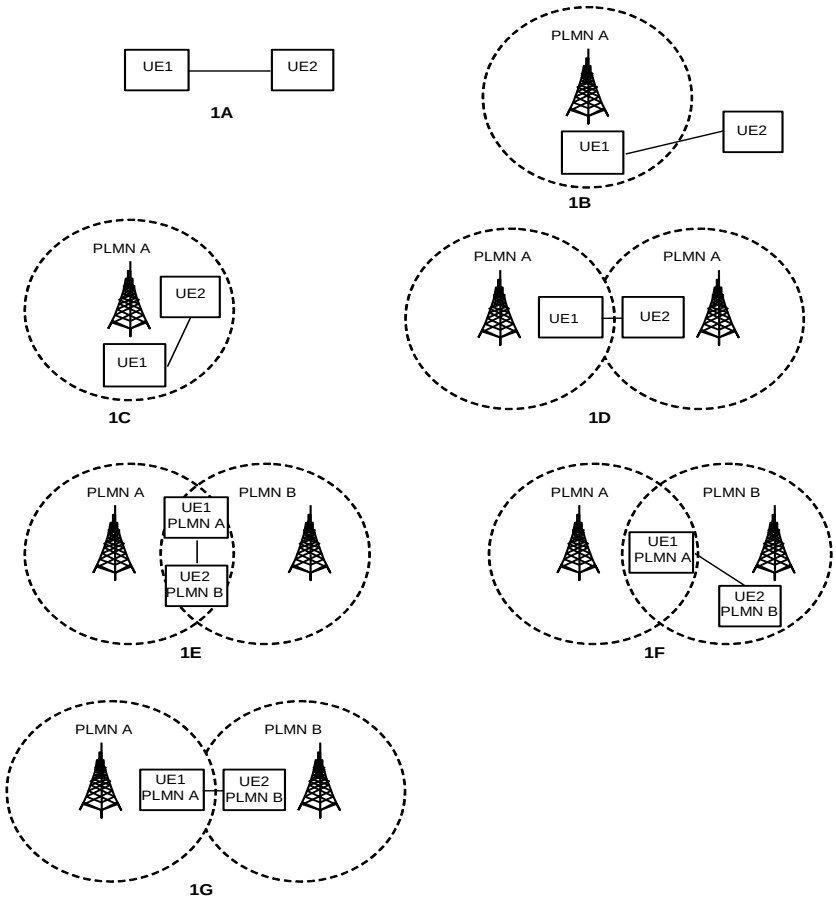

Figure 1.5: ProSe direct communication scenarios without a relay.

and privacy. The management of D2D communications is studied in [17], in which management objects that are used to configure the D2D UEs are defined.

1.3 The Application Areas of D2D

The D2D proximal discovery services provide an always-on device discovery of friends, services and offers in UEs' proximity [18]. D2D enabled mobile devices can discover things relevant to you, knowing what is around you, sensing your environment, and learning your preferences. There are plenty of applications for the D2D communications, mainly commercial use and public safety.

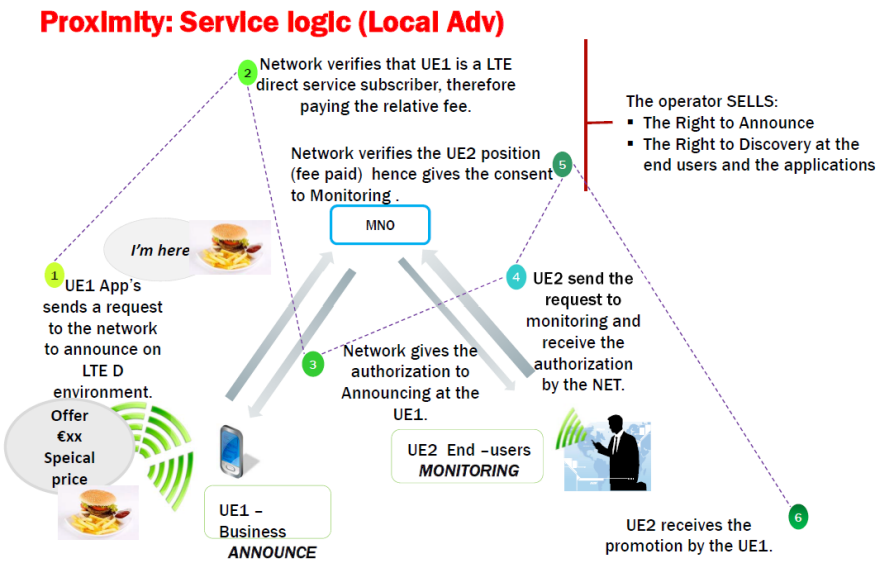

Figure 1.6: Proximity: Service logic (Local Advertising) [19].

1.3.1 Commercial services

The D2D commercial services are based on the D2D proximity discovery service, and the connected D2D UEs are always managed by the LTE network. As an example of the nearby alerted services, Figure 1.6 shows a case study of the precision advertising application presented by Telecom Italy Group [19]. A vendor launch a nearby announcement, once the request is verified by the LTE network, the vendor can send the promotion to the nearby D2D enabled UEs. Similar applications are gaming, entertainment and social media. Each UE could be a social media which launched a new social networking [20].

1.3.2 Public safety applications

One of the key requirements of the public safety network is that it should be stable (not affected by the environment or network traffic) and be able to communicate irrespective of whether the network infrastructure is fixed [21].

In almost all outdoor and most indoor areas, the cellular network can provide network coverage and communication demands. However, for some scenarios it is impossible, e.g. in long tunnels, deep inside a building with severe wall penetration loss or if the CC network suffers severe damage from either natural disasters or targeted attacks. D2D communication can be used for relaying to provide expanded network coverage, or to boost network capacity when the cellular network is congested.

Another advantage of D2D communication for public safety is group communication. The D2D communications allows a one-to-many communication feature; for an emergency situation the dispatcher can broadcast information to multiple UEs at same time, which can significantly shorten the emergency response time. Some research proposes D2D communication to provide public protection and disaster relief (PPDR) and national security and public safety (NSPS) services [22, 23].

1.4 Research Contributions

For conventional wireless multi-hop, current research has focused on: i) how to incorporate feedback mechanisms to ensure greater routing reliability [24]; ii) how to optimise partner selection to exploit spatial diversity [25–27]; and iii) how to optimise spectrum sharing and power control for increased energy- and spectral-efficiency [28–30].

When one considers multi-hop routing in the context of D2D communications, a major modeling consideration is the mutual interference between the overlay macro-BS tier and the temporarily formed underlay D2D tier, as well as intra-tier interference when the D2D shares a cellular band spectrum.

This is a dynamic problem with many variables such as the location of the source-destination UE pair and the overall network state. Multi-hop routing selection under a cellular interference environment has not been extensively studied at the time of conducting my research and my research mainly focus on the D2D multi-hop routing.

D2D communication can utilize unlicensed spectrum as well [31], such as the LTE-unlicensed spectrum specifically 5 GHz spectrum [32]. The existing 5 GHz unlicensed networks (802.11.n/802.11.ac) are using Carrier Sense Multiple Access (CSMA) for channel collision avoidance, but the D2D network is a demand-based system.

In this thesis, my contributions are summarised as follows:

1. An extensive and detailed overview of D2D multi-hop routing, the protocol exchange between D2D UEs and coexisting technologies between D2D using unlicensed and Wi-Fi system. Related to the publication of: "Y. Wu, W. Guo, H. Yuan, S. Wang, X. Chu, J. Zhang,"Device-to-device Meets LTE-Unlicensed", in *IEEE Communications Magazine*, vol. 54, no. 5, May 2016, pp. 154-159.".

2. An improved broadcasting algorithm (BR), restricted broadcasting algorithm (RBR), is addressed by solving the overload signaling challenge of BR. Furthermore, an interference aware routing (IAR) is introduced for the D2D multi-hop routing, which efficiently reduces the mutual interference between D2D and CC networks. For an emergency D2D communications, the application of RBR, shorted-path-routing (SPR), and IAR is addressed and the performance is compared. Related to the publication of "H. Yuan, W. Guo, and S. Wang, "Emergency route selection

for D2D cellular communications during an urban terrorist attack", in *IEEE International Conference on Communications Workshops* (ICC), Sydney, Jun. 2014, pp. 237-242.".

3. An analytical stochastic geometry framework comparing the performance of SPR and IAR is developed and the spatial operational envelopes for different D2D routing algorithms and CC transmissions based on the UEs physical location are defined. Related to the submitted to: " H. Yuan, W. Guo, Y. Jin, S. Wang, M. Ni, "Interference-Aware Multi-Hop Path Selection for Device-to-Device Communications in a Cellular Interference Environment" Submitted to *IET Communications*, 2016.".

4. Based on a spatial operational zone, it is found that there is an area not suitable for D2D communication because of the interference from BS. The possibility of D2D routing path passing through the area is analysed. As a result, a gradient based switching mechanism between D2D and CC is devised. Related to the publication of: "H. Yuan, W. Guo, and S. Wang, "D2D Multi-Hop Routing: Collision Probability and Routing Strategy with Limited Location Information", in *IEEE International Conference on Communications Workshops (ICC)*, London, Jun. 2015, pp. 681-685.".

5. The fairness of the channel occupation time between the D2D operating in the industrial, scientific, and medical radio band (ISM) and the 802.11 network is examined, and the network performance and time delay for both D2D and Wi-Fi UEs are analysed. Related to the publications of: "H. Yuan, W. Guo, S. Wang, "Device-to-device Communications in LTE-Unlicensed Heterogeneous Network", in *IEEE International workshop*

on Signal Processing advances in Wireless Communications (SPAWC), Edinburgh, July, 2016, pp. 1-5." and "Y. Wu, W. Guo, H. Yuan, S. Wang, X. Chu, J. Zhang,"Device-to-device Meets LTE-Unlicensed", in *IEEE Communications Magazine*, vol. 54, no. 5, May 2016, pp. 154-159.".

1.5 Thesis Outline

The main topic of this thesis is the D2D multi-hop routing selection, which includes routing selection in underlaying cellular networks and the LTE-Unlicensed spectrum. The thesis is organised as follows.

Chapter 2 presents a overview of D2D communications. A review of different band spectrums for D2D communications is provided, where their performance merits and limitations are discussed. A review of D2D multi-hop routing algorithms is also presented, where the difference between the D2D routing and the traditional Ad hoc routing is discussed.

In Chapter 3 the wireless communication network modelling is explained, with the two main modelling theories: Stochastic Geometry modelling and Monte Carlo simulation.

In Chapter 4 the dynamic selection of multi-hop routes for D2D communications co-existent with a fully loaded urban cellular network is addressed, when the cellular network is congested during an unexpected event. Three different wireless routing algorithms, shortest-path-routing (SPR), interference-aware-routing (IAR) and restricted broadcast-routing (RBR), are analysed.

Chapter 5 develops a theoretical stochastic geometry framework, which is used to generalize the performance comparison of IAR and SPR. Operational

bounds on the operation envelopes of the different D2D routing algorithms can be entirely characterized by clear geometric regions in the coverage area of the cell.

In Chapter 6, a collision area (which is defined as that the D2D communication cannot satisfy the minimum SINR requirement because of the interference from BSs) in a heterogeneous cellular network for the purpose of interference management between D2D and CC is defined. In the absence of accurate location information, the collision probability of the D2D multi-hop path hitting the defined collision area is analysed.

Chapter 7 considers how the envisaged D2D networks can efficiently scale its capacity by utilising the unlicensed spectrum with appropriately designed LTE-Unlicensed (LTE-U) protocols are examined. The LTE-U Listen Before Talk (LBT) algorithm with multi-hop routing is adapted for collision avoidance between traditional unlicensed UEs, e.g. Wi-Fi UEs, and the LTE-U enabled D2D UEs.

The research results and findings presented in the thesis are summarised in Chapter 8, and possible future work directions are also discussed.

Chapter 2

Review of Device-to-Device Communication

In this chapter, the motivation to study D2D communications and its status within the cellular network eco-system is discussed. Then, two prominent research challenges in multi-hop D2D communications underlaying cellular networks are reviewed: band selection (inband and outband) and a variety routing algorithms for multi-hop D2D communications are presented. Before that, the communication performance benefits for D2D are reviewed, and then the communication spectrum is investigated, inband and outband unlicensed spectrum (802.11 protocol).

2.1 Overview of Communication Performance Benefits

D2D communications, which is a part of the LTE-Direct standard [33], is a technique of allowing UEs to communicate directly with each other, via

relaying messages using neighboring UEs [34, 35]. In terms of command and control, each D2D connection will anchor on the serving BS, but the BSs are avoided in terms of data-bearing channels. Hence, D2D communication protocols are semi-distributed.

The conditions for establishing D2D communications in a cellular environment include insufficient channel resources in the BS and the transmission of delay tolerant data [36]. As for device discovery between potential D2D UEs, it has been proposed that the UEs can utilize recent 3GPP ProSe standardization [37].

The potential advantages of D2D communications include throughput enhancement, UE energy saving and coverage expansion [38,39]. The economic attraction for mobile operators is that significant capacity and coverage gains can be achieved without having to invest in network-side hardware upgrades or new cell deployments. However, there are technical challenges related to D2D and conventional cellular (CC) communications in co-existence, especially the mutual interference due to spectrum sharing.

Enhanced Throughput. The rate of CC network can be enhanced by exploiting D2D communications as a relay [40, 41]. The idle UEs can act as relay to help the CC UEs when they are in a poor link quality to transmit data [42], so that the network throughput is enhanced. There is an obvious challenge, how to manage the transmission model (whether via D2D relay or CC). A transmission graph solution is presented in [43], where each UE (D2D or CC) is represented by a vertex. The transmission mode selection (whether to use D2D relay or CC) is formulated as a flow maximization problem.

Another approach to improve the network throughput is reusing the cellular spectrum with the CC network. The main challenge for reusing is

how to manage the mutual interference of D2D and CC communication. Several techniques have been investigated to suppress interference between D2D and CC links, such as Successive Interference Cancellation (SIC) [44], Radio Resource Management (RRM) [45] with game theory to prioritize transmitters [46]. An SIC is proposed in [47], which is by reducing the interference to D2D communication link can get capacity without dropping CC network capacity. Radio spectrum management [48], whether the D2D UEs reuse the cellular spectrum or the dedicated spectrum for D2D UEs by BS, is another efficient way to reduce the mutual interference.

Extension of Coverage. D2D UEs serve as relays to cover UEs outside the cellular coverage. When a UE is not in the cellular coverage, another D2D-enabled UE within the cellular coverage is selected as a relay to help the UE communicate with the BS or other UEs with in coverage. The authors in [49] describe the D2D acting as a relay for national security and public safety (NSPS) services when the network coverage is partial or missing.

Energy Efficiency. Generally D2D communication is a shorter distance communication network compared with the CC network. So D2D needs lower transmission power to get the same signal-to-interference-noise-ratio (SINR) under the same interference environment. D2D communication can effectively offload the CC network traffic [50, 51], and after the traffic is offloaded to D2D UEs, the BS can set up as a sleeping control model when the network traffic volume is below the threshold [52].

Spectrum Efficiency. The D2D communications can enhance the spectrum efficiency by reusing the cellular spectrum. How to allocate the cellular spectrum is a challenge. A cognitive spectrum access technology for spectrum allocation has been proposed [53]. The cognitive D2D UEs are capable of sens-

ing the received interference for any D2D receiver. When the two D2D UEs prepare to communicate, the transmitter sends a communication request to the intended receiver first. Then the receiver senses the channel interference; if the SINR is over the set threshold, the intended receiver replies a communication confirm message for establishing the D2D communication link. While if the SINR is below the threshold, the D2D communication is not allowed.

2.2 D2D Band Selection

The D2D communication can utilize either the cellular spectrum (inband) or unlicensed spectrum (outband). The outband spectrum can be unlicensed spectrum or allocated spectrum by BS [54]. For inband D2D, there are two models to reuse cellular spectrum resources [55]: underlay inband or overlay inband.

The licensed band of Frequency Division Duplex (FDD) LTE network which is operated in Figure 2.1 shows the full frequency band allocations. Industrial, scientific and medical (ISM) radio bands mainly focus on 433 MHz, 915 MHz, 2450 MHz and 5000 MHz.

2.2.1 Inband D2D

In underlay inband, D2D links use the same cellular network spectrum band at the same time as the CC network. The underlay D2D would enhance the spectrum efficiency by reusing the CC spectrum with CC network at the uresame time but an obvious challenge is to manage the mutual interference between D2D and CC network. In overlay inband D2D, the cellular network allocates dedicated resources such as allocated spectrum channels or different

FDD LTE BANDS & FREQUENCIES				
LTE BAND NUMBER	UPLINK (MHZ)	DOWNLINK (MHZ)	WIDTH OF BAND (MHZ)	BAND GAP (MHZ)
1	1920 - 1980	2110 - 2170	60	130
2	1850 - 1910	1930 - 1990	60	20
3	1710 - 1785	1805 -1880	75	20
4	1710 - 1755	2110 - 2155	45	355
5	824 - 849	869 - 894	25	20
6	830 - 840	875 - 885	10	25
7	2500 - 2570	2620 - 2690	70	50
8	880 - 915	925 - 960	35	10
9	1749.9 - 1784.9	1844.9 - 1879.9	35	60
10	1710 - 1770	2110 - 2170	60	340
11	1427.9 - 1452.9	1475.9 - 1500.9	20	28
12	698 - 716	728 - 746	18	12
13	777 - 787	746 - 756	10	41
14	788 - 798	758 - 768	10	40
15	1900 - 1920	2600 - 2620	20	680
16	2010 - 2025	2585 - 2600	15	560
17	704 - 716	734 - 746	12	18
18	815 - 830	860 - 875	15	30
19	830 - 845	875 - 890	15	30
20	832 - 862	791 - 821	30	71
21	1447.9 - 1462.9	1495.5 - 1510.9	15	33
22	3410 - 3500	3510 - 3600	90	10
23	2000 - 2020	2180 - 2200	20	160
24	1625.5 - 1660.5	1525 - 1559	34	135.5
25	1850 - 1915	1930 - 1995	65	15
26	814 - 849	859 - 894	30 / 40	10
27	807 - 824	852 - 869	17	28
28	703 - 748	758 - 803	45	10
29	n/a	717 - 728	11	
30	2305 - 2315	2350 - 2360	10	35
31	452.5 - 457.5	462.5 - 467.5	5	5

Figure 2.1: FDD LTE frequency band allocations.

time slots of the channel to D2D links. The spectrum sharing is illustrated in Figure 2.2.

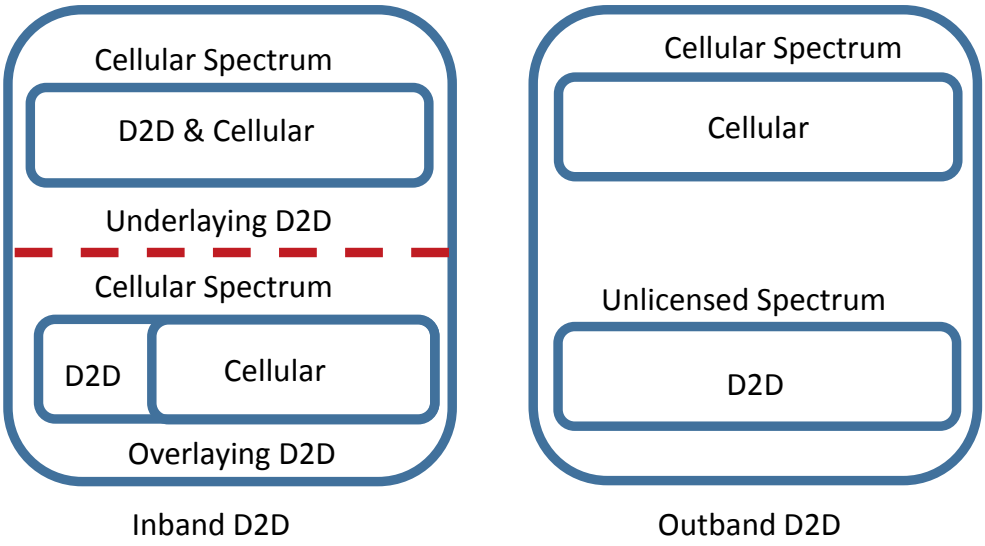

Figure 2.2: The band spectrum situation for inband and outband D2D communication.

In overlaying D2D communications, BS allocates dedicated resources for D2D communications [56–58]. The overlaying D2D eliminates the mutual interference between the CC networks and D2D communications, however it reduces the resources efficiency and the available resources for the CC network.

The communication channel is partitioned to different sub-channels on the time domain for overlaying D2D communication, which is addressed in [40], in which the authors considered a pair of D2D UEs as a two way relay between CC UE and BS while the D2D can communicate with each other. At the first time slot, BS and CC UE transmit data to the two D2D UEs and for the second time slot the two D2D UEs transmit the data to CC UE and BS shown in Figure 2.3. At each time slot, only one D2D UE can send message to the other D2D UE. According to the channel throughput, the CC UE selects the

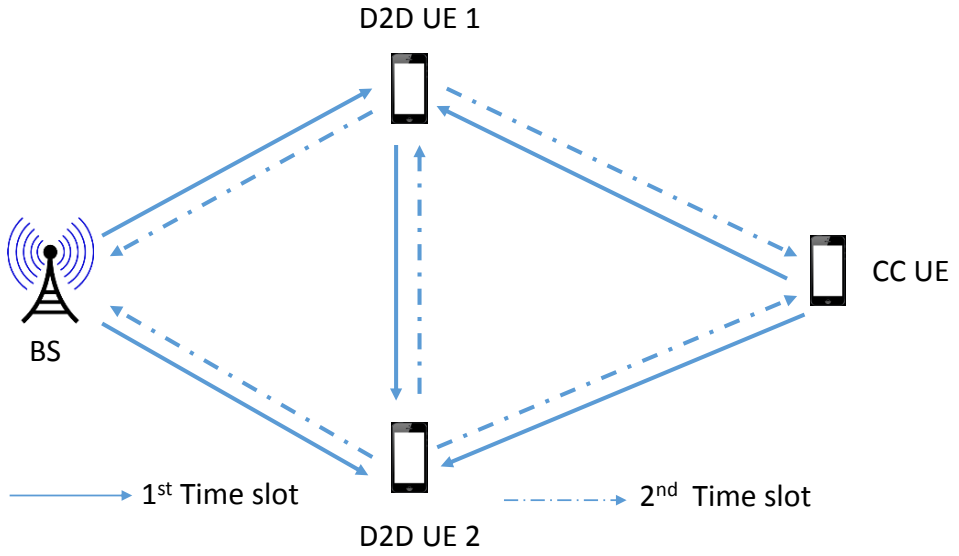

Figure 2.3: The two different time slot protocol.

D2D UEs as a relay to communicate with the BS . The results shown in [40] are that the overall network achievable rate increases for both the cellular links and the D2D communications.

A frequency overlaying D2D communication with the different time slot allocation is presented in [59]. The authors proposed an overlaying D2D communications of a two-tier cellular network for offloading the network traffic and enhancing the network rate. Each macro BS (distributed as a hexagon) has six pico BSs at the end points of its borders, and the pico BSs maintain a mapping table (which includes available frequency resource block (RB), channel state information (CSI) and QoS requirements) to assist the D2D communication establishment. The average rate of macro BSs, pico BSs and D2D communications is optimized based on the user density and pico cell coverage range. The results show that D2D communication can significantly improve the per CC UE average rate, however the D2D average rate depends on the frequency

allocation between pico BS and D2D communications. Similar work was presented in [60], where the authors addressed a downlink (DL) overlaying D2D communications. The D2D UEs are allocated the dedicated DL spectrum acting as a relay to extend the CC coverage; D2D UEs communicate with the CC UEs who are outside the CC coverage.

2.2.2 Outband D2D Communication

The outband spectrum can be either unlicensed spectrum or allocated spectrum taken from the licensed band [31]. Outband D2D is advantageous compared with underlaying D2D because there is no mutual interference between D2D and CC UEs. For example, in [61] the industrial, scientific and medical (ISM) band is selected for D2D communications in LTE. The D2D UEs are grouped based on the different QoS requirements, whereby only one UE per group can use the ISM band for communication.

D2D on Unlicensed Spectrum

During the past few years, the concept of LTE-U (LTE for Unlicensed Spectrum) has been addressed, which suggests that LTE can operate in the unlicensed spectrum with significant modifications to its transmission protocols. LTE-U must adhere to unlicensed spectrum requirements, i.e., set transmit power limits and collision avoidance [32]. By utilizing the considerable amount of unlicensed spectrum available, low power D2D transmissions can potentially avoid cross-tier interference with CC channels, at the cost of complicating the unlicensed spectrum usage [62]. LTE-U has been included in 3GPP Release 13 standardization along with optional carrier aggregation to improve peak data

rates [62].

Wi-Fi is a contention-based system with an appropriate mechanism taken to avoid interference, i.e., CSMA. However LTE is a demand-based system, so a critical element of LTE-U is to ensure fairness for Wi-Fi and other unlicensed users. There are two main algorithms for a fairness to sharing the unlicensed channel.

Idle Channel Sense

A straight approach is to sense the Wi-Fi channel. If the channel is empty, the unlicensed communication is actived. If the channel is occupied then wait for a clean channel. The difference between CSMA and Idle Channel Sense (ICS) is that a CSMA system is applied with a collision avoidance (CA) mechanism. When the transmitter senses a clear channel, it will send a ready to send (RTS) frame. If the receiver is ready to receive it will send a Clean to Send (CTS) package to inform transmitter. This protocol is also called RTS/CTS handshake.

In [63], an example of LTE-U channel access scheme is presented, where the femtocell base station (fBS) senses the unlicensed channel by detecting the received power strength [64]. Before the fBS accesses the unlicensed channel, it will detect the channel for a period T_{sensing}. If the channel is clean during the sensing time, then the fBS accesses the unlicensed band and occupy the channel for a fix time T_{cellTx}. If not, the fBS assigns the LTE licensed resource.

Another protocol is addressed in [65], which proposes an approach for LTE-U UEs co-existence with the 802.11 protocol controlled by eNB. The eNB is divided into two components, 802.11 part and LTE part. At the beginning, the 802.11 part of eNB senses the unlicensed channel. If the unlicensed channel

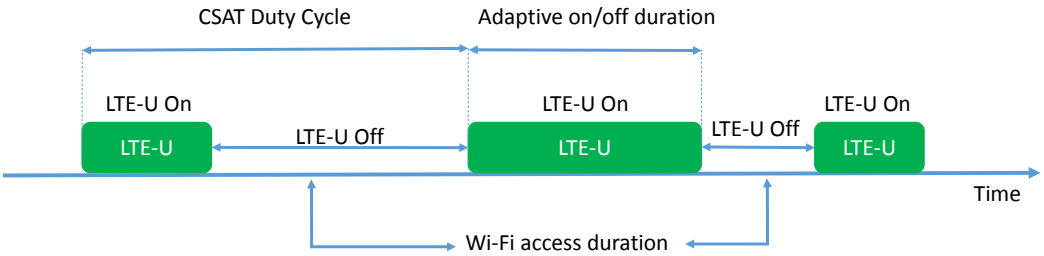

Figure 2.4: CSAT enables LTE-U and Wi-Fi to share the same channel.

is empty, the LTE part of eNB will launch the communication with LTE UEs on unlicensed band. At the same time, 802.11 part of eNB will broadcast a Wi-Fi frame that notices the channel occupancy time to 802.11 UEs. If there exists an 802.11 UE using the channel, the 802.11 part decodes the PHY frame from 802.11 device and obtains its length and attributes information (e.g. transmission power, maximum interference power that is tolerable by 802.11 receiver UE). According to the decoded information, the LTE part uses a lower power communication with the LTE UEs on unlicensed band to satisfy the interference requirement of the 802.11 UEs.

Carrier-Sensing Adaptive Transmission

Different from the ICS, Carrier-Sensing Adaptive Transmission (SCAT) is based on duty cycle to control the LTE signal on and off, duty cycled configuration does not sense the channel before transmitting [66]. As shown in Figure 2.4 when the LTE-U is on, the LTE occupies the channel; while in the LTE-U off period, the channel is unoccupied to neighboring Wi-Fi which can resume normal Wi-Fi transmissions. During the LTE-U off period, the utilization of Wi-Fi medium will be measured by LTE (normally LTE fBS), and adaptively adjust LTE-U *On* duty cycle according to the Wi-Fi traffic load.

The duty cycle can be set to a few hundred milliseconds, which can effectively accommodate the QoS requirement while controlling the data transmission delay.

Compared with ICS, SCAT does not sense the channel before transmission so that there is a probability of that two different different UEs are transmission at same time(which is defined as a communication collision). The collision reduces both LTE and Wi-Fi capacity. The research in [67] shows that when the LTE-U on period is shorter than off period, the network capacity of using SCAT is 13% lower than using ICS.

2.3 Review of Multi-hop Routing Algorithms

In D2D communications multi-hop network, how to select the best path is a challenge. Routing is the process of selecting best paths in a network. In wireless communication networks, routing directs data forwarding from the source node to the destination through the specific nodes in the same network. How to select the specific nodes is called the routing algorithm. A qualitative comparison of multi-hop routing algorithm is given in Table 2.1.

2.3.1 Broadcasting Wireless Routing

Broadcasting (BR) refers to transmitting data to all other nodes within the transmitter's transmission range [68]. There are two main replication algorithms: Flooding and Controlled flooding.

Flooding: The source node sends a copy of the data to all of its neighbors. When a node receives a broadcast data, it duplicates the data and forwards it to all of its neighbors. At the end of the process every node will

Table 2.1: Qualitative comparison of multi-hop routing algorithms.

Example	Algorithm	Routing Information	Control	Interference Aware	Routing Direction
[68]	BR	-	Self organised	No	No
[69]	GFR	Physical location	Self organised	No	Yes
[70]	FR	Physical location	Self organised	No	Yes
[71]	GPSR	Physical location	Self organised	No	Yes
[72]	FLQ	SINR, RB, Traffic	Self organised	-	Yes
[73]	ILA	Physical location, SIR	Controlled by BS	Yes	Yes

have a copy of the packet. As shown in Figure 2.5, the source node s broadcasts data to node j_1. Then j_1 duplicates to all its neighbors.

However, when a node is connected to more than two other nodes, it will create and forward multiple copies of the broadcast data. It is result to the endless multiplication of broadcast data [68]. As shown in Figure 2.5, an endless multiplication of broadcasting is between node j_1, j_2, and j_3.

Controlled flooding: By solving the problem of endless multiplication in BR, a controlled flooding algorithm is addressed in [74] which is also known as Controlled flooding BR. The process of the algorithm is shown as:

1. A source node puts its sequence number i into a broadcast data, which is set up as 1.

2. The source sends the packet to all of its neighbors.

3. When nodes receive the data from source node, they set their sequence

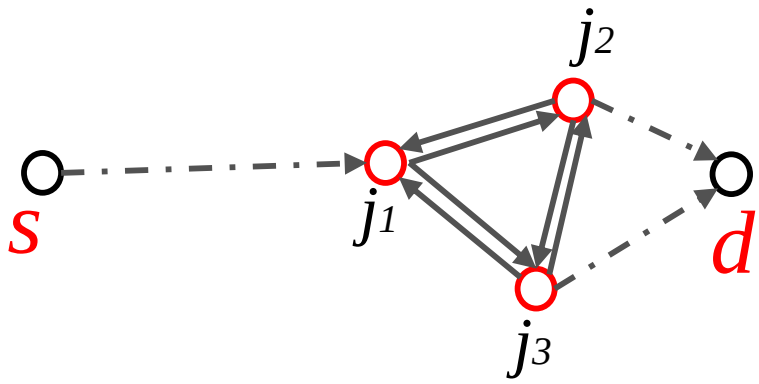

Figure 2.5: The broadcasting routing with flooding.

number as $i + 1$, then broadcast data they have received. Each process of broadcasting increases the sequence number by 1.

4. When a node receives a broadcast data, it checks the data sequence. If smaller than its own sequence number, the packet is duplicated and forwarded, otherwise, the packet is dropped.

As shown in Figure 2.6, the BR with controlled flooding. Source UE s wishes to transmit data to the destination UE d, but there is no direct communication link between s and d. In this figure, the source UE s is broadcasting data to destination UE d. At the beginning, s sets its sequence as 1 and broadcasts to j_1. After receives the data from s, j_1 sets its sequence as 2 and forwards to j_2 and j_3. But j_2 and j_3 cannot replay back because their sequences are bigger than j_1. Therefore, the controlled broadcasting avoids the endless multiplication of broadcast data.

However, BR causes overload signaling and when the data reaches the destination node and how to inform other nodes to stop BR remains challeng-

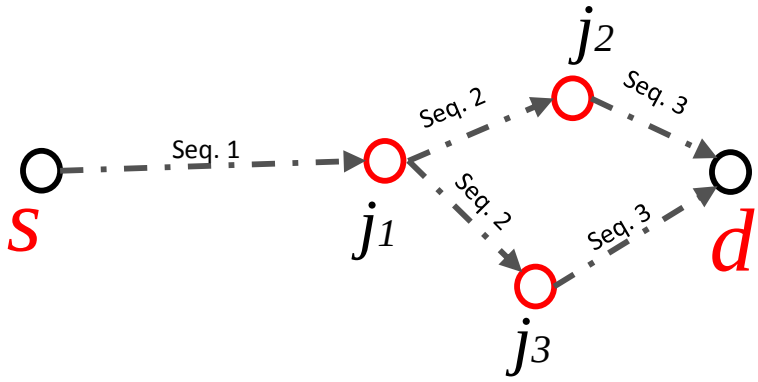

Figure 2.6: The broadcasting routing with controlled flooding.

ing.

2.3.2 Geographical Wireless Multi-hop Routing

The problem of BR is lack of direction, there is no route direction for where the data should be transferred. For solving those problems, a geographical location based routing algorithm is proposed in the 1980s by Hideaki Takagi [75].

Geographical routing is a routing protocol using information about the geographic location of the neighbors of the current node to direct a packet to its destination. In geographic routing protocols, it is assumed that all UEs have the information of their own locations and that the source UE knows location information of the destination UE. As we will see below, the destination location information is passed from source UE to every relay node during the relay nodes selections. Normally, UEs obtain their own geographic coordinates with a Global Positioning System (GPS) [76] or a grid location service [77] (e.g. in D2D BS acts as a grid location provider). In the following,

three popular Geographical multi-hop routing methods in the literature are reviewed.

Greedy Forwarding Routing

Greedy Forwarding Routing is an improved BR. As reviewed earlier in Section 2.3.1, in BR any UEs re-broadcast the data after receive the data, but in Greedy Forwarding only the selected UEs can relay. Greedy forwarding is a routing algorithm based on the network UEs' physical locations, and it works by forwarding a packet closer to destination [69]. When the source UE needs to send data to a specific destination UE, it first checks its available neighbour UEs to select the neighbour UE which is closest to the destination as the first relay. Once the data is received, the relay UE will perform the same approach, to determine the neighbours which is closest to destination and forward the data to it as the next relay. The process is continued until the data reaches the destination.

Figure 2.7 illustrates a greedy forwarding algorithm under the same network scenario with BR. It is can be seen that the routing has a definite directivity from s to d. Following the greedy forward routing, s selects its neighbour UE j_1 as which is closest to d within s transmission range. The relay UE j_1 repeats greedy process forward to next UE j_2, repeating this process until data reaches d.

A successful greedy forward routing requires among all the UEs participating in the routing process, there should be at least one neighbour closer to the destination than itself such as shown in 2.7. Realistically, this might be impossible for a dynamic wireless network, therefore the UE cannot find a UE to forward data. For example in Figure 2.8(b), at the first step s cannot find

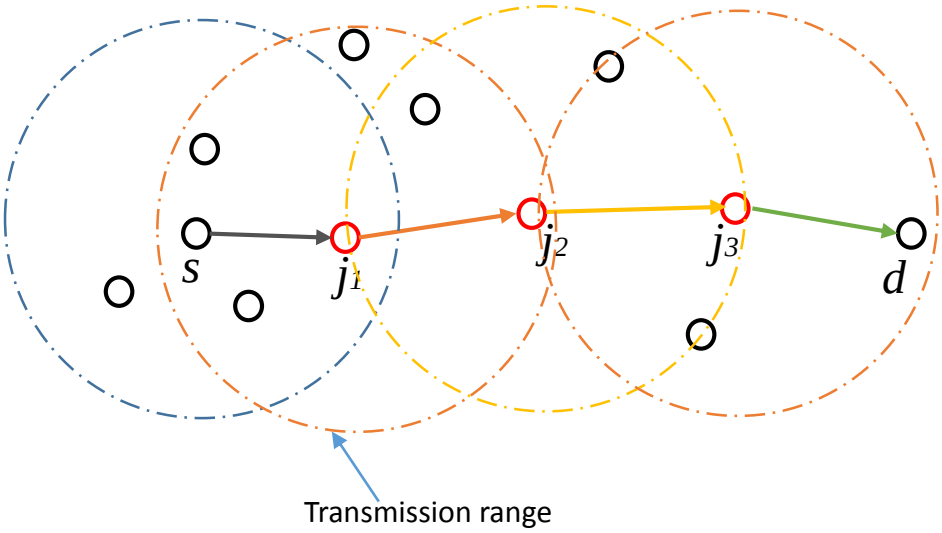

Figure 2.7: Wireless relay network via greedy forwarding algorithm.

a closer neighbour than itself to d. When a UE cannot find a neighbour closer than itself to the destination, it will drop the data to avoid routing loop [78]. An alternative to greedy routing is face routing which avoids this problem.

Face Routing

In face routing, a geometric routing algorithm is applied to a planned subgraph of network topology [70]. A planar subgraph divides the network topology plane into different faces, where each planar subgraph contains no intersecting edges and is composed of polygonal regions separated by edges [79,80]. Figure 2.8(a) shows an example of planar graphs.

Once the planar subgraph has been obtained, the data from source UE is forwarded along the first face boundary in anticlockwise (from the source to the destination) order until it reaches the source-destination-line (S-D-line) shown in Figure 2.8(b). The routing path traverses around the face and changes to

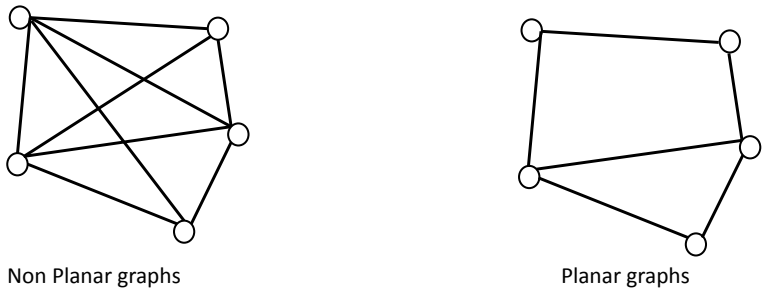

(a) An example of non planar and planar graphs.

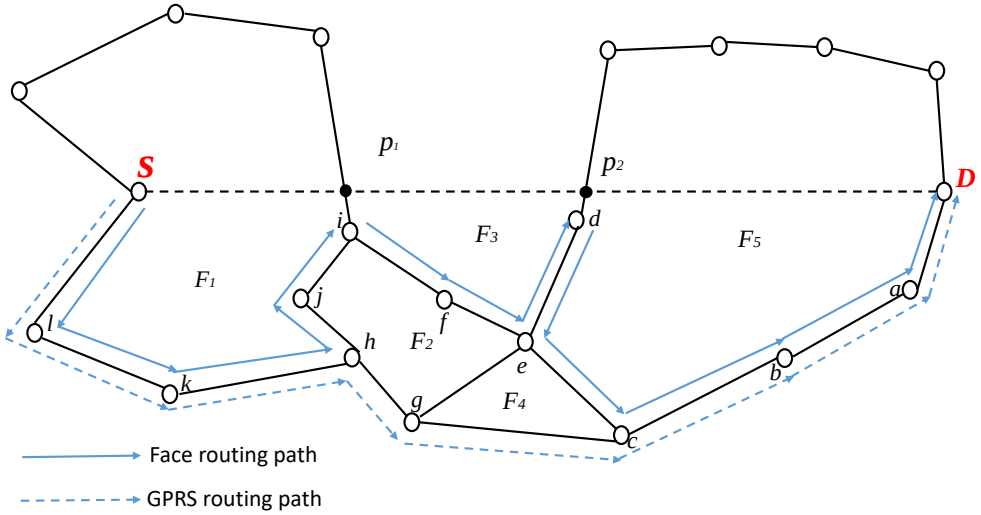

(b) An example of the path followed by a packet using a face routing protocol and Greedy Perimeter Stateless Routing.

Figure 2.8: The planar graphs and face routing.

other faces at the edges crossing the S-D-line until it reaches the destination UE [81]. Figure 2.8(b) shows an example of the routing computed by face routing protocol. The route starts from source UE S to destination UE d, it first travels inside the face F_1 until reaches UE i. If continuing to route in F_1 it will reach the intersection point by S-D line and face boundary line, called a face broken point p_1. Therefore, it has to change routing face, under the right hand rule then routing path changes to the face F_3. Subsequently, the data

travels along the boundaries of faces F_3 when reaches d and then changes to F_5 until delivered to destination D.

Ideally, planar subgraphs are connected as planarization with full connectivity, but in reality specifics of a wireless environment mean planar subgraphs may lack connectivity, such as node a does not exist in Figure 2.8(b), when node b cannot find a next relay, and it will switch to anticlockwise order. If anticlockwise and clockwise order both fail, the network routing fails to connect the destination.

Another problem is that it is not the shortest route. As shown in Figure 2.8(b) when data arrives the relay UE h, the shortest path is $h-g-c$ but for facing routing it is $h-j-i-f-e-d-c$. The longer routing path causes longer time delay and more energy consumption due to a larger number of hops. A combined greedy routing and face routing called greedy perimeter stateless routing (GPSR) algorithm to enhance the routing efficiency is proposed.

Greedy Perimeter Stateless Routing (GPSR)

The greedy perimeter stateless routing (GPSR) algorithm uses graph-theoretic techniques to find routes, and exploits the correspondence between geographic positions and connectivity in a wireless network to make packet forwarding decisions [71]. It will start in greedy forward routing and then switch to face routing when the current UE cannot find a neighbour closer to the destination than itself. In particular, it employs:

1. *greedy mode* which is the priority mode, forward data to neighbour UE that is closer to the destination;

2. *face mode* in regions of the network where a greedy path does not exist,

data traverses successively closer faces of a planar sub-graph of the full connectivity graph until reaching a UE closer to the destination, and then the greedy mode resumes.

Geographical Routing based on the location information can provide a definite directivity for the routing path. However, for a wireless communication network the channel status (such as channel throughput, traffic volume or SINR) is also an important parameter for the network. Geographical Routing does not consider the channel status when selecting the routing path. Attentively, a channel status based routing algorithm called FlashLinQ is reviewed in the next section.

2.3.3 FlashLinQ Routing Algorithm

FlashLinQ (FLQ) is a technology of PHY/MAC network architecture for synchronous and distributed D2D communication [72], which was introduced by QualComm, aiming to find a maximal channel-state-aware subset of channel links. FLQ is suitable for D2D coexisting communication under a condition of QoS, e.g. SINR, traffic volume. In FLQ, a synchronous Time Division Duplex (TDD) Orthogonal Frequency Division Multiplexing (OFDM) system is designed at 2.586 GHz carrier frequency with 5 MHz bandwidth. Each device identifies its neighbouring devices by receiving single-tone discovery signals.

In the architecture of FlashLinQ, the available links between D2D UEs are distributed as two matrices for both transmitter and receiver, and each one has 112 RB, where an RB represents a sub-channel and an OFDM symbol. The links are assigned to different priorities ordered from $1st$ to nth. For a link with the nth priorities scheduled for communication it has to satisfy the

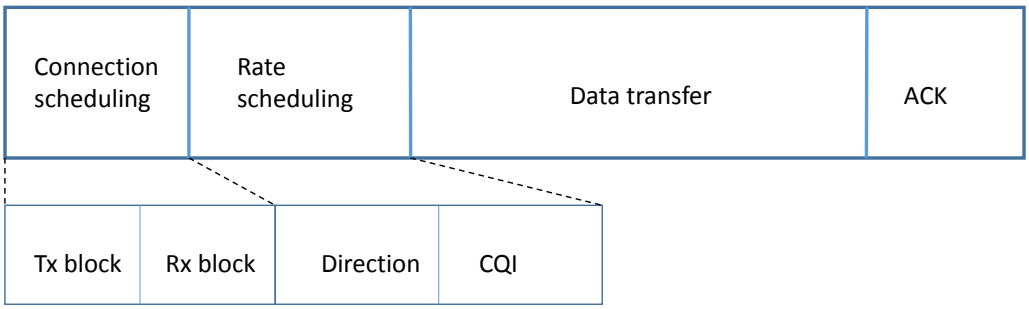

Figure 2.9: The structure of traffic channel (TCCH)

following requirements:

1. Both transmitter UE and receiver UE agree the channel SIR;
2. The signal over link n will not cause interference to any already scheduled link with a higher priority, e.g. link {1, 2, 3, ..., n-1};
3. Both transmitter and receiver UEs' corresponding RBs are available.

D2D links perform link scheduling according to the scheduling results in a traffic channel (TCCH) frames in the data transfer phase shown in Figure 2.9. In the link scheduling period of the traffic channel, in order to determine whether to access the link, transmitter (Tx) and receiver (Rx) in each active D2D link schedules process by transmitting and detecting direct power signal (DPS) and inverse power echo (IPE) signals in Tx and Rx OFDM blocks respectively. Finally, Tx transmits data frames to Rx and Rx acknowledges results of the data reception in the Data transfer and Acknowledgement (ACK) periods.

The priority of different links is assigned randomly at each time slot, so FLQ is fair for all links. A locally unique connection identifier (CID) is allocated for each D2D link. If the two links have the same CID, those links

can transmit simultaneously. A two-hop D2D communication with FLQ is presented in [82]. The hop links are connected as:

- Source D2D UE m discovers destination D2D UE m' based on FLQ;
- m identifies UE j as a relay for multi-hop communication based on the first discovery results;
- m establishes the link $m - j - m'$ and transmits data from m to m' relaying by j;
- m' replay the confirm ACK to m through j, transmission completed, release the link.

The RBs are limited to 112 in FLQ, for a high D2D UEs density, which is not enough for dedicating the RB to each D2D communication link, furthermore dedicates RBs to D2D also reduces the cellular spectrum efficiency.

FLQ is a routing algorithm which depends on each UE maintaining a routing table containing information of all available relay UEs and geographical routing protocol does not need to maintain the entire network topology. On one hand, geographical routing reduces network cost due to the relatively low amount of coordination and information exchange. On the other hand, geographical routing only requires information about neighbour UEs so it reduces reliance of complete network topology.

2.3.4 BS Assistance for D2D Communications Routing

BR, geographical routing and FLQ are self-organised routing algorithms. They lack central control and need a complex self-organised mechanism to deal with

the routing environment changes such as the movement of UEs and communication channel status changes. Furthermore, when the routing process fail, there is not an efficiency backup algorithm. D2D communications is part of LTE-Direct standard. The entire communication is controlled and authorised by the BS. Therefore, the BS plays a significant role for D2D routing.

The BS assistance for D2D communication contains three main functions at each hop: (1) register the identification (ID) of D2D UEs (such as IMSI) and the D2D UE link layer identifier; (2) authorise the D2D UEs proximity discovery whereby the open discovery technology is used (in open discovery, the UEs can be detected by any other UE in its proximity [34] [83]); (3) provide the destination UE location to the relay UEs. In the event that the D2D multi-hop process fails, the BS will take over the communications and establish a CC link.

Device Proximity Discovery

Before a source UE can communicate with the destination UE, it needs to identify its neighboring UEs so that the data can be routed through the optimal set of relay UEs to the destination. In order to set up a D2D link, the UE transmits a device discovery signal for its nearby UEs to detect the signal. The device discovery process can be classified into **restricted discovery** and **open discovery** [34]. In restricted discovery, D2D UEs must have a permission from the BS to be detected by other UEs, while in open discovery, the UEs can be detected by any other UE in its proximity.

As Figure 2.10 shows, the user of UE m (the discoverer) wishes to discover whether there are any other D2D UEs in proximity. UE m broadcasts a discovery request message:

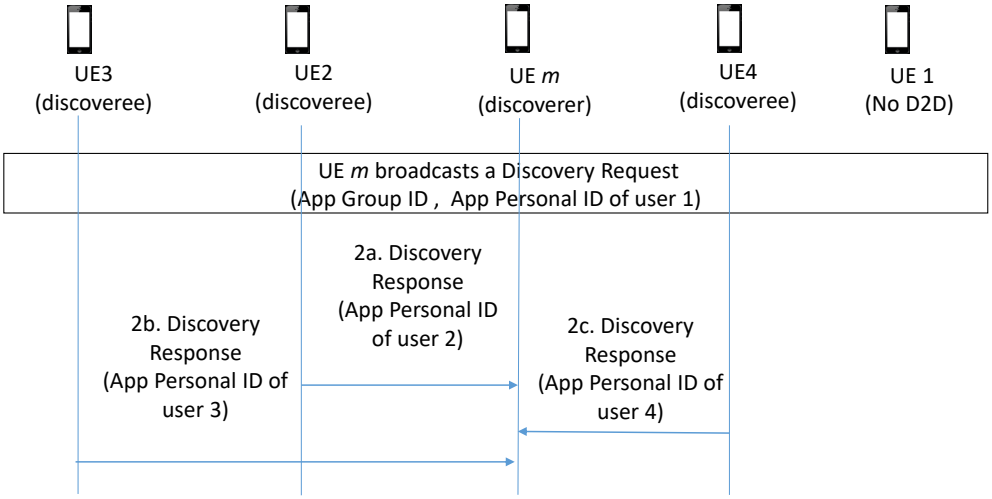

Figure 2.10: The D2D UE proximity discovery

- If a mobile UE is an active D2D UE, it replies a data frame with its identifier ID set to the discover UE's neighbour group, which is marked as a potential D2D relay UE in the group;
- Alternatively, if the UE is not an active D2D UE, it may keep quiet to the discoverer UE.

The discovery request message is received by UE1, UE2, UE3 and UE4. Apart from the user of UE1, all other UEs are active D2D UEs. Each of UEs responds directly to discoverer UE with a discovery response message which may contain the unique personal ID of its user.

Data Relay Between UEs

As shown in Figure 2.11, the BS provides assistance between the D2D source UE m and the relay UE j to the BS when the data is relaying from source to

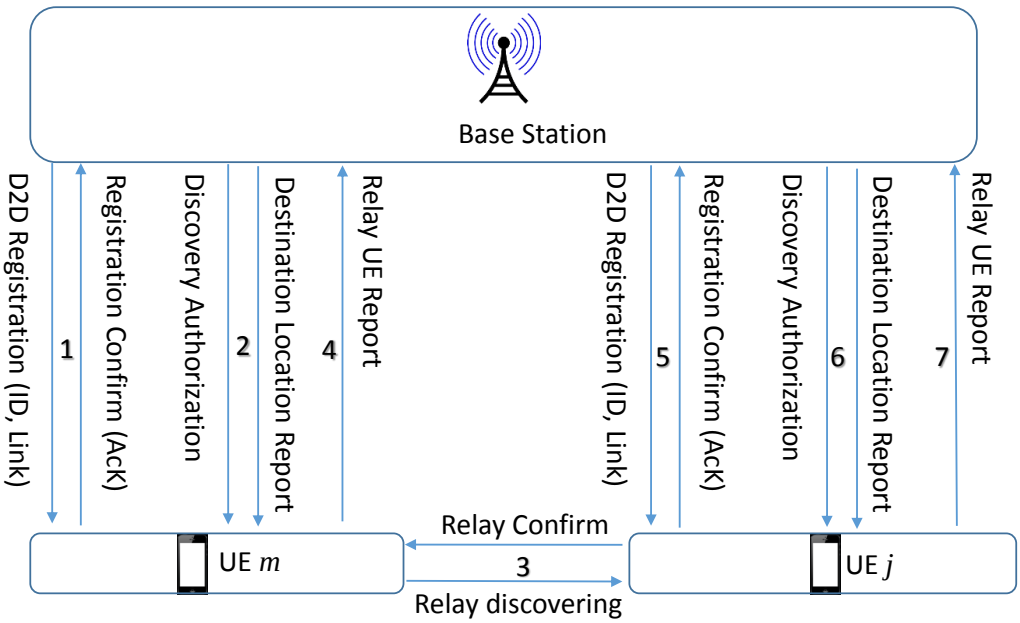

Figure 2.11: The D2D communication data relay

destination.

- After the discovery has finished, the candidate UE is reported to BS by source UE m, and then the BS registers the UE j as a relay UE.
- The UE j confirms the registration (ACK) to the BS, which includes the relay ID and communication link.
- When the UE j is confirmed, the BS authorises the UE j to discover its proximity devices and reports the destination UE m location information.
- The UE j selects the next relay UE j' and reports to the BS.

For D2D routing, the neighbour discovery and data routing are controlled by BS. When one routing algorithm fails, BS can choose a corresponding backup, such as switching to CC communication or other algorithms. For

a mobile communication system, the movement of UEs affects the routing chosen and the BS accordingly adjusts the routing path direction.

2.4 Interference Aware Multi-hop

The D2D has mutual interference between D2D links and the underlay CC network. How to deal with the interference when relaying data is a challenge.

2.4.1 Exclusion Zone Strategy

In order to limit the mutual interference, a popular approach is to introduce and optimise an exclusion zone, wherein only D2D transmissions can occur while CC UEs are strictly outside the exclusion zone. By controlling the size and location of the exclusion zone through power control, exclusion-zone based partner selection can ensure low outage probabilities for both D2D and CC UEs.

Two analytical upper-bounds for the radius of exclusion zone centred at the receiving D2D UE are presented in [84]. The exclusion zone radius is defined such that up to a certain number of UEs can transmit simultaneously without causing failed reception at the central D2D UE, for all possible combinations of UE locations therein.

In [73], the exclusion zone is defined in terms of the interference-to-signal ratio (ISR) at the D2D receiver in a model that consists of one D2D pair and multiple CC UEs. More specifically, the exclusion zone is defined as a δ_D-interference limited area (ILA), in which cellular UEs could generate an interference level larger than $\delta_D P_{D,R}$ to the D2D receiver, where δ_D and $P_{D,R}$ are the ISR threshold and the received power at the D2D receiver, respectively.

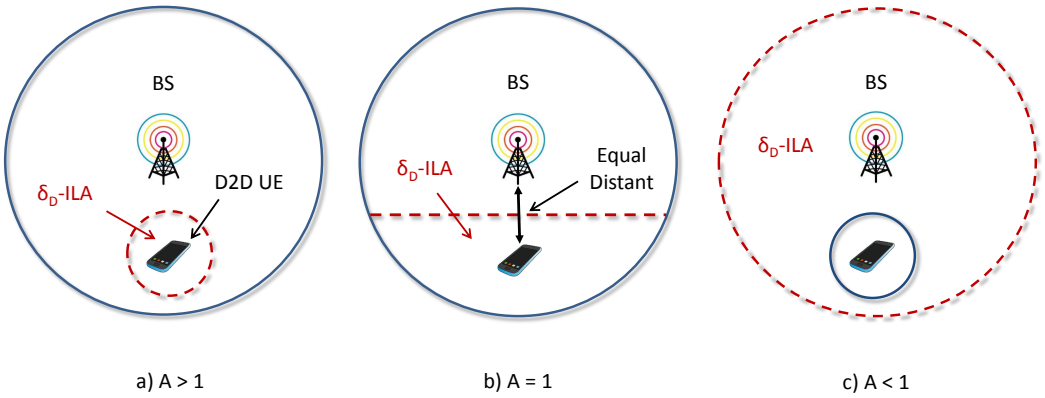

Figure 2.12: D2D to cellular interference regions for different A values.

The authors also proposed a power control scheme to limit the transmit power of D2D UEs so as not to generate any harmful interference to CC links. They focused on reducing the uplink (UL) interference from CC UEs to D2D UEs as they noted that the downlink (DL) interference from BS to D2D UEs can be efficiently managed by transmitting beam forming techniques.

Figure 2.12 illustrates different possible shapes of the δ_D-ILA, where the parameter A is proportional to the transmission power of D2D UEs [73]. If $A > 1$, the δ_D-ILA area is a circular area centred at the D2D receiver. If $A = 1$, it is the smaller region within the coverage area of BS. It is divided into two parts by a chord passing through the midpoint perpendicular to the straight line between the BS and the D2D UE. If $A < 1$, the δ_D-ILA area is the whole cellular coverage area without the region shown in case $A > 1$. We can see that the shape of the δ_D-ILA is not always a circular area centred at the D2D receiver, but depends on the ratio of the transmit power of D2D transmitter and the received power at the BS. This indicates that network optimisation solutions assuming circular small-cell or D2D coverage areas may

lead to inaccurate results.

2.5 Conclusions

In this chapter, the two prominent research challenges have been reviewed: how to avoid collision with unlicensed network (specifically, Wi-Fi network) when D2D communication operated with Unlicensed spectrum, and multi-hop routing algorithms.

In the first part, the collision avoidance of D2D operation on LTE-U spectrum with Wi-Fi system is discussed. Two main coexistence technologies are reviewed: SCAT and ICS. SCAT is based on duty cycle to control the LTE-U signal on and off, and it does not sense the channel before transmitting. However, it gets a possibility of collision due to the lack of sensing before transmission. ICS is similar with the Wi-Fi regulation CSMA, however ICS would not test the channel before transmission.

In the second part, the base line routing algorithm BR is analysed. Because of BR lacking of direction, a definite directivity routing algorithm Geographical wireless multi-hop routing is reviewed, which is based on the physical location information of UEs. For a wireless communication system, QoS is important. FLQ is a algorithm based on a routing table and it is suitable for D2D communication under a certain conditions of QoS(e.g. SINR or traffic volume).

For D2D routing, BS plays a role for assistance D2D proximity discovery and provides location information. However, the CC network (specially the BS) is also a significant interference source to D2D communications. The interference aware D2D routing has also been addressed in this chapter.

Chapter 3

Methodologies for Wireless Network Modelling

3.1 Introduction

Before analyse the D2D performance with the different routing algorithms, the modeling methods for wireless communication systems are reviewed and analysed. There are two main approaches: Monte Carlo simulation [85] and Stochastic Geometry [86].

Monte Carlo simulation is a broad class of computational algorithms that rely on repeated random sampling to obtain numerical results. Their essential idea is using randomness to solve problems that might be deterministic in principle. For the wireless network modelling, the Monte Carlo simulation aims to generate the locations of the BSs and UEs. For each single simulation, a random UE location and a BS location are generated. Based on the locations of UEs and BSs the performance of the network is analysed. A large number of the simulations is used to get the normal or average performance. In this

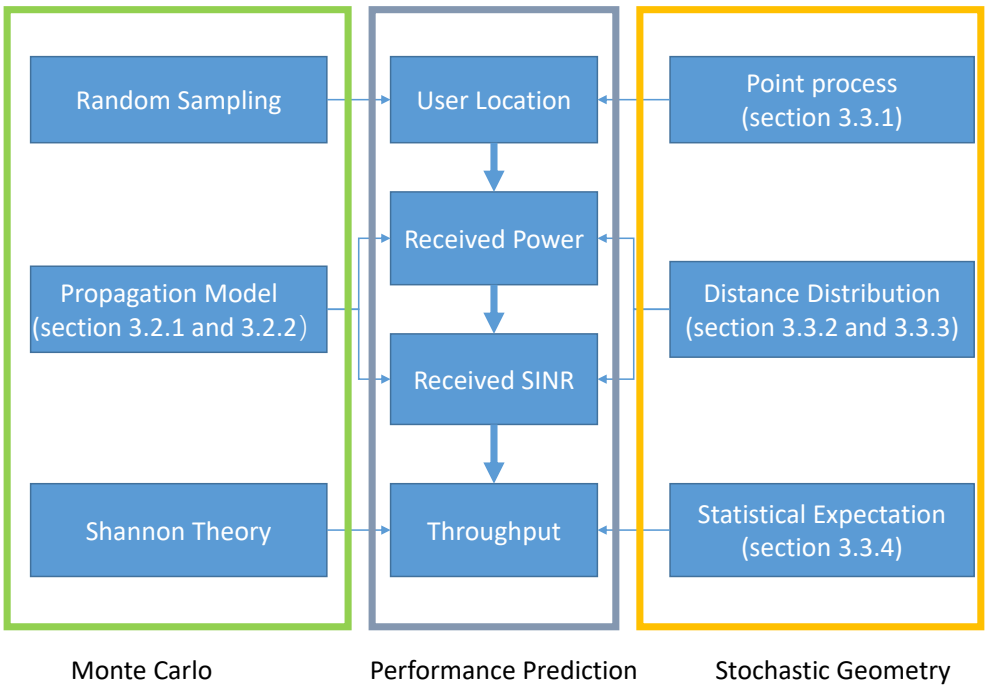

Figure 3.1: A comparison of Monte Carlo simulation and Stochastic Geometry.

thesis, the simulation times for Monte carlo simulation is 100,000.

The Stochastic Geometry uses the point process to generate the nodes locations distribution, then uses the statistical methods to expect the network performance, such as network capacity and success communication probability. A comparison of Monte Carlo simulation and Stochastic Geometry is shown in Figure 3.1.

3.2 Monte Carlo Simulation

Monte Carlo simulation started in the 1940s for the purpose of testing engineering systems subjects to real behaviour [87]. It is a broad class of computational algorithms that rely on repeated random sampling to obtain numerical

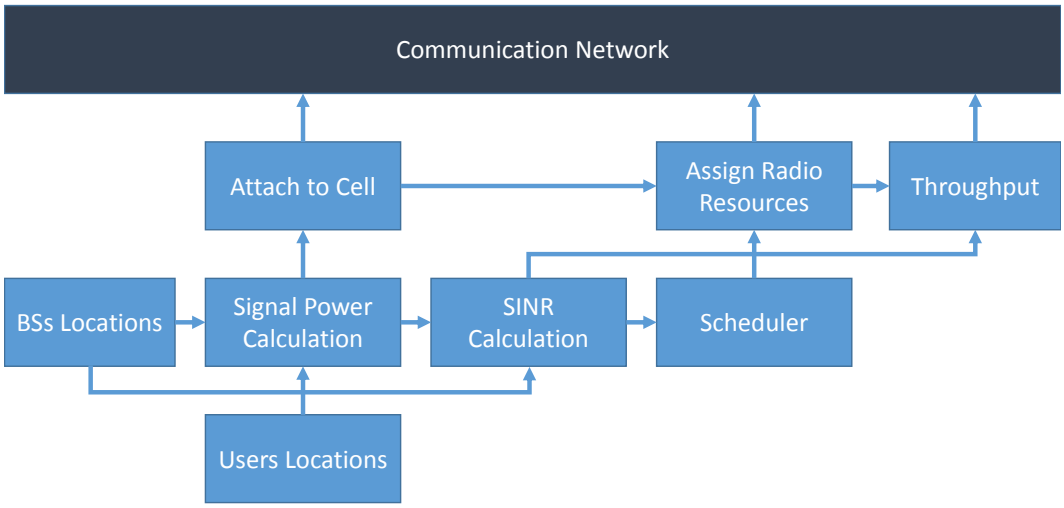

Figure 3.2: A typical Monte Carlo simulation for cellular communication system.

results. When planning a wireless network, design must be proved to work for a wide variety of scenarios that depend mainly on the number of users and their locations [88]. Monte Carlo simulation is typically used to generate these users and their locations. The network performance is then evaluated and optimised.

As Figure 3.2 shows a typical Monte Carlo simulation structure for cellular communication system. The main random variables are: users' locations, BSs locations, network traffic and channel conditions.

By knowing the locations of BSs and UEs, the received signal power and SINR can be calculated using the propagation and pathloss model. The channel throughput highly depends on the receive SINR by using the Shannon capacity theory.

3.2.1 Statistical Pathloss Model

The signal strength of an electromagnetic wave would result from a line-of-sight path through free space, with no obstacles nearby to cause reflection or diffraction, which is defined in "Standard Definitions of Terms for Antennas", IEEE Std 145-1983, as "The loss between two isotropic radiators in free space, expressed as a power ratio." Free-space path loss (FSPL) is proportional to the square of the distance between the transmitter and receiver.

$$PL_{\mathrm{FS}} = \left(\frac{4\pi r f}{c}\right)^2 \tag{3.1}$$

where f is the signal frequency (in Hz), r is the distance from the transmitter (in m), and c is the speed of light in a vacuum.

The statistical Pathloss Model approach includes two components: an estimate of the median path loss and a random component that depends upon the physical features of the local terrain. The measurement of the field strength in various environments is a function of the distance r, and from the transmitter to the receiver motivates a simple propagation model for median path loss having the form:

$$\frac{P_{\mathrm{R}}}{P_{\mathrm{T}}} = \frac{\lambda}{\alpha} \tag{3.2}$$

Where P_{R} is the received power, P_{T} is the transmission power, λ represents a gain that is related to the frequency and antenna gains, and α is the pathloss distance exponent typically rangesfrom 2 to 5 depending on the environment

Table 3.1: Example Path-loss exponents

Environments	α
Free space	2
Flat rural	3
Rolling rural	3
Suburban rural	3.5
Dense urban, skyscrapers	4.5

shown in Table 3.2.1.

3.2.2 Ray Tracing by Wireless InSite

The simulation is based on the software Wireless InSite[1], which is a suite of ray-tracing models and high-fidelity electromagnetic solvers for the analysis of site-specific radio propagation and wireless communication systems. The Shooting and Bouncing Ray method (SBR) is used to find the propagation paths from the transmitters to the receiver points [89], [90]. A dense grid of geometric bouncing optics rays representing the transmission electromagnetic wave is shooting into the propagation medium and follow the rays bounce, reflection off materials, diffraction off materials and penetrate through materials. These rays interact with environmental features (dielectric constant of obstruction material, obstruction size shape and location, location of transmitter and receiver) and make their way to receivers. In this simulation, the maximum number of reflections for each single ray is 30 and the maximum number of diffractions is 5. The SBR for the number of ray paths is more than 2 interactions, image method for Ray paths is within 2 interactions.

However, the Monte Carlo simulation strongly depends on the known UEs or BSs locations for a particular network. If the UEs locations change

[1]http://www.remcom.com/wireless-insite

Table 3.2: Symbol Notation

Symbol	*Definition*	*Parameter*	*Value*
γ	link SINR	Bandwidth	20 MHz
m	source D2D UE	Transmit Frequency	2.1 GHz DL
m'	destination D2D UE	macro-BS Number	19
j	Relay D2D UEs	CC UE Number/BS	120
o	nearest BS	D2D UE Number/BS	150
H	fading gain	Environment	Ottawa City
σ^2	AWGN power	Propagation Model	3GPP UMi [91]
λ	pathloss constant	UE Distribution	PPP
P_{BS}	BS transmission power	ζ	-6 dB
P_{D2D}	D2D transmission power	AWGN Power	-132 dBm
ζ	SINR threshold	BS Antenna Height	45 m
R	max. D2D trans. distance	D2D User Height	1.5 m
$r_{j,j'}$	average hop distance	P_{BS}	40 W
$r_{j,j'}^{\text{SPR}}$	average hop distance for SPR	P_{D2D}	0.1 W
$r_{j,j'}^{\text{IAR}(i)}$	average hop distance for IAR	Λ_{D2D}	400/km^2
$K_{\text{SPR,IAR}}$	number of hops	Wall Loss	20 dB
R_{BS}	BS coverage range	Traffic Model	full buffer
Ψ	Macro-BSs coverage size	Multi-path Fading	Rayleigh
Λ_{D2D}	available D2D density	Fading Variance	6 dB
Λ'_{D2D}	co-frequency D2D density	Macro-BSs coverage	1650 m

or the network structure changes, the simulation model would be changed. Stochastic Geometry is a general analytical model that applies for all cellular networks' realizations. The simulation parameters and symbols are defined in Table 3.2.

3.3 Stochastic Geometry

Stochastic geometry has been used as a tool for modelling wireless networks as early as 1978 [92] in the past ten years, stochastic geometry and associated techniques have been applied and adapted to cellular systems [93, 94], ultra-

wideband [95], cognitive radio [96, 97], femtocells [98], relay networks [99] and other types of wireless systems.

In practice, cellular networks are already deployed and, for a given city, the locations of BSs are already known. However, in the Stochastic Geometry analysis, it is not concerned with the performance of a specific realization of the cellular network at a specific geographical location. Instead, it focuses on a general analytical model that applies on average for all cellular networks' realizations. If it needs to analyse the average capacity in a cellular network, instead of repeating the analysis for each and every geographical setup of the cellular networks, Stochastic Geometry can obtain general performance analysis, guidelines and design insights that apply when averaging over all distinct realizations [86].

For this point of view, the locations of the BSs are considered unknown. Furthermore, following the studies in [100, 101], the locations of the BSs are considered random. Stochastic Geometry models the BS locations by a point process (PP) [102–104], which describes the random spatial patterns formed by points in space. According to the properties of the selected PP, the network performance (such as outage probability and network capacity) is analysed.

3.3.1 Spatial Point Process

A spatial point process is a random pattern of points in a space. Spatial point processes are useful as statistical models in the analysis of observed patterns of points, where the points represent the locations of BSs or UEs.

A one-dimensional point process can be handled as the arrival times $T_1 < T_2 < T_3 < ...$ where T_i is the time at when the i-th point arrives, which

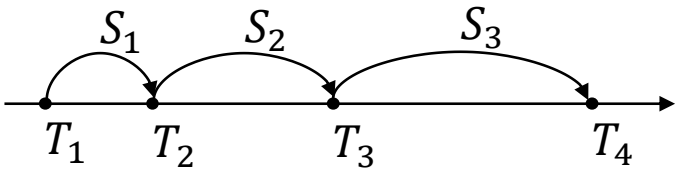

Figure 3.3: A point process in time.

is the random variables and $T_i < T_{i+1}$. The inter-arrival times $S_i = T_{i+1} - T_i$ are independent for the Poisson process as shown in Figure 3.3.

Poisson point process

A spatial point process is a model for a random pattern of points in d-dimensional space, where $D \geq 2$ in this thesis only 2 dimensions is considered. For example, if we make a map of the locations of the number of a group of people; this map constitutes a random pattern of points in two dimensions. There will be a random number of such points, and their locations are also random. A spatial Poisson point process (PPP) is defined as follow.

For any set of Euclidean space $\mathcal{B}$, $\mathcal{B} \subset \mathbb{R}^d$, $\mathbb{R}^d$ is a d-dimensional Euclidean space. $N(\mathcal{B})$ is the number of points in the set $\mathcal{B}$, the number $N(\mathcal{B})$ has a Poisson distribution with the density Λ of a space set of $\mathcal{B}$. Therefor the probability of the number of random points in the set $\mathcal{B}$ is [86]:

$$\mathbb{P}(N(\mathcal{B}) = k) = \exp\left(-\int_{\mathcal{B}} \Lambda(x)\mathrm{d}x\right) \frac{\left(\int_{\mathcal{B}} \Lambda(x)\mathrm{d}x\right)^k}{k!} \tag{3.3}$$

For a 2-D Poisson process, $\int_{\mathcal{B}} \Lambda(x)\mathrm{d}x = A\Lambda$, where A is the area of the 2-D

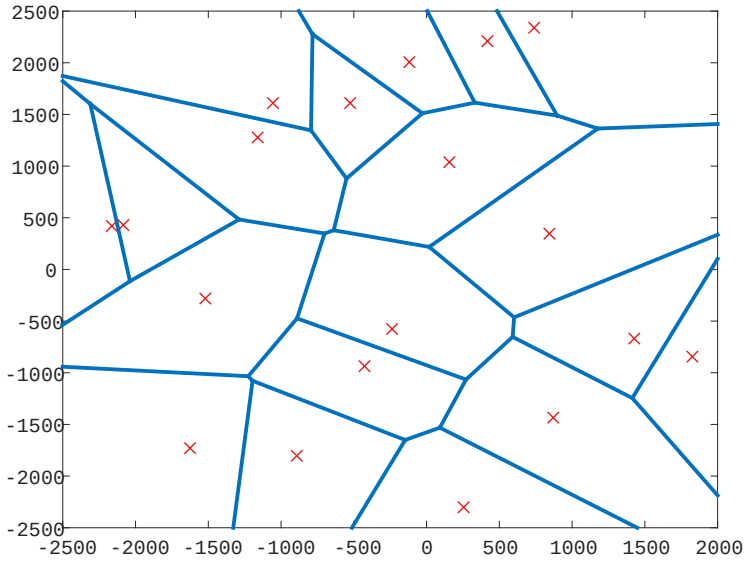

Figure 3.4: Cellular BSs location modeled va PPP.

space $\mathcal{B}$.

So the the probability of the number of random points in the 2-D set $\mathcal{B}$ is,

$$\mathbb{P}(N(\mathcal{B}) = k) = \exp(-\Lambda A)\frac{(\Lambda A)^k}{k!}. \tag{3.4}$$

In Stochastic Geometry model, the location of the BSs are modeled via a PPP. The transmission power of BSs are assumed to be equal, each user associates with the nearest BS, the coverage of the BSs from a Voronoi tessellation [105]. So a line bisecting the distance between each two neighbouring BSs separate their coverage regions. Figure 3.4 shows a PPP modeled cellular network, the blue lines are the boundaries of the BSs coverage, red stars are the locations of BSs.

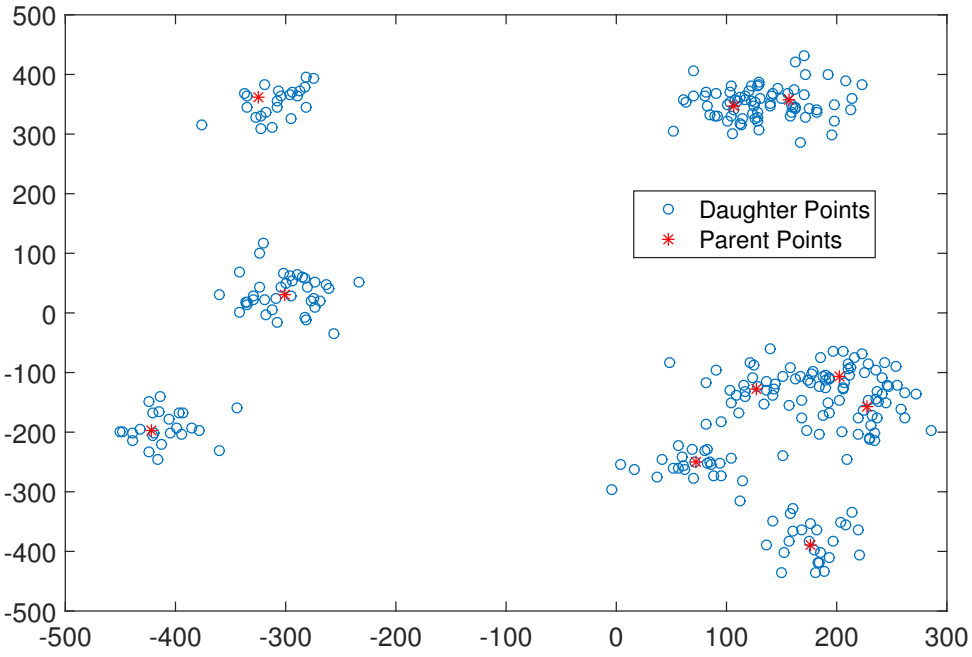

Figure 3.5: A PCP modeled network, the red stars are the parent points (BSs) and the blue circles are the UEs

Poisson Cluster Process

Due to the variation of the capacity demand across the service area (e.g., downtowns, residential areas, parks, sub-urban and rural areas), the BSs will not exactly follow a grid-based model. With independent deployment of small cells (e.g., femto cells, Heterogeneous networks) will have a topological randomness of the network. The Poisson Cluster Process (PCP) is widely used for modelling the heterogeneous networks [106–108] and multi-tier cellular networks [109, 110].

A general PCP is generated by taking a parent PPP and daughter point processes. At first, using PPP to generate the parent points, and then translating the daughter processes to the position of their parent. The cluster process is then the union of all the daughter points. Denote a parent PPP by $\Phi_{\mathrm{P}} = \{x_1, x_2, ...\}$ of with density Λ_{P}. The daughter processes are generated

by another PCP, which applies homogeneous independent clustering to an existing parent process [111]. The daughter clusters are $\mathfrak{N}_{x_i} = \mathfrak{N} + x_i$ for each $x_i \in \Phi_{\mathrm{P}}$ and the random point process $\mathfrak{N}$. The whole process of Φ is: $\Phi = \bigcup_{x \in \Phi_{\mathrm{P}}} \mathfrak{N}_x$. A double PPP is used for generating the PCP distribution. The UEs are scattered on a circle with the radius r_{P} centred at each parent node as shown in Figure 3.5, which is a heterogeneous network generate by PCP.

3.3.2 Distance to the Nearest BS

An important quantity is the distance r separating a typical user from its tagged base station. Since each user communicates with the closest base station, no other base station can be closer than r. In other words, all interfering base stations must be farther than r. The UEs are attached to the closest BS, with a random variable distance R, and from the Eq. (3.4), $k = 0$ so the probability of no BS closer than r is:

$$\mathbb{P}\left[R > r\right] = \mathbb{P}\left[\text{no BS closer than } r\right] = e^{-\Lambda_{\mathrm{BS}} \pi r^2}, \tag{3.5}$$

where Λ_{BS} is the density of BSs.

Therefore, the cumulative distribution function (CDF) of to the closest BS is:

$$F_R(r) = 1 - e^{-\Lambda_{\mathrm{BS}} \pi r^2} \tag{3.6}$$

and the probability density function (pdf) of to the closest BS can be found as

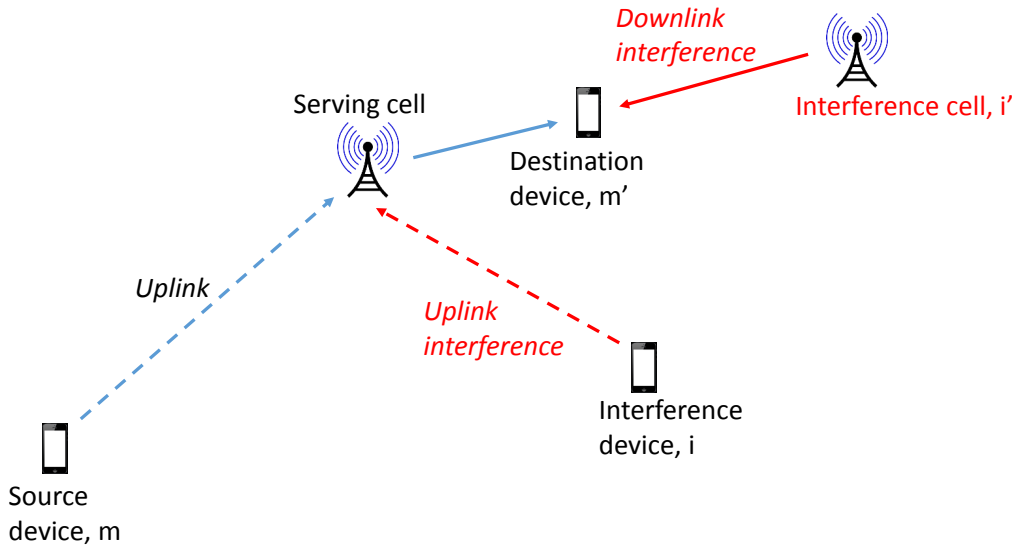

Figure 3.6: CC between two UEs with interference from neighbouring BSs and other UEs

$$f_R(r) = \frac{\mathrm{d}F_R(r)}{\mathrm{d}r} = 2\Lambda_{\mathrm{BS}}\pi r e^{-\Lambda_{\mathrm{BS}}\pi r^2}. \tag{3.7}$$

3.3.3 Signal-to-Interference-plus-Noise Ratio Model

For the CC network, as Figure 3.6 shows the source the UE communicates with the destination UE via the BS. The interference are from the other CC UEs who are sharing the same frequency at the uplink and the neighbouring BSs at the downlink. For the underlaying inband D2D, the D2D UEs can both share the downlink or the uplink channel with the cellular networks.

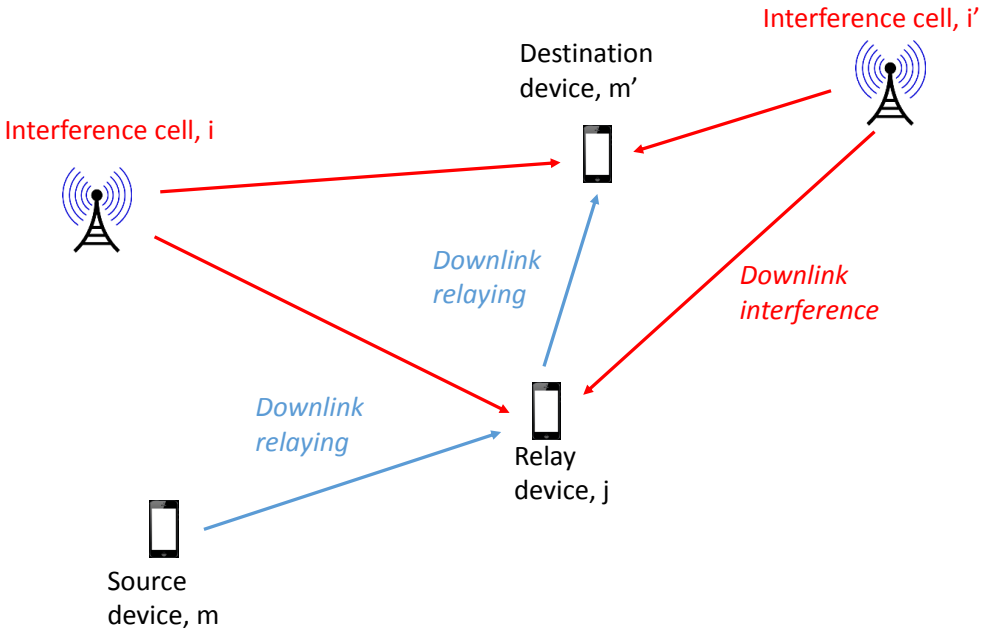

Figure 3.7: D2D downlink communications between two UEs with interference from neighbouring BSs.

SINR for D2D Communication

When the D2D share the cellular DL band, as shown in Figure 3.7, the main interference is from the nearby BSs. In general, the centre of the BS's coverage area is off-limits to D2D transmissions using the cellular DL band due to the high DL interference from the nearby macro-BS. The cell edge is generally off-limits to D2D transmissions using the cellular UL band due to the high UL interference from cell-edge CC UEs transmitting at high power levels.

For the DL D2D communications, the SINR from any D2D UEs j to j' at DL is:

$$\gamma\left(r_{o,j'}\right) = \frac{H_{j,j'} P_{\mathrm{D2D}} \lambda r_{j,j'}^{-\alpha}}{\sigma^2 + I_{\mathrm{BS}}\left(r_{o,j'}\right) + I_{\mathrm{D2D}}}. \tag{3.8}$$

where P_{D2D} is the D2D transmission power, $H_{j,j'}$ is the channel fading between

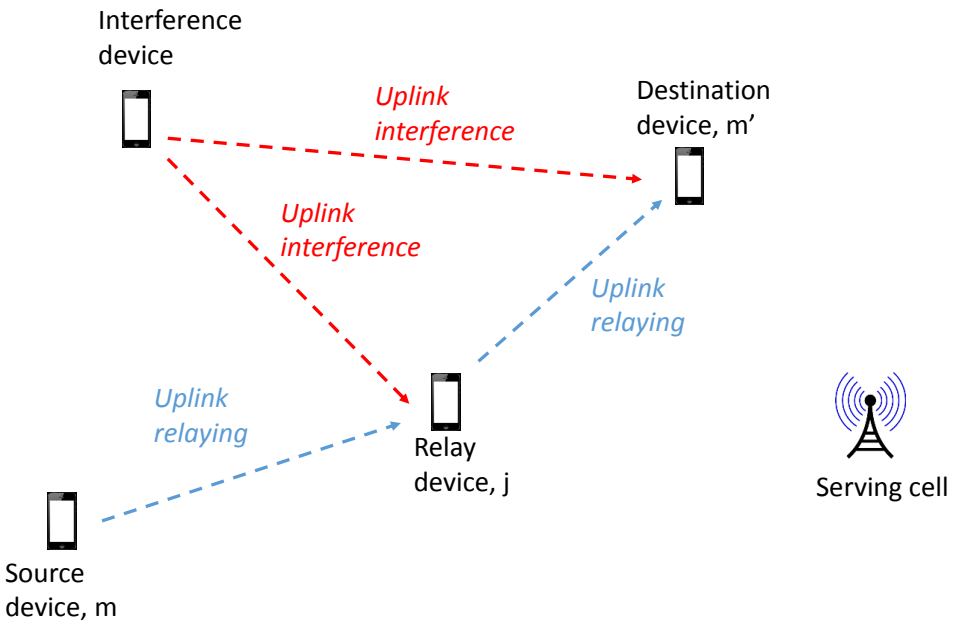

Figure 3.8: D2D uplink communications between two UEs with interference from other UEs.

UE j and UE j', σ^2 is the AWGN power, $r_{o,j'}$ is the distance between the nearest BS and UE j', $r_{j,j'}$ is the distance between UE j and UE j', H is the fading gain, λ is the frequency dependent pathloss constant, and α is the pathloss distance exponent. I_{BS} is the interference from BSs, and I_{D2D} is the interference from co-frequency D2D UEs.

Figure 3.8 shows the D2D is sharing the cellular UL spectrum, the interference to D2D UEs is from the other CC UEs and co-frequency D2D UEs. So the SINR for the UL is:

$$\gamma\left(r_{j,j'}\right) = \frac{H_{j,j'} P_{\mathrm{D2D}} \lambda r_{j,j'}^{-\alpha}}{\sigma^2 + I_{\mathrm{D2D}}}. \tag{3.9}$$

Expectation of BSs Interference

For the DL D2D communication, the interference from BSs is a big challenge to the D2D interference. By managing the interference, we need to know how much the expected interference is. The interference to D2D UEs is from the 1^{st} nearest BS to the Nth nearest BS, which is

$$I = \sum_{i=1}^{N} P_{\text{BS}} \lambda r_i^{-\alpha} \tag{3.10}$$

where P_{BS} is the BS transmission power, λ is pathloss constant and r_i is the distance to the i-th BS.

The average interference power from the second nearest BS to further BS is [112]:

$$I_{\text{BS}}^{2nd-n} = \left[\frac{\pi \Lambda_{\text{BS}} \Xi(r, \Psi, 4)}{2\sqrt{1/P_{\text{BS}}\lambda_{\text{BS}}} \text{erfc}^{-1}(0.5)} \right]^2, \tag{3.11}$$

so the total BS interference is comprised of the interference from the nearest BS that is of distance $r_{o,j'}$ away, and other further BSs.

$$\begin{aligned} I_{\text{BS}} &= \sum_{i=1}^{N} P_{\text{BS}} r_i^{-\alpha} \\ &= P_{\text{BS}} \lambda_{\text{BS}} r^{-\alpha} + \left[\frac{\pi \Lambda_{\text{BS}} (\arctan(\Psi) - \arctan(r_{o,j'}))}{2\sqrt{1/P_{\text{BS}}\lambda_{\text{BS}}} \text{erfc}^{-1}(0.5)} \right]^2. \end{aligned} \tag{3.12}$$

. The parameters for the above equations are as follows: P_{BS} is the transmission power, λ is the frequency dependent pathloss constant, Ψ is the radius of the network coverage area for an accurate BS density Λ_{BS} and α is the pathloss distance exponent.

3.3.4 Network Capacity

AS the Shannon theory defined, the network capacity related to SINR is shown in [113] as:

$$C = B \log_2 (1 + \gamma), \tag{3.13}$$

where B is the channel bandwidth and γ is the received SINR. The expectation of a non-negative continuous random variable X is $\mathbb{E}[X] = \int_{t>0} \mathbb{P}(X > t) \mathrm{d}t$. With the PPP and fading distribution, the expectation capacity for any single UE with the cellular DL is [100]:

$$\begin{aligned} \mathbb{E}(C_i) &= \int_0^{+\infty} \mathbb{P}\left\{ B \log_2 \left[1 + \frac{H_i P_{\mathrm{BS}} \lambda r^{-\alpha}}{\sigma^2 + I_{\mathrm{BS}-i}} \right] > \zeta \right\} \mathrm{d}\zeta \\ &= \int_0^{+\infty} \mathbb{P}\left[H_i > r^{\alpha} \frac{1}{P\lambda} \left(\sigma^2 + I_i\right) \left(2^{\frac{\zeta}{B}} - 1\right) \right] \mathrm{d}\zeta, \end{aligned} \tag{3.14}$$

where H_i is the channel fading from the BS i to receiver UE, P_{BS} is the BS transmission power, B is the bandwidth, and $I_{\mathrm{BS}-i}$ is the interference from the BS i. The multi-path fading is a distribution of $\sim \exp(\beta)$, $f_R(I|r)$ is the joint interference distribution, and where $\beta = 1/P_{\mathrm{BS}}\lambda$. Inserting the fading distribution yields:

$$\begin{aligned} \mathbb{E}(C_i) &= \int_0^{+\infty} \exp\left[-\beta r^{\alpha} \sigma^2 \left(2^{\frac{\zeta}{B}} - 1\right) \right] \int_0^{+\infty} \exp\left[-\beta r^{\alpha} I_i \left(2^{\frac{\zeta}{B}} - 1\right) \right] f_R(I|r) \mathrm{d}I \mathrm{d}\zeta \\ &= \int_0^{+\infty} \exp\left[-\beta r^{\alpha} \sigma^2 \left(2^{\frac{\zeta}{B}} - 1\right) \right] \mathcal{L}\left[-\beta r^{\alpha} \left(2^{\frac{\zeta}{B}} - 1\right) \right] \mathrm{d}\zeta, \end{aligned} \tag{3.15}$$

where $\mathcal{L}$ is the Laplace transform of the interference term I_i:

$$\mathcal{L}(I_i) = \int_0^{+\infty} \exp\left[-\beta r^\alpha \left(2^{\frac{\zeta}{B}} - 1\right) I_i\right] f_R(I|r)\mathrm{d}I, \tag{3.16}$$

which is given by [114]:

$$\mathcal{L}(I_i) = \exp\left[-\Lambda_{\mathrm{BS}} \pi r^2 Q(\zeta, \alpha)\right], \tag{3.17}$$

where the Q function is:

$$\begin{aligned} Q(\zeta, \alpha) &= \int_{2^{\frac{\zeta}{B}}-1}^{+\infty} \frac{\left(2^{\frac{\zeta}{B}} - 1\right)^{\frac{2}{\alpha}}}{1 + u^{\alpha/2}} \mathrm{d}u \\ &= \sqrt{\frac{\zeta}{B} - 1} \arctan\left(\sqrt{\frac{\zeta}{B} - 1}\right) \qquad \text{for } \alpha = 4. \end{aligned} \tag{3.18}$$

The mean rate for the multi-user capacity is:

$$\begin{aligned} \overline{C} &= \int_0^{+\infty} \mathbb{E}\left(C_i\right) f_R(r) dr \\ &= \int_0^{+\infty} e^{-\pi \Lambda_{\mathrm{BS}} r^2} \int_0^{+\infty} \mathbb{P}\left\{B \log_2\left[1 + \frac{H_i P_{\mathrm{BS}} \lambda r^{-\alpha}}{\sigma^2 + I_i}\right] > \zeta\right\} \mathrm{d}\zeta \mathrm{d}r \\ &= \int_0^{+\infty} \int_0^{+\infty} -\Lambda_{\mathrm{BS}} \pi r^2 \exp\left\{-\beta r^\alpha \sigma^2 \left(2^{\frac{\zeta}{B}} - 1\right) - \Lambda_{\mathrm{BS}} \pi r^2 \left[Q(\zeta, \alpha) + 1\right]\right\} \mathrm{d}\zeta \mathrm{d}r. \end{aligned} \tag{3.19}$$

3.4 Conclusion

In this chapter, the modelling methods of wireless communication systems are reviewed. The Monte Carlo simulation started in the 1940s for the purpose of testing engineering systems subjects to real behaviour. It is a broad class of computational algorithms that rely on repeated random sampling to obtain numerical results. The the Monte Carlo simulation is strongly depending on the known UEs or BSs locations for a particular network. By knowing the locations of BSs and UEs, the received signal power and SINR can be calculated using the propagation and path loss model. Furthermore the network capacity can be calculated based on the SINR. Stochastic geometry has been used as a tool for modelling wireless network as well. It focuses on a general analytical model that applies on average for all cellular networks realizations. Stochastic Geometry can obtain general performance analysis, guidelines and design insights that apply when averaging over all distinct realizations. In this chapter, the spatial point process and its fundament are discussed. Then how to catch the nearest BS based on the BSs and UEs locations is analysed, and the network capacity is studied.

Chapter 4

Emergency D2D Route Selection in an Urban Environment

4.1 Introduction

Terrorist attacks generally target dense urban areas to deliver the greatest casualty and the high impact. In the event of such an attack, such as the 9/11 attack in New York City and the 7/7 bombing in London, the wireless communication network becomes overloaded or even shuts down. This is due to the fact that the number of UEs that a BS can serve is limited, and the number of radio resource blocks (RRBs) to support services is also limited. In this chapter, the cellular network is assumed fully loaded with traffic, and a large set of UEs are seeking alternative ways to relay vital data.

D2D communication is a way of allowing UEs to act as relays for each other with the potential integration of public safety applications [115, 116].

The BSs of the cellular network are avoided in terms of data-bearing channels, but may or may not serve as a coordinator or facilitator to D2D channels. D2D channels are treated as emergency data channels [117, 118], whereby the end-to-end outage performance is one of the major priorities for low rate data transfer (i.e., safety messages).

As described in Chapter 2, a major modeling consideration is the mutual interference between the overlay macro-BS tier and the temporarily formed underlay D2D tier, as well as intra-tier interference. One of the unresolved, and must be resolved challenges are, how to efficiently select D2D relay partners in such an interference environment. This is a dynamic problem with many variables such as the location of the source-destination UE pair and the overall network situation. In terms of existing work on multi-hop routes that mitigate interference, one approach used is to introduce and optimise an artificial exclusion zone, where D2D transmissions can occur only inside the zone, and CC transmissions are restricted to outside the zone [119]. The caveat with this approach is that a large number of exclusion zones can severely degrade CC transmission capacity and cause areas of outage.

In this chapter a novel interference-aware routing algorithm is introduced for emergency transmission in urban environments. Several routing algorithms strategies and performances are compared and results for an urban environment with varying UE densities and building materials are presented.

4.2 Experiment Setup

4.2.1 Cellular Network

The system considered is an OFDMA based multiple-access network. It consists of 3 macro BSs located in the city of Ottawa [1]. In this chapter, it is considered that the communications between 2 arbitrary UEs, routing data via: CC channels or D2D channels.

In terms of the traffic load, every BS in the cellular networks experiences a full buffer traffic from CC sources during the aftermath of a terrorist attack. Furthermore, UEs that wish to communicate to each other need to share the DL spectrum and use D2D multiple relaying. Therefore, the dominant issue is the mutual interference from CC and D2D channels in co-existence.

The communication environment is a specifically urban scenario, Ottawa city centre. As analysed in Chapter 3, in this chapter the problem is to analyse the performance in a particular network structure so the Monte Carlo Simulation is selected as the network modelling method.

4.2.2 Urban Propagation Model

D2D Propagation Model

The propagation environment used in this study is a real city centre in Ottawa City in Canada. A 0.92 km $\times$ 0.55 km grid that comprises of approximately 80 buildings of various shapes and dimensions is selected. The 3D city model is shown in Figure 4.1. The UE Path loss models are shown in Figure 4.2. If there is a direct transmission path between transmitter UE and receiver UE

[1]The reasons why Ottawa is selected are: The city of Ottawa layout is regular metric shapes (streets and building); and Ottawa is a typical developed urban environment.

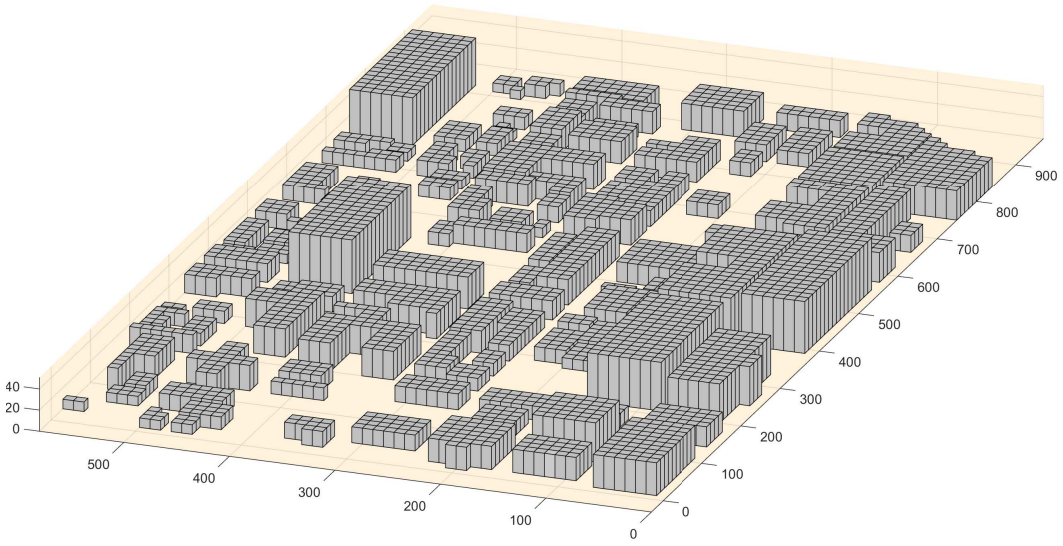

Figure 4.1: 3D building model (m^2) of a section in Ottawa city model.

which is called the Line-of-Sight (LOS) propagation path, the path loss model is [91]:

$$PL_{\text{LOS}}(r) = 22\log_{10}(r) + 28 + 20\log_{10}(f_c). \tag{4.1}$$

where r is the distance between transmitter and receiver, and f_c is the carrier frequency.

If there is no direct transmission path between transmitter UE and receiver UE which is called as the Non-Line-of-Sight (NLOS) propagation path shown in Figure 4.2, the path loss model is [91]:

$$PL_{\text{NLOS}} = \max\left(2.7 + 42.8\log_{10} r, 38.46 + 20\log_{10} r\right) + 0.7r_{\text{indoor}} + nL_w \tag{4.2}$$

where r_{indoor} is the distance of propagation path inside the building, n is the number of the all propagation path through walls and L_w is the propagation path loss of wall.

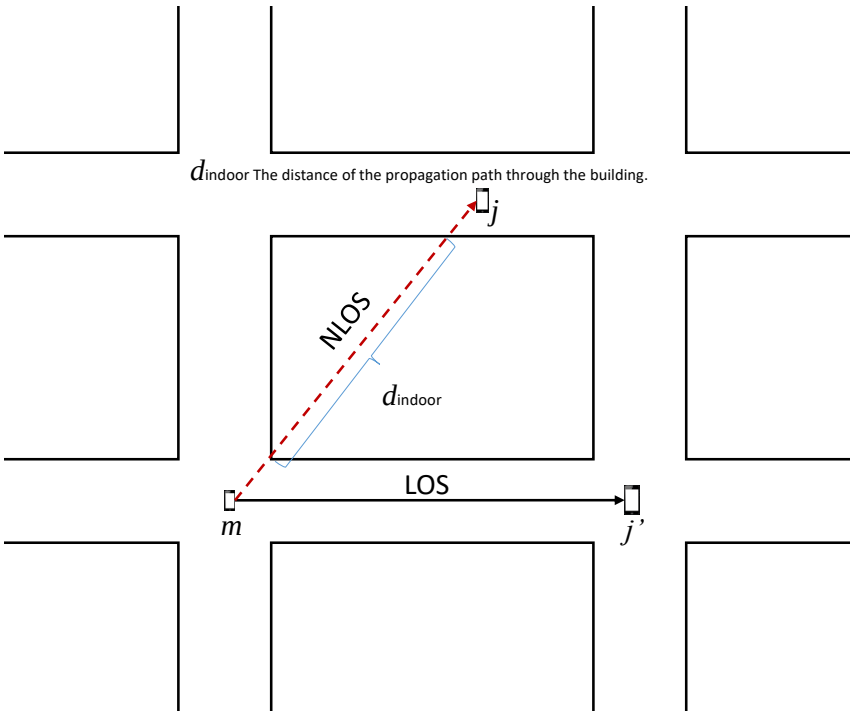

Figure 4.2: UE propagation path loss models in urban environment.

CC Propagation Model

For the interference power from BS, the LOS and NLOS is shown in Figure 4.3. Where h_{BS} is the height of BS, h_{d} is the height of building, r_u is the distance of D2D UE to the highest building between UE and BS, and r_{d-b} is the distance of the highest building between UE and BS to the BS. Path loss model of LOS (which $\frac{r_u}{r_{d-b}} > \frac{h_{\mathrm{d}}}{h_{\mathrm{BS}}}$) is [91]:

$$PL_{\text{BS-LOS}} = 40\log_{10}(r_u + r_{d-b}) + 7.8 - 18\log_{10}(h_{\mathrm{BS}}) - 18\log_{10}(h_{\mathrm{UE}}) + 2\log_{10}(f_c) \tag{4.3}$$

where h_{UE} is the height of UE.

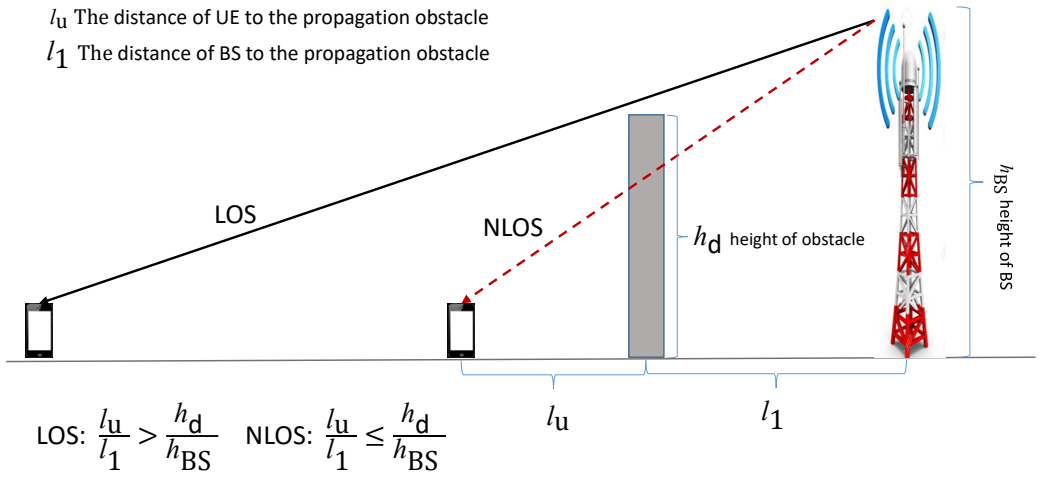

Figure 4.3: BS Path Loss model of LOS and NLOS.

The NLOS path loss model (which $\frac{r_u}{r_{d-b}} \leq \frac{h_d}{h_{BS}}$) is [91]:

$$\begin{aligned} PL_{\text{BS-NLOS}} =& 161.04 - 7.1\log_{10}(W) + 7.5\log_{10}(h) - \left[24.37 - 3.7\left(\frac{h}{h_{\text{BS}}}\right)^2\right]\log_{10}(h_{\text{BS}}) \\ &+ \left[43.2 - 3.1\log_{10}(h_{\text{BS}})\right]\left[\log_{10}(r) - 3\right] + 20\log_{10}(f_c) \\ &- \left[3.2\left(\log_{10}(11.75h_{\text{UE}})^2\right) - 4.97\right]. \end{aligned} \tag{4.4}$$

where h is the average building height and W is the street width.

The minimum SINR required for data flow is -6 dB in the urban environment, the broadcasting threshold is -4 dB, simulation area is 0.51 km^2, street width is 20 m and D2D Source-Destination distance is 250 m to 450 m. A full list of experimental parameters and corresponding values is found in Table 3.2. The assumption is made that all UEs are outdoors in the event of a terrorist attack, but communication signals can go through buildings.

4.3 Outage Probability Definition

4.3.1 CC Outage Probability

This section introduces the concept of the outage probability. Two arbitrary UEs m and m', which have an end-to-end distance of $r_{m,n}$ and $r_{n,m'}$ to their serving BS respectively. The instantaneous SINR of a communication link from m to n is defined in Eq.(3.7):

The minimum SINR for data communication is ζ (-6 dB). The end-to-end outage probability (which is defined that the received SINR falling below ζ) of UE m communicating to UE m' is given as a function of the uplink and downlink outage probabilities:

$$\mathbb{P}_{\mathrm{CC,out}}(m, m') = 1 - \mathbb{P}(\gamma_{m,n} > \zeta)\mathbb{P}(\gamma_{n,m'} > \zeta). \tag{4.5}$$

4.3.2 D2D Outage Probability

For D2D communications, each single hop has to satisfy the SINR requirement. The outage probability for non-cooperative decode-and-forward (DF) relaying is given as a function of the product of the success probability for each link:

$$\mathbb{P}_{\mathrm{D2D,out}} = 1 - \prod_{j=1}^{J} \left[1 - \mathbb{E}\left(\mathbb{P}_{\mathrm{D2D-j,out}}\right)\right] \tag{4.6}$$

where $\mathbb{E}\left(\mathbb{P}_{\mathrm{D2D-j,out}}\right)$ is the probability of a single D2D hop; and the total number of hops J is determined by the density of UEs in the network, the distance between the source and destination UEs and the route selected.

4.4 D2D Routing Strategies

4.4.1 Restricted Broadcast-Routing (RBR) Algorithm

As discussed in Chapter 2, the traditional BR routing causes overload signaling when relay the information. Therefore the traditional BR algorithm would cause a great interference to the CC network. To reduce the interference by reducing the number of relay nodes, a Restricted Broadcast-Routing (RBR) is presented.

Figure 4.4: RBR data frame structure.

In RBR, the source UE m broadcasts its data, and the UEs within the transmission range of sources UE who will to act as relay UEs simply continue to broadcast this data. The step by step algorithm is as follow:

1. The source UE m broadcasts its transmission data, with a frame structure shown in Figure 4.4. It includes the frame ID, destination location information and broadcasting SINR threshold ζ'. The UEs with the received SINR $\zeta < \gamma < \zeta'$ is selected as a broadcasting UE rather than all UEs broadcasting.

2. The D2D UEs broadcasts the data by following the algorithm:

   function RBR($r_{o,j}$, $r_{o,m'}$, r_{CA}, Λ_{BS})

   if Destination UE reached **then** *Broadcasting finished*

   else Not reach the destination UE

For each hop UE j, check the frame ID and γ

if $\zeta < \gamma < \zeta'$ **then**

Broadcasting the data

else $\gamma \geq \zeta'$

Keep quiet

end if

end if

end function

3. When the data reached the destination UE, the destination informs the BS and then BS broadcasts a RBR *stop* signalling to all UEs.

4.4.2 Shortest-Path-Routing (SPR) Algorithm

SPR is a kind of Greedy Forwarding Routing reviewed in Chapter 2 but it is assisted and controlled by BS. The SPR step-by-step D2D algorithm needed to achieve the shortest path routing from a generic UE pair (m to m') operates in the following manner:

1. The source UE m requests communication with a destination UE m' through standard authentication via the Evolved Packet Core (EPC) network. The serving BS allocates D2D authorization for this request and provides the location of destination UE m' to the source UE m, which is used for route selection.

2. If m' is not in single hop range of m, UE m broadcasts a relay request and the request is received by neighbouring UEs in its communication range, which is the maximum distance for which reliable data transmission can

take place. Available UEs will send back an acknowledgement signal to source UE m.

3. UE m receives feedback of the potential relay UEs and sends the data packet to the relay UE j that is the closest to the destination UE m'. The pseudo code is as follows: let Γ_K be the total set of available relay UEs j' at hop sequence $K = \{1, 2, 3, ..., k\}$, k is the hop number and $r_{m,j'} \in L_k$ be the set of distances between the potential forwarding UEs and m'.

   While The communication data has not reached m'

   1 *Calculate distance* L_k *between* Γ_k *and UE* m';

   2 *Find the UE* j' *with distance* $\min L_k$;

   3 *Transmit the data to UE* j' ;

   End While

In the event that the D2D multi-hop process fails, the BS will take over the communications and establish a standard CC link between the last successful relay UE and the destination UE. Whilst D2D transmissions are taking place, the regular CC channels will suffer additional interference.

4.4.3 Interference Aware Routing (IAR) Algorithm

The idea behind IAR is to reduce the CC interference to the D2D UEs received in the DL band. This is intuitively achieved if the D2D routing process occurs along the BS's cell boundary, where the distance to adjacent BSs is maximised and the aggregate interference to adjacent BSs is minimised. The IAR path has 3 distinct stages (Figure 4.5):

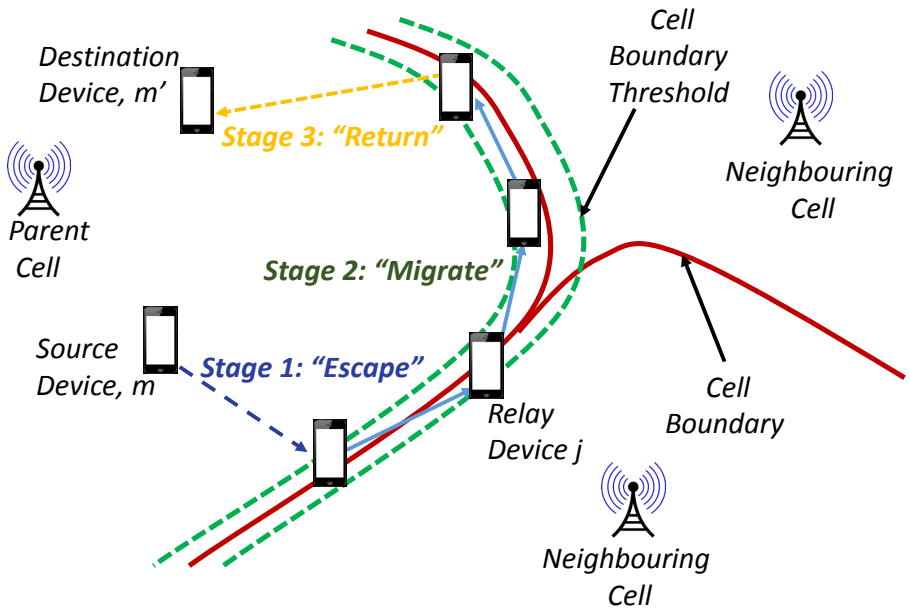

Figure 4.5: Interference-Aware-Routing (IAR): 3-Stage Process

- *Stage 1 (Escape to Cell Boundary):* from source UE m to closest boundary UE j;
- *Stage 2 (Migrate along Cell Boundary):* from boundary UE closest to the source to a boundary UE closest to the destination;
- *Stage 3 (Return from Cell Boundary):* from the boundary UE closest to the destination to the destination UE m'.

Each stage of the IAR actually utilizes the SPR algorithm. Clearly the route is longer than the SPR path, but the advantages are that the interference from CC UEs can be reduced significantly due to the increased distance from the parent-BS.

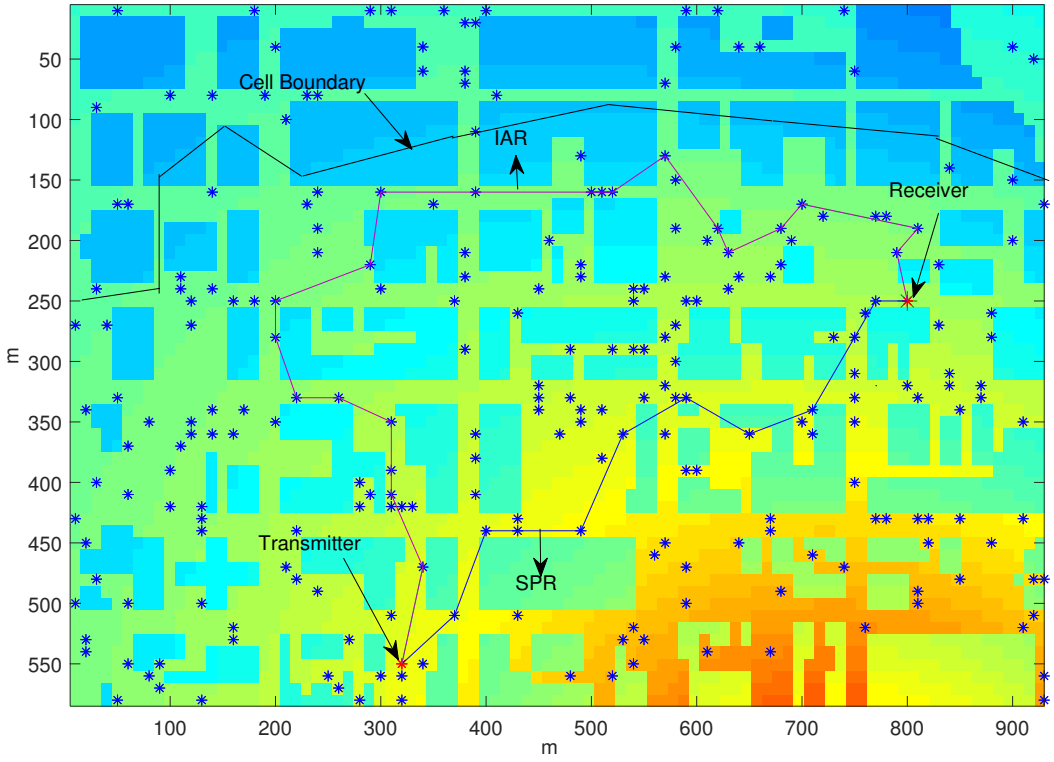

Figure 4.6: Simulated D2D Routing Paths in Ottawa city between Transmitter UE and Receiver UE for Shortest-Path-Routing (SPR) and Interference-Aware-Routing (IAR). The diagram is under-laid with the interference power received at each location. Stars represent outdoor UE positions.

4.5 Results and Analysis

This chapter first examined the feasibility of D2D routing when the BS is fully loaded. In Figure 4.6, the simulation results show the simulated end-to-end D2D routing paths between an arbitrary transmitter UE and receiver UE for both SPR and IAR in Ottawa city. The D2D communication propagation is shown in Eq.(4.1) and Eq.(4.2) for LOS and NLOS respectively. The propagation between BS and D2D is shown in Eq.(4.3) and Eq.(4.4).

Figure 4.6 also shows the DL received SINR of CC links in the Ottawa city centre. The first observation is that the IAR path (1278 m) is approxi-

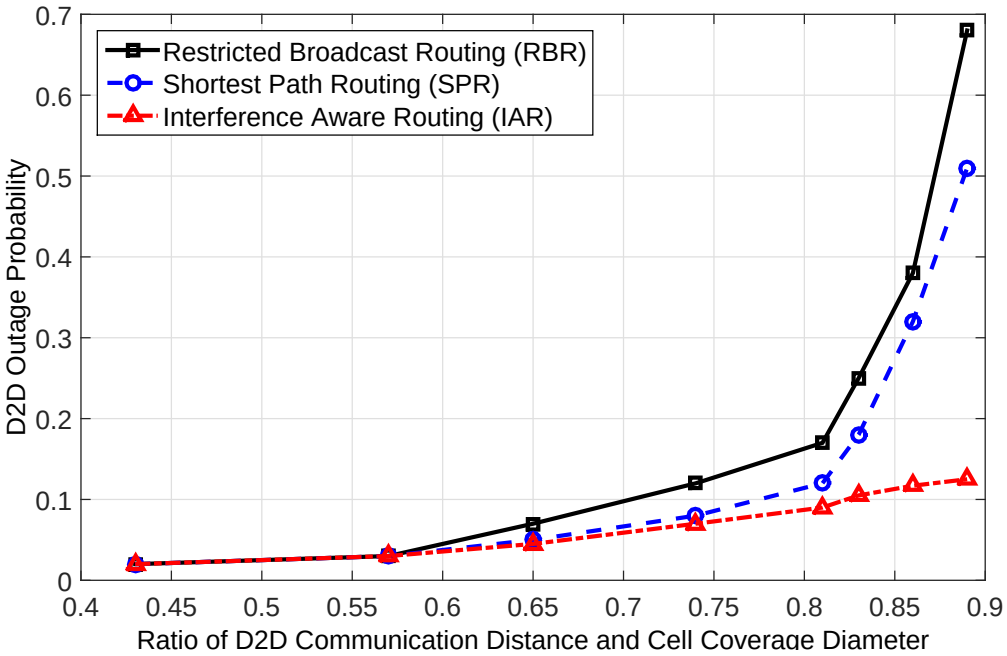

Figure 4.7: D2D outage probability as a function of the ratio between D2D distance and cell coverage diameter.

mately 35% longer tothan the SPR path (921 m) in this particular case. So the IAR would suffer a longer delay than SPR. Consequently, for time-sensitive communication SPR is a better choice than IAR.

However, the IAR path mostly travels in the low interference power regions (green to light blue), whereas the SPR path travels in the high interference power regions (yellow). Therefore, the interference from BS to the IAR D2D UEs is lower than the SPR case. Therefore, the IAR has a higher network throughput than the SPR.

4.5.1 D2D Routing Distance

Figure 4.7 compares the outage probability of the three routing algorithms for different D2D communication distances: SPR, RBR, and IAR. The parameters setting are all using DL bands, and with the UE density is 400/km^2 (The

population density in New York city at 2010 is 10,431.1 per km^2) and wall path loss is 5 dB. It is found that for small D2D communication distances, both SPR and RBR achieve lower outage probabilities than IAR. This is intuitive as the IAR routing algorithm stipulates that even when communicating short distances, the route must escape to the cell edge and return. The increase in route distance is likely to be several folds higher than the SPR and RBR cases.

Whilst RBR achieves a slightly better performance of outage probability than SPR in Figure 4.7 when the D2D communication distance is shorter than 125 m, the interference it causes to CC UEs is more significant as more transmissions are required. For D2D communication distances that are significantly greater than the cell radius, there is a high probability that the RBR and SPR paths will pass near the BS. This will cause significant interference between CC links (via the BS) and D2D links. The IAR mechanism allows the routing to avoid the BS' site location and maximise the mutual distance between the D2D multi-hop path and the BS. This reduction in mutual interference leads to an improved overall performance, despite increasing the overall hop length.

4.5.2 D2D User Density

For addressing the effect of user density to the success probability, an assumption is made that only a pair of D2D or CC UEs is considered. By reducing the interference of other parameters, the distance ratio of m and m' is 0.7 and wall path loss is 5 dB. If those parameters change the results may not be exactly the same but the tendency is the same. Figure 4.8 shows the D2D routing success probability as a function of D2D UE density, varying from 0

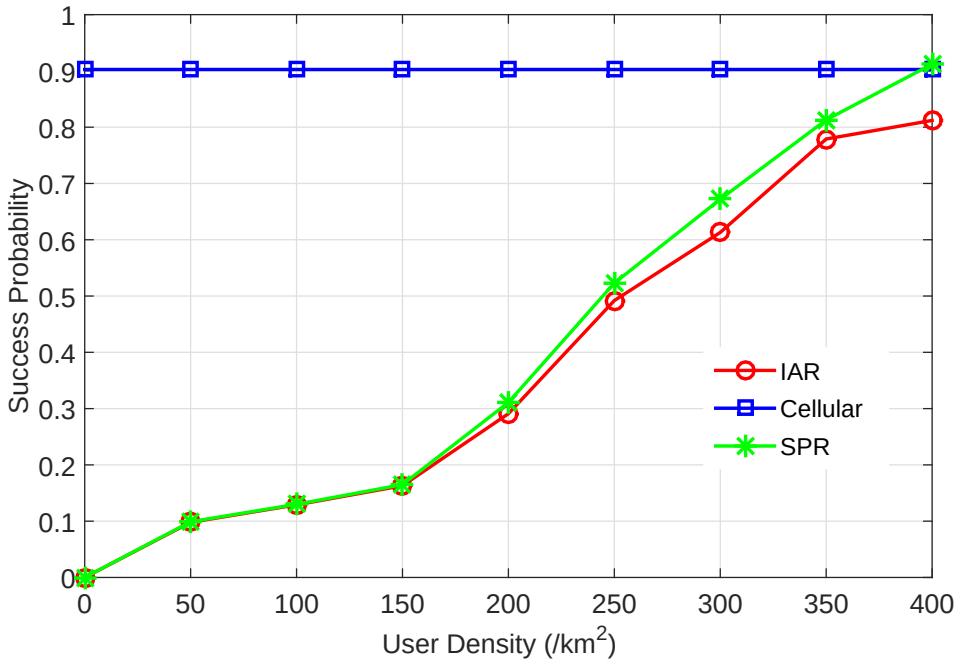

Figure 4.8: D2D routing success probability as a function of D2D UE density.

to 400 UEs per square km. The success probability rises to over 80% when the UE density is over 400/km^2 and the results for IAR and SPR are remarkably similar. That is to say, IAR is just as effective as SPR, whilst minimizing interference to CC UEs in the centre regions of the cell's coverage area.

4.5.3 Wall Penetration Loss

Figure 4.9 shows the D2D routing success probability as a function of the building outer wall penetration loss (dB), varying from 5 to 30 dB. The success probability falls to below 50% when the building outer wall penetration loss is at 30 dB (thick wall). The IAR outage probability performs are consistently better than SPR for this set of results by up to 10%. Therefore, D2D is possible under certain environmental and user density scenarios. More specifically, when the co-network UE density is over 400/km^2 and when the walls in the

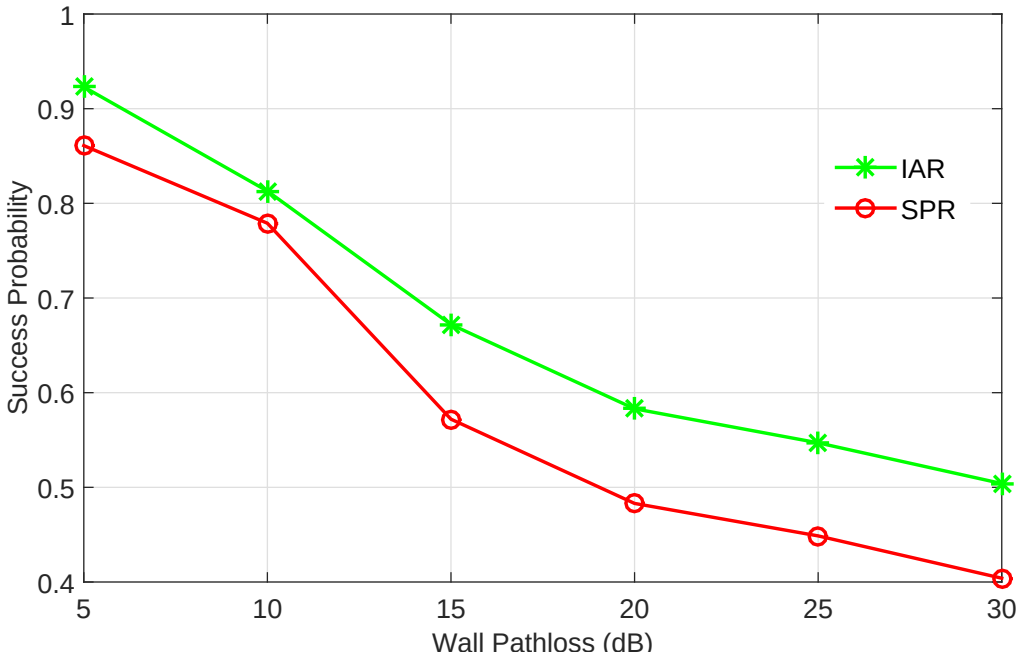

Figure 4.9: D2D routing success probability as a function of building outer wall penetration loss (dB).

city are not very thick (wall loss is less than 10 dB), D2D communication gets a good performance. One of the key advantages of IAR routing over SPR routing is that it reduces the interference to regular CC UEs. By picking a routing path that travels predominantly along the traditional cell-edge, it maximizes the distance to the majority of CC UEs.

4.5.4 CC Performance Constraint with D2D

When the D2D UEs share the spectrum with CC, CC UEs would suffer interference from D2D UEs. Figure 4.10 shows the CC success probability with various number of D2D active UEs pairs. In those results only one CC pair is considered. The results show that the increasing number of active D2D UEs are reducing the CC success probability. Specially for RBR when there are

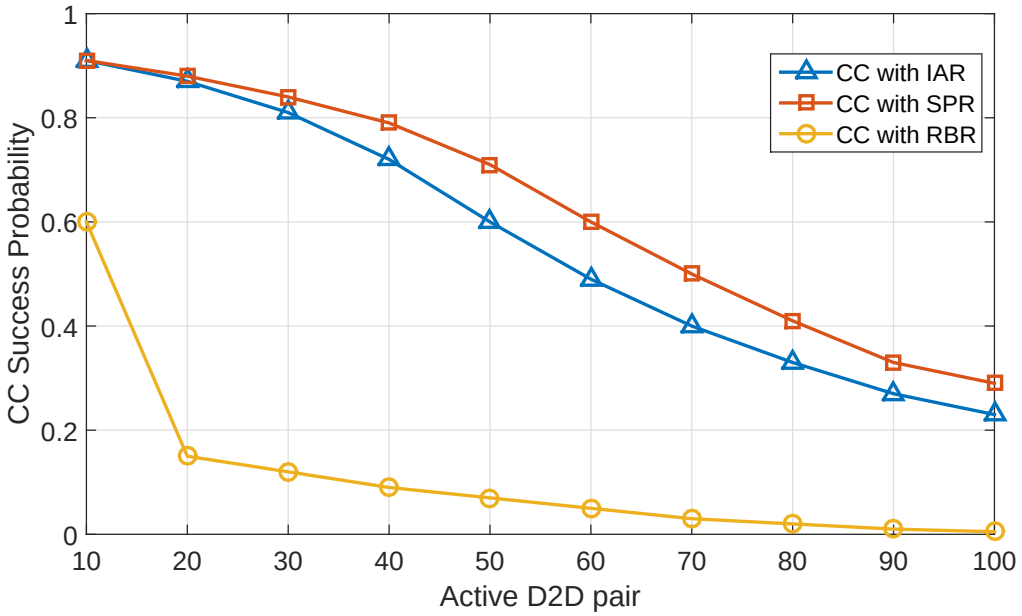

Figure 4.10: The CC success probability with different number of D2D active UEs pairs.

10 active pairs of D2D UEs, the success probability decrease to 0.6 and it is under 0.1 when the active number is bigger than 40. The similar trend of CC success probability is also shown for IAR and SPR.

There is trade-off in success probability between CC and active D2D UEs number. For a stringent CC success probability constraint, D2D transmission is not permitted. As the CC constraint gets relaxed, the D2D routing methods change between RBR, IAR and SPR, and the active number varies from 10 to 50. More specifically, the results show that for:

- CC success probability $> 95\%$: no D2D is permitted;
- CC success probability $> 80\%$: D2D using IAR or SPR with maximum active number 30;
- CC success probability $> 75\%$: D2D using IAR or SPR with maximum

active number 40;

- CC success probability $>$ 40%: D2D using RBR, SPR or IAR with maximum active number 10;

4.6 Conclusions

In this chapter, the communication scenario is that a terrorist attack is in a real city and that the cellular network is congested. Emergency D2D communication needs to co-exist with CC communication. The results shows that in such a co-existence and mutually interfering scenario, IAR is superior to the intuitive SPR and broadcasting algorithms, if the overall transmission range is over 80% of a cell's coverage diameter. Otherwise, for short distance D2D communications, the SPR and RBR algorithms perform better. In terms of D2D feasibility, the results show that the D2D emergency channel can achieve up to a high success communication probability of 91% when the user density is high (400 available users per square km), but can drop to 50% when the user density falls or when the building's wall penetration loss is relatively high (30 dB). Therefore, there is significant challenges related to whether D2D communications in urban areas are feasible in the event of an emergency that overloads the cellular network. In general, there is a fundamental trade-off between active D2D UEs number and CC success probability performances, due to their mutual interference. For different CC outage constraints and D2D distances, the results shows how different D2D routing strategies should be selected.

Chapter 5

Multi-Hop Path Selection in a Cellular Interference Environment

5.1 Introduction

In Chapter 4, the simulation results show that SPR and IAR can get over 85% success probability. The mathematic fundament of success probability of SPR and IAR and general performance of network performance analysis are presented in this chapter.

This chapter hypothesizes and goes on to prove that a longer multi-hop route (IAR), one that minimizes mutual interference, in some certain circumstances, it is more beneficial than a greedy SPR scheme. This chapter attempts (1)provide a stochastic geometry theoretical framework to generalize the performance comparison mathematically, (2) provide geometric boundaries that define the spatial operational envelopes for different D2D routing algorithms

and CC transmissions and (3) analyse the DL co-channel performance. Furthermore, the capacity analysis for each routing algorithm is addressed and the total volume of the offloaded traffic.

5.2 System Setup

. This chapter aims to get a general performance of different routing algorithms. As analysed in Chapter 3, Stochastic Geometry is suitable to model the communication network.

5.2.1 Spectrum Allocation

The underlaying D2D allocation can enhance the spectrum efficiency but has to manage the cross-tier interference. For inband underlay spectrum, both the up-link (UL) and DL bands for co-channel D2D communications have their advantages and caveats [35]. In general, the centre of the BS's coverage area is off-limits to D2D transmissions using the cellular DL band due to the high DL interference from the nearby macro-BS. The cell edge is generally off-limits to D2D transmissions using the cellular UL band due to the high UL interference from cell-edge CC UEs transmitting at high power levels.

5.2.2 D2D UEs Distribution

The multi-hop communication between two arbitrarily located UEs within the coverage area of a BS is considered. In the current analysis of a large random wireless network, the UE's location distribution is assumed to be the Poisson point process (PPP). For example, in [120] the authors assumed the

UE location as a PPP for the transmission capacity of a wireless network. The tutorial [121] is about the stochastic geometry for modeling analysis, and design of the wireless networks, PPP is also one of the methods for the UE location distribution. The similar work is addressed in [122, 123], PPP is one of the tools for generating the UE locations as well. In this chapter, the D2D UEs are distributed as the PPP with density Λ_{D2D}, and BSs are distributed as the PPP with density Λ_{BS}. The system parameters are shown in Table 3.2.

5.3 Routing Strategies

In this chapter, two routing algorithms are addressed, SPR and IAR. Figure 5.1 illustrates the SPR algorithm between m and m', where the solid line (in blue) shows the D2D multi-hop path, which can be approximately modelled by a straight line. θ is the angle of the straight line between m, o, m', which is $\angle mom'$.

Figure 5.4 shows a D2D UEs, its maximum coverage range R, and how it selects a new relay UE j to forward the message to. The selection of D2D relay UE is dynamic and real-time, when the UE finished the relaying it would be released from the D2D communication link. Furthermore, the relay UE can modify the routing path according the periodically signal from the BS. The average D2D communication duration is less than 0.5 s by research in [124], so the movement of the UE cannot cause the routing algorithm operation switch.

Each individual stage of the IAR algorithm will use the SPR scheme. If there are no D2D UEs that satisfies the condition of IAR, the routing will switch to the previously mentioned SPR scheme. In most cases, the IAR algorithm increases the path length significantly in comparison to the SPR

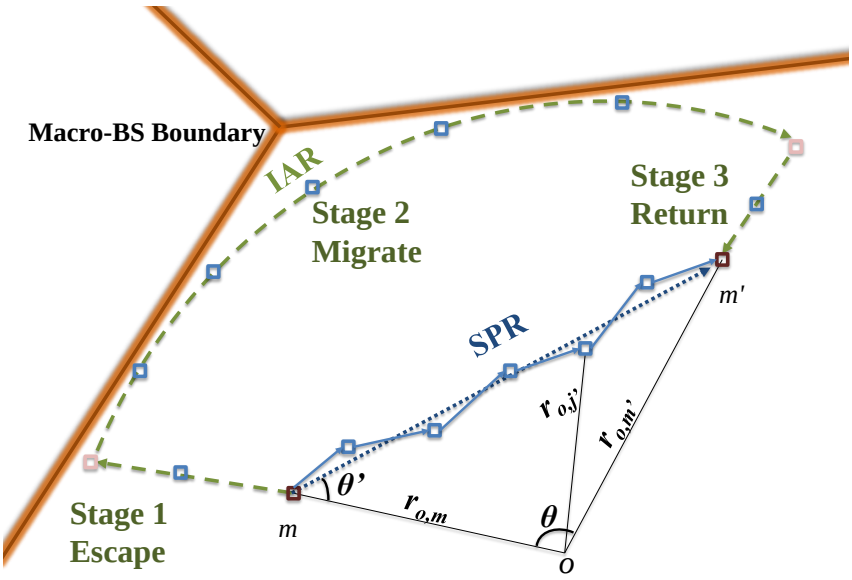

Figure 5.1: D2D multi-hop communications from m to m' under SPR or IAR algorithms.

algorithm, but the advantage is that the interference from the BS can be reduced significantly due to the increased average distance from the nearest BS.

5.4 Success Probability of D2D Multi-hop Communication

The performance metrics associated with D2D are primarily related to success probability, as the data is usually for services that demand a low rate and can tolerate a high latency. This is therefore the main focus of this chapter. The success probability of D2D multi-hop communication is defined as the probability of receiving the data bearing signal at the receiver with the SINR greater than a data communication threshold ζ at each of the multi-hop stages.

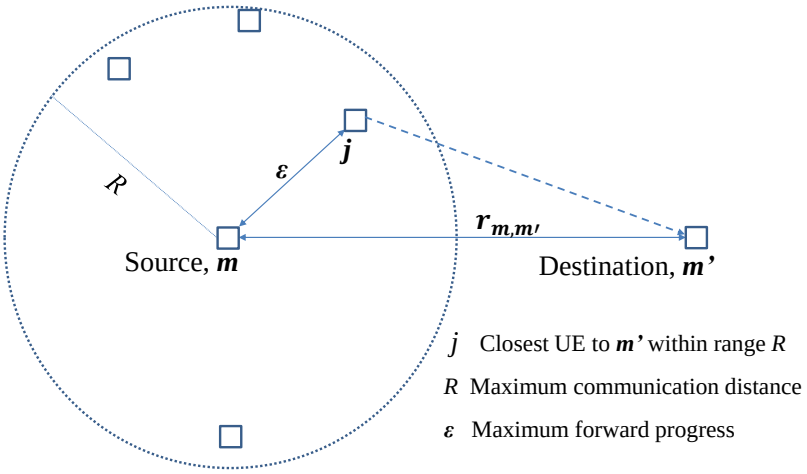

Figure 5.2: D2D UEs coverage boundary and maximum potential forwarding distance for each single hop.

Particularly in this charter, the SINR at a receiver UE j', which is one of the many relay UEs in the D2D multi-hop link. The aggregated interference power at a receiver arises from two sources: (1) co-frequency D2D transmissions in the same BSs; (2) the transmission on CC links from all the BSs. Therefore, for a relay UE that is of distance $r_{o,j'}$ from the nearest BS, the received SINR γ between any D2D relay j and j' is:

$$\gamma\left(r_{o,j'}\right) = \frac{H_{j,j'} P_{\mathrm{D2D}} \lambda_{\mathrm{D2D}} r_{j,j'}^{-\alpha}}{\sigma^2 + I_{\mathrm{BS}}(r_{o,j'}) + \sum\limits_{\substack{i \in \Phi \\ i \neq j}} H_{i,j'} P_{\mathrm{D2D}} \lambda_{\mathrm{D2D}} r_{i,j'}^{-\alpha}}, \tag{5.1}$$

where $I_{\mathrm{BS}}(r_{o,j'})$ is the total interference from all BSs shown in Eq. (3.12). Typically, the aggregate interference power is significantly higher than the additive noise power σ^2, and one can be assumed that the noise power is negligible.

5.4.1 Average Hop Distance

Maximum Transmission Distance

In order to characterize the success probability performance of the SPR and IAR algorithms, it is necessary to determine the average hop distance of each scheme first. As shown in Figure 5.4, each UE is capable of transmitting a signal of up to an average range R, which covers an area $A = \pi R^2$. The averaged is defined by ignoring instantaneous effects of UE movement and channel fading. For each hop, the D2D UE within the range R closest to the destination is selected as a relay UE for the next hop, the hop distance is ε. For the QoS requirement of the data communication, the minimum SINR required is ζ. The maximum transmission distance is that the SINR of the D2D receiver is bigger than the SINR threshold ζ.

$$\arg\max \left\{ \frac{H_{j,j'} P_{\mathrm{D2D}} \lambda_{\mathrm{D2D}} [R(r_{o,j'})]^{-\alpha}}{W + I_{\mathrm{BS}}(r_{o,j'}) + \sum\limits_{\substack{i \in \Phi \\ i \neq j}} H_{i,j'} P_{\mathrm{D2D}} \lambda_{\mathrm{D2D}} r_{i,j'}^{-\alpha}} \geq \zeta \right\}, \tag{5.2}$$

where the $I_{\mathrm{BS}}(r_{o,j'})$ is shown in Eq. (3.12). Without considering instantaneous fading effects, the R is:

$$R(r_{o,j'}) = \frac{\zeta^{-1/\alpha} \left(H_{j,j'} P_{\mathrm{D2D}} \lambda_{\mathrm{D2D}} \right)^{1/\alpha}}{\left(H_{j,j'} P_{\mathrm{D2D}} \lambda_{\mathrm{D2D}} \right)^{-1/\alpha}} \left(I_{\mathrm{BS}}(r_{o,j'}) + \sum_{\substack{i \in \Phi \\ i \neq j}} H_{i,j'} P_{\mathrm{D2D}} \lambda_{\mathrm{D2D}} r_{i,j'}^{-\alpha} \right)^{-1/\alpha} \tag{5.3}$$

Therefore, using Eq. ((5.1)) to find the maximum value of $r_{j,j'}$ under the condition of $\gamma(r_{o,j'}) \geq \zeta$,the maximum of D2D transmission distance for a

single hop is:

$$R = \arg\max \left\{ r_{j,j'} | \gamma(r_{o,j'}) \geq \zeta \right\} = \left[\xi \frac{I_{\mathrm{BS}}(r_{o,j'})}{P_{\mathrm{D2D}} \lambda_{\mathrm{D2D}}} + \zeta \sum_{\substack{i \in \Phi \\ i \neq j}} r_{i,j'}^{-\alpha} \right]^{-1/\alpha} \tag{5.4}$$

Average Hop Distance for Single Hop

Given the maximum hop distance, then the average hop distance can be found. As mentioned before, the assumption was made that the D2D UEs are randomly and uniformly distributed. Let the Euclidean distance between source UE m and destination UE m' be $r_{m,m'}$. The probability density function (PDF) of the maximum single hop distance ε presented as Eq. (5.5) is given by [125]:

$$f_{\epsilon, r_{m,m'}}(\varepsilon) = \begin{cases} \sum_{n=0}^{\infty} G(n) 2n (r_{m,m'} - \varepsilon) \arccos(1 + \frac{\varepsilon^2 - R^2}{2r_{m,m'} - (r_{m,m'} - \varepsilon)}) \\ \quad \times \left[\frac{1}{2} \sqrt{4R^2 r_{m,m'}^2 - (R^2 - \varepsilon^2 + 2r_{m,m'}\varepsilon)^2} \right. \\ \quad -(r_{m,m'} - \varepsilon)^2 \arccos(1 + \frac{\varepsilon^2 - R^2}{2r_{m,m'} - (r_{m,m'} - \varepsilon)}) \\ \quad \left. + R^2 \arcsin(\frac{R^2 - \varepsilon^2 + 2r_{m,m'}\varepsilon}{2lR}) \right]^{n-1} & 0 \leqslant \varepsilon \leqslant R \\ \\ 0 & \text{elsewhere,} \end{cases} \tag{5.5}$$

There is an assumption that there are minor interference differences in the D2D relay UEs at different locations because the interference in the DL channel is from a BS, the resulting interference differences in a small spatial circle are small. The mean hop distance for each single hop under these

assumptions is therefore:

$$r_{j,j'} = \mathbb{E}[\varepsilon] = \int_0^{R(r_{o,j'})} \varepsilon f_{\varepsilon, r_{m,m'}}(\varepsilon) \mathrm{d}\varepsilon, \tag{5.6}$$

subject to the maximum hop distance R constraint given by Eq. (5.4).

5.4.2 Success Probability for Single Hop D2D

The assumption is made that the interference distances are always greater than the D2D transmission distance. This is reasonable given that the distance to the BS is farther compared the distance of a D2D hop, and that interference D2D UEs are located in neighbouring BSs. Success probability of any single D2D hop is $\mathbb{P}[\text{SINR} > \zeta]$. Defining $g_{j,j'} = H_{j,j'} P_{\text{D2D}} \lambda_{\text{D2D}}$ and $I_{\text{D2D}}\left(r_{i,j'}, H_{i,j}\right) = \sum_{\substack{i \in \Phi \\ i \neq j}} H_{i,j'} P_{\text{D2D}} \lambda_{\text{D2D}} r_{i,j'}^{-\alpha}$, the probability is:

$$\begin{aligned} \mathbb{P}_{\text{Success}} &= \mathbb{P}\left[\frac{g_{j,j'} r_{j,j'}^{-\alpha}}{I_{\text{BS}}(r_{o,j'}) + I_{\text{D2D}}\left(r_{i,j'}, H_{i,j}\right)} > \zeta\right] \\ &= \mathbb{P}\left[g_{j,j'} > r_{j,j'}^{\alpha}\left(I_{\text{BS}}(r_{o,j'}) + I_{\text{D2D}}\left(r_{i,j'}, H_{i,j}\right)\right)\right] \\ &= \int_0^{+\infty} \int_{\xi}^{+\infty} f_G(g) f_R(I_{D2D}|r_{i,j}) \mathrm{d}g \mathrm{d}I_{D2D}, \end{aligned} \tag{5.7}$$

where $\xi = r_{j,j'}^{\alpha}\left(I_{\text{BS}}(r_{o,j'}) + I_{\text{D2D}}\left(r_{i,j'}, H_{i,j}\right)\right)$. The multipath fading has a PDF of $f_G(g) \sim \exp(\beta)$ where $\beta_{\text{D2D}} = 1/P_{\text{D2D}}\lambda_{\text{D2D}}$ and $f_R(I_{D2D}|r_{i,j})$ is the

joint interference distribution. Applying the fading distribution:

$$\begin{aligned}\mathbb{P}_{\text{Success}} &= \exp\left[-\beta_{\text{D2D}} r_{j,j'}^{\alpha} I_{\text{BS}}(r_{o,j'})\right] \int_0^{+\infty} f_R(I_{D2D}|r_{i,j}) e^{-\beta_{\text{D2D}} r_{i,j'}^{\alpha} I_{\text{D2D}}\left(r_{i,j'}, H_{i,j}\right)} \mathrm{d}I_{\text{D2D}} \\ &= \exp\left[-\beta_{\text{D2D}} r_{j,j'}^{\alpha} I_{\text{BS}}(r_{o,j'})\right] \mathcal{L}\left(\beta_{\text{D2D}} r_{i,j'}^{\alpha}\right),\end{aligned} \tag{5.8}$$

where $\mathcal{L}()$ is the Laplace transform of the interference term I_{D2D}.

The Laplace transform of the interference signal power by D2D UEs is:

$$\begin{aligned}\mathcal{L}\left(\beta_{\text{D2D}} r_{i,j'}^{\alpha}\right) &= \int_{r_{i,j'}}^{+\infty} \int_0^{+\infty} \exp\left(-\sum_{\substack{i\in\Phi \\ i\neq j}} \beta_{\text{D2D}} r^{\alpha} g_i r_{i,j'}^{-\alpha}\right) f_G(g_i) f_R(r_{i,j'}) \mathrm{d}g_i \mathrm{d}r_{i,j'} \\ &= \int_{r_{i,j'}}^{+\infty} \int_0^{+\infty} \prod_{\substack{i\in\Phi \\ i\neq j}} \exp\left(-\beta_{\text{D2D}} r^{\alpha} g_i r_{i,j'}^{-\alpha}\right) f_G(g_i) f_R(r_{i,j'}) \mathrm{d}g_i \mathrm{d}r_{i,j'} \\ &= \exp\left[-\Lambda'_{\text{D2D}} \pi r_{i,j'}^2 Q(\zeta,\alpha)\right],\end{aligned} \tag{5.9}$$

where the D2D is distributed as a Poisson point distribution, and Λ'_{D2D} is the intensity of the co-frequency D2D UEs. The $Q(\zeta,\alpha)$ function is:

$$\begin{aligned}Q(\zeta,\alpha) &= \int_{\zeta^{-2/\infty}}^{+\infty} \frac{\zeta^{2/\alpha}}{1+u^{\alpha/2}} du \\ &= \sqrt{\zeta}\arctan(\sqrt{\zeta}) \qquad \text{for } \alpha = 4.\end{aligned} \tag{5.10}$$

Substituting in the expressions for $\mathcal{L}(\beta_{\text{D2D}} r_{i,j'}^{\alpha})$ Eq. (5.9) and $I_{\text{BS}}(r_{o,j'})$ Eq. (3.12) into Eq. (5.8) gives the success communication probability for any single hop is:

$$
\begin{aligned}
\mathbb{P}_k &= \mathbb{P}[\gamma > \zeta] \\
&= \exp\Bigg\{ - \beta_{\mathrm{D2D}} r_{j,j'}^{\alpha} P_{\mathrm{BS}} \lambda_{\mathrm{BS}} r_{o,j'}^{-\alpha} \\
&- \frac{P_{\mathrm{BS}}\lambda_{\mathrm{BS}}}{P_{\mathrm{D2D}}\lambda_{\mathrm{D2D}}} r_{j,j'}^{\alpha} \left[\frac{\pi \Lambda_{\mathrm{BS}} \Xi(r_{o,j'}, \Psi, 4)}{2\mathrm{erfc}^{-1}(0.5)} \right]^2 - \Lambda'_{\mathrm{D2D}} \pi r_{i,j'}^2 Q(\zeta, \alpha) \Bigg\},
\end{aligned}
\tag{5.11}
$$

where $\beta_{\mathrm{D2D}} = 1/P_{\mathrm{D2D}}\lambda_{\mathrm{D2D}}$. The parameter $\Lambda'_{\mathrm{D2D}} = N'_{\mathrm{D2D}}/\pi R_{\mathrm{BS}}^2$ is the density of co-frequency D2D UEs and should not be confused with Λ_{D2D}, which is the density of potential D2D UEs in existence. The parameter $r_{i,j'}$ is the distance of a hop and ζ is the minimum data connectivity SINR threshold for realistic modulation and coding schemes (MCS).

5.4.3 Success Probability for multi-hop SPR Scheme

The success probability calculation is given as Algorithm 1 Success Probability.

For the scenario of SPR shown in Figure 5.1, the average distance of each hop $r_{j,j'}^{\mathrm{SPR}}$ is defined in Eq. (5.4) and Eq. (5.6) as:

$$
\begin{aligned}
& r_{j,j'}^{\mathrm{SPR}}(k) = \int_0^{R[r_{o,j'}(k)]} \varepsilon f_{\varepsilon, r_{m,m'}}(\varepsilon) \mathrm{d}\varepsilon \\
& r_{o,j'}(k) = \sqrt{r_{o,m}^2 + \Big(\sum(.)\Big)^2 - 2 r_{o,m} \sum(.) \cos\theta'} \\
& \text{where} \quad \sum(.) = \sum_{1}^{K_{\mathrm{SPR}}} r_{j,j'}^{\mathrm{SPR}}(k-1) \\
& \text{and} \qquad \cos\theta' = \frac{r_{o,m}^2 + r_{m,m'}^2 - r_{o,m'}^2}{2 r_{o,m} r_{m,m'}},
\end{aligned}
\tag{5.12}
$$

where the hop distance is relatively short such that the assumption is $r_{o,j'} \approx$

Algorithm 1 Success Probability

procedure PROBABILITY $\mathbb{P}_{\text{SPR}}$ $(r_{o,m}, r_{o,m'}, \theta, \zeta)$
  if $\gamma(r_{o,m}) \geq \zeta$ **then** % The 1st hop SINR requirement
    Calculate the distance to the BS is assumed $r_{o,j'} = r_{o,j}$
    Calculate the Max. range $R(r_{o,m})$ from (5.4)
    Calculate the hop forward distance $r_{j,j'}$ from (5.6)
    Calculate the probability $\mathbb{P}_{\text{SPR},1}$ from (5.10) and (5.13)
    From the second hop to the k-th hop
    while destination node m' not reached **do**
      Calculate the distance to the BS $r_{o,j'}(k)$ from (5.12)
      Calculate the Max. range $R(r_{o,j'}(k))$ from (5.4)
      Calculate the hop forward distance $r^{\text{SPR}}_{j,j'}(k)$ from (5.12)
      Calculate the probability $\mathbb{P}_{\text{SPR},k}$ from (5.10) and (5.13)
    end while
  end if
  $\mathbb{P}_{\text{SPR}} = \prod_{k=1}^{k} \mathbb{P}_{\text{SPR},k}$
end procedure

$r_{o,j}$, so $r_{o,j'} = r_{o,m}$. The flow chart in Figure 5.3 shows the IAR and SPR hop forward algorithm.

From Eq. (5.11), the success communication probability for the multi-hop SPR at the k-th hop is:

$$\mathbb{P}_{\text{SPR},k} = \exp\Bigg\{ - \left[\frac{r^{\text{SPR}}_{j,j'}(k)}{r_{o,j'}(k)}\right]^{\alpha} (\frac{P_{\text{BS}}}{P_{\text{D2D}}}) - \frac{P_{\text{BS}}}{P_{\text{D2D}}} [r^{\text{SPR}}_{j,j'}(k)]^{\alpha} \left[\frac{\pi \Lambda_{\text{BS}} \Xi(r_{o,j'}(k), \Psi, 4)}{2\text{erfc}^{-1}(0.5)}\right]^2 - (\frac{r^{\text{SPR}}_{j,j'}(k)}{R_{\text{BS}}})^2 N'_{\text{D2D}} Q(\zeta, \alpha) \Bigg\}, \tag{5.13}$$

where the D2D shares the band link with the BS, so that the frequency dependent pathloss constant $\lambda_{\text{BS}} = \lambda_{\text{D2D}}$. It can be seen that the success probability is a function of the distance from the closest BS to the relay UE j ($r_{o,j'}$).

The total hop distance is the Euclidean distance between m and m': $r_{m,m'} = \sqrt{r^2_{o,m} + r^2_{o,m'} - 2r_{o,m} r_{o,m'} \cos\theta}$. Therefore the total number of hops is

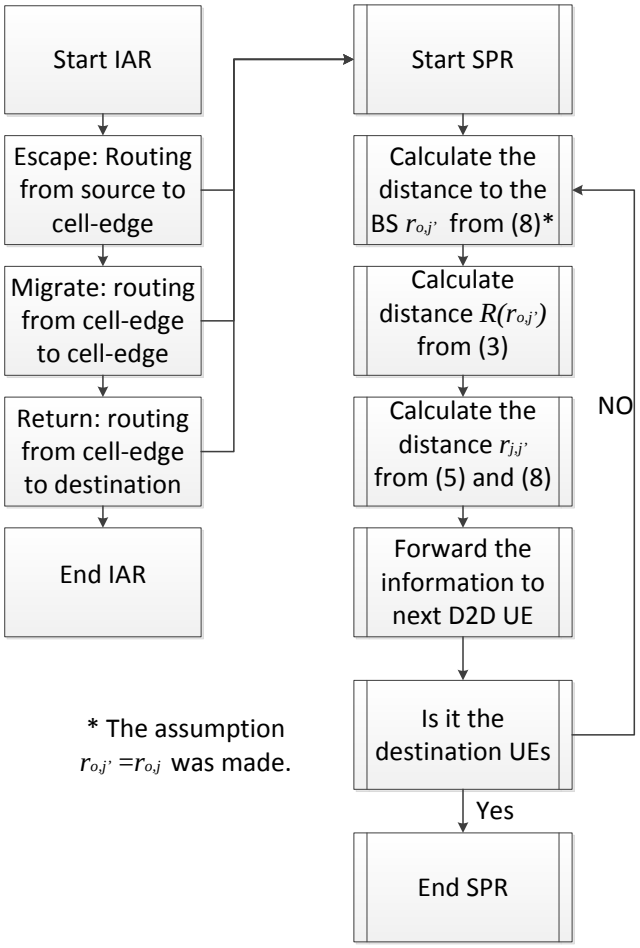

Figure 5.3: The flow chart of the IAR and SPR.

K_{SPR} satisfies:

$$r_{m,m'} = \sum_{k=1}^{K_{\mathrm{SPR}}} r_{j,j'}^{\mathrm{SPR}}(k). \tag{5.14}$$

Given that the successful probability of a multi-hop transmission is the product of the success at each link, the overall success probability is therefore:

$$\mathbb{P}_{\mathrm{SPR}} = \prod_{k=1}^{K_{\mathrm{SPR}}} \mathbb{P}_{\mathrm{SPR},k}. \tag{5.15}$$

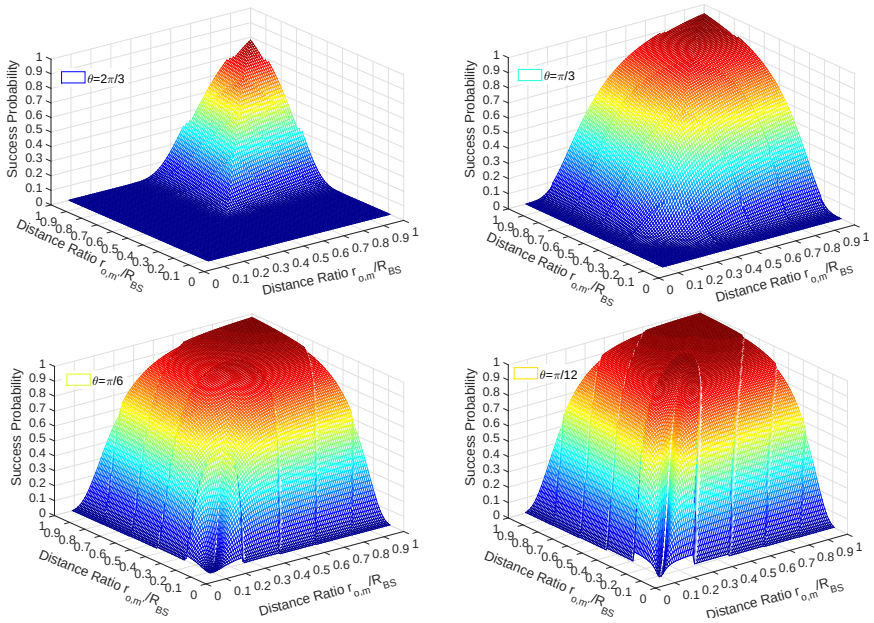

Figure 5.4: The success probability of SPR D2D at different locations: x and y axes are the distance ratio scale of $r_{o,m}$ and $r_{o,m'}$ to R_{BS}.

The results in Figure 5.4 for different values of θ show the theoretical success probability of D2D UEs at any location in a BS using the multi-hop SPR algorithm. As the angle θ decreases, the success probability increases significantly. For large angles (approaching π), the SPR route will inevitably cross near the BS, incurring greater mutual interference. In terms of the distance from the BS to the source or destination UEs, the greater the distance the stronger the success probability, which means that D2D communications should be avoided close to the BS.

5.4.4 Success Probability for IAR Scheme

As mentioned previously, there are three main *stages* to the IAR algorithm: (1) Escape, (2) Migrate, and (3) Return. Each *stage* of the IAR utilizes the aforementioned SPR algorithm, and the success probability for each IAR stage

can be derivation from Eq. (5.13) and 5.15.

Stage 1: Escape

For the first multi-hop stage (IAR(1)), the source UE m attempts to use SPR to transmit to the nearest point on the cell-edge, so the total routing distance for this stage is $\left[R_{\mathrm{BS}} - r_{o,m}\right]$. At the k-th hop, the distance from the BS to the relay UE is: $r_{o,j'}(k) = r_{o,m} + \sum_2^k r_{j,j'}^{\mathrm{IAR}(1)}(k-1)$, where the average hop distance for each single k-th hop is $r_{j,j'}^{\mathrm{IAR}(1)}(k) = \int_0^{R[r_{o,j'}(k)]} \varepsilon f_{\varepsilon,r_{m,m'}}(\varepsilon)\mathrm{d}\varepsilon$ and $r_{o,j'}(1) = r_{o,m}$. From Eq. (5.13), the probability of success at the k-th hop in this stage is:

$$\mathbb{P}_{\mathrm{IAR}(1),k} = \exp\Bigg\{ - \left[\frac{r_{j,j'}^{\mathrm{IAR}(1)}(k)}{r_{o,m} + \sum_2^k r_{j,j'}^{\mathrm{IAR}(1)}(k-1)}\right]^{\alpha} (\frac{P_{\mathrm{BS}}}{P_{\mathrm{D2D}}}) - \frac{P_{\mathrm{BS}}}{P_{\mathrm{D2D}}}[r_{j,j'}^{\mathrm{IAR}(1)}(k)]^{\alpha} \left[\frac{\pi\Lambda_{\mathrm{BS}}\Xi(r_{o,m} + r_{j,j'}^{\mathrm{IAR}(1)}(k), \Psi, 4)}{2\mathrm{erfc}^{-1}(0.5)}\right]^2 - (\frac{r_{j,j'}^{\mathrm{IAR}(1)}(k)}{R_{\mathrm{BS}}})^2 N'_{\mathrm{D2D}} Q(\zeta, \alpha)\Bigg\}, \tag{5.16}$$

The total number of hops in the first stage is $K_{\mathrm{IAR}(1)}$, where $R_{\mathrm{BS}} - r_{o,m} = \sum_{k=1}^{K_{\mathrm{IAR}(1)}} r_{j,j'}^{\mathrm{IAR}(1)}(k)$. Therefore the success probability for the entire *Escape* stage is $\mathbb{P}_{\mathrm{IAR}(1)} \approx \prod_{k=1}^{K_{\mathrm{IAR}(1)}} \mathbb{P}_{\mathrm{IAR}(1),k}$.

Stage 2: Migrate

For the second multi-hop stage (IAR(2)), the route is from the cell-edge UE closest to source to another cell-edge UE that is closest to the destination. At any given point along the route, the distance from the BS to any of the relay UEs is approximately R_{BS} (i.e. the cell coverage area is modelled as a circle). The total hop distance for the stage is $\theta \times R_{\mathrm{BS}}$. Therefore, the average hop

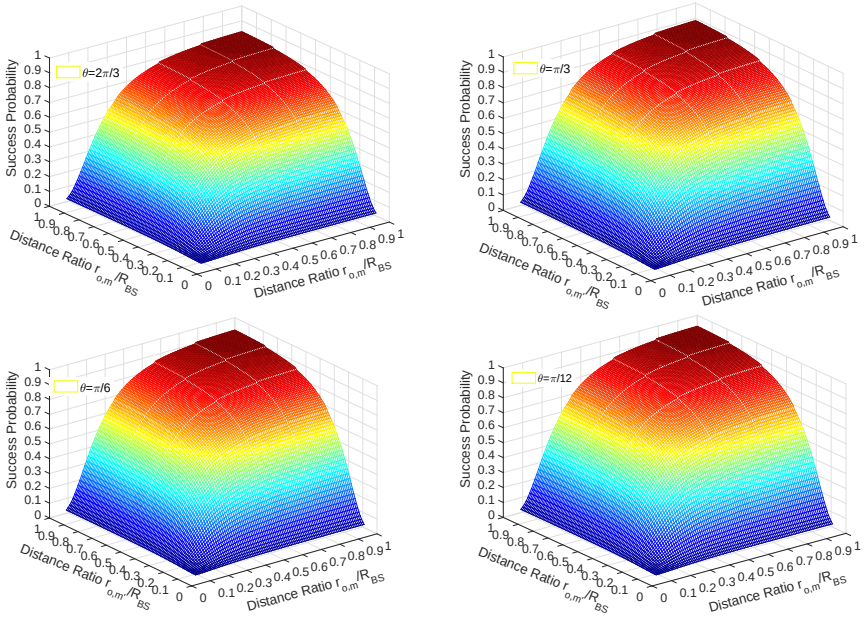

Figure 5.5: The success probability of IAR D2D at different locations: x and y axes are the distance ratio of $\frac{r_{o,m}}{R_{\mathrm{BS}}}$ and $\frac{r_{o,m'}}{R_{\mathrm{BS}}}$.

distance through the stage is $r_{j,j'}^{\mathrm{IAR}(2)}(k) = \int_0^{R_{\mathrm{BS}}} \varepsilon f_{\varepsilon, r_{m,m'}}(\varepsilon)\mathrm{d}\varepsilon$. From Eq. (5.13), the probability of success for each hop is:

$$\mathbb{P}_{\mathrm{IAR}(2),k} = \exp\left\{ -\left[\frac{r_{j,j'}^{\mathrm{IAR}(2)}}{\theta \times R_{\mathrm{BS}}}\right]^{\alpha} (\frac{P_{\mathrm{BS}}}{P_{\mathrm{D2D}}}) \right.$$
$$\left. - \frac{P_{\mathrm{BS}}}{P_{\mathrm{D2D}}} [r_{j,j'}^{\mathrm{IAR}(2)}]^{\alpha} \left[\frac{\pi \Lambda_{\mathrm{BS}} \Xi(\theta \times R_{\mathrm{BS}}, \Psi, 4)}{2\mathrm{erfc}^{-1}(0.5)}\right]^2 - (\frac{r_{j,j'}^{\mathrm{IAR}(2)}}{R_{\mathrm{BS}}})^2 N'_{\mathrm{D2D}} Q(\zeta, \alpha) \right\}. \tag{5.17}$$

The total number of hops in the second stage in the IAR algorithm is $K_{\mathrm{IAR}(2)} = (\theta \times R_{\mathrm{BS}})/r_{j,j'}^{\mathrm{IAR}(2)}$. Therefore the success probability of the entire *Migrate* stage is $\mathbb{P}_{\mathrm{IAR}(2)} \approx \prod_{k=1}^{K_{\mathrm{IAR}(1)}} \mathbb{P}_{\mathrm{IAR}(2),k}$.

Stage 3: Return

For the third multi-hop stage, it is a multi-hop from the boundary relay UE back to the destination UE so the distance from BS to the k-th hop UE is: $r_{o,j'}(k) = R_{\mathrm{BS}} - \sum_2^k r_{j,j'}^{\mathrm{IAR}(3)}(k-1)$,where the hop forward distance for each single hop through the entire IAR *Escape* stage is $r_{j,j'}^{\mathrm{IAR}(3)}(k) = \int_0^{R[r_{o,j'}(k)]} \varepsilon f_{\varepsilon, r_{m,m'}}(\varepsilon)\mathrm{d}\varepsilon$ and $r_{o,j'}(1) = R_{\mathrm{BS}}$ and $r_{o,j'} = R_{\mathrm{BS}}$. The total UE hop distance for this stage is $R_{\mathrm{BS}} - r_{o,m'}$. From Eq. (5.13), the probability of success for the k-th hop is:

$$\mathbb{P}_{\mathrm{IAR}(3),k} = \exp\Bigg\{ - \left[\frac{r_{j,j'}^{\mathrm{IAR}(3)}(k)}{R_{\mathrm{BS}} - \sum_{k=2}^{k} r_{j,j'}^{\mathrm{IAR}(3)}(k-1)}\right]^{\alpha} \times (\frac{P_{\mathrm{BS}}}{P_{\mathrm{D2D}}}) - \frac{P_{\mathrm{BS}}}{P_{\mathrm{D2D}}}[r_{j,j'}^{\mathrm{IAR}(3)}(k)]^{\alpha} \times \left[\frac{\pi\Lambda_{\mathrm{BS}}\Xi(R_{\mathrm{BS}} - \sum_2^k r_{j,j'}^{\mathrm{IAR}(3)}(k-1), \Psi, 4)}{2\mathrm{erfc}^{-1}(0.5)}\right]^2 - (\frac{r_{j,j'}^{\mathrm{IAR}(3)}(k)}{R_{\mathrm{BS}}})^2 N'_{\mathrm{D2D}} Q(\zeta, \alpha)\Bigg\}, \tag{5.18}$$

The total number of hops in the third stage in the IAR algorithm is $K_{\mathrm{IAR}(3)}$ where $R_{\mathrm{BS}} - r_{o,m'} = \sum_{k=1}^{K_{\mathrm{IAR}(3)}} r_{j,j'}^{\mathrm{IAR}(3)}(k)$. Therefore, success probability for the entire stage *Return* is $\mathbb{P}_{\mathrm{IAR}(3)} \approx \prod_{k=1}^{K_{\mathrm{IAR}(3)}} \mathbb{P}_{\mathrm{IAR}(3),k}$.

Synthesis

The overall success probability from source D2D user to destination D2D user by IAR is:

$$\mathbb{P}_{\mathrm{IAR}} = \prod_{i=1}^{3} \mathbb{P}_{\mathrm{IAR}(i)}, \tag{5.19}$$

and the total number of hops is: $K_{\mathrm{IAR}} = \sum_{i=1}^{3} K_{\mathrm{IAR}(i)}$.

Figure 5.5 shows the theoretical success probability of D2D UEs in

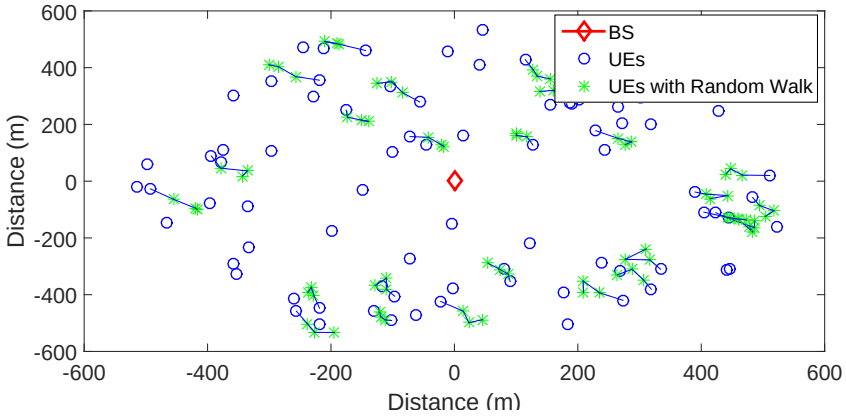

Figure 5.6: A snapshot of the simulation setup consisting of D2D UEs moving inside the coverage area of a single BS.

different locations employing the IAR algorithm. Compared with the SPR algorithm shown previously in Figure 5.4, the angle θ for IAR is not a significant parameter, the difference angle values do not change the success probability of the IAR much. Whereas the distances of the source and destination UEs to the BS are important parameters for the performance of IAR success probability. Generally the IAR has better performance of success probability than SPR for D2D routes that are of longer distance and are further away from the BS. In terms of distance from the BS of the source or destination UEs, the greater the distance the stronger the success probability, which means that D2D communications should be avoided close to the BS.

5.5 Results and Analysis

We now consider a specific urban terrain, which is covered by 19 macro-BSs. A central macro-BS as shown in Figure 5.6, where a number of D2D UEs are located. A Random Walk model is added to the simulation to model user mobility (each circle represents a new position of the user with connecting

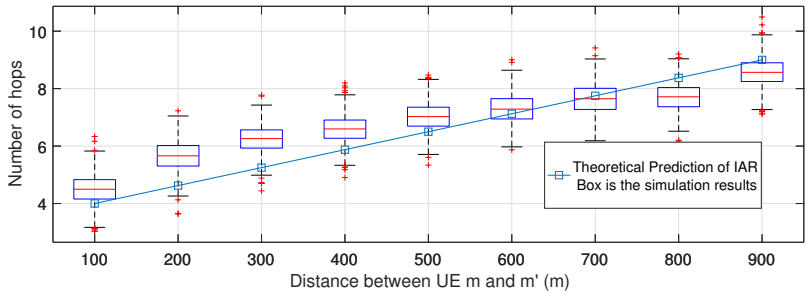

(a) The theoretical number of hops for IAR compared with box plot simulation results.

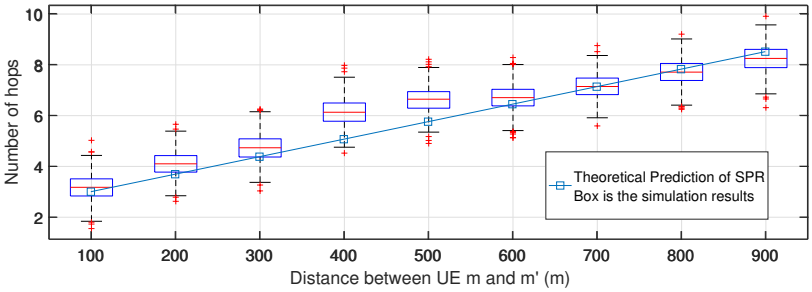

(b) The theoretical number of hops for SPR compared with box plot simulation results.

Figure 5.7: The theoretical number of hops for IAR and SPR routing schemes compared with the box plot plot of their simulation results.

lines to show the movement trace). Within that set of UEs, a source UE and a destination UE are randomly selected. The specific system and propagation parameters are in accordance to Table 3.2.

5.5.1 Number of Hops

The detailed performance of the D2D underlay tier is now considered. The number of hops of each scheme is an important indication of relay UE utilization level. The more hops each scheme uses, the greater the chance of data loss, privacy violation, and the less efficient the scheme is in terms of hardware utilization. Figure 5.7 shows the number of hops for the two respective schemes, as a function of the Euclidean distance between source and destination UEs.

In the box plot the central rectangle spans the first quartile to the third quartile (the interquartile range or IQR). A segment inside the rectangle shows the median and black segments above and below the box show the locations of the minimum and maximum. The first set of observations is that the number of hops is increasing *linearly* with the distance for both SPR and IAR. Whilst for the same distance between source and destination the average number of hops for IAR is greater than SPR, the difference becomes smaller for longer distances between UEs. That means the advantage of IAR at long distances is significant, as it can dramatically reduce interference between D2D and CC UE channels. The second set of observations is that the theory matches the simulation data well. The accuracy diminishes for distances below 400 m, because the noise due to random UE placements causes the routing path to resemble an arc as opposed to a straight line.

5.5.2 Network Capacity

The capacity at each hop link is given in Eq. (5.20) [126]:

$$\mathcal{C}_k = a \arctan(\frac{\gamma\left(r_{o,j'}\right) + b}{c}), \tag{5.20}$$

where $\mathcal{C}$ is the data-rate formula proposed, and the parameters a, b and c are determined by the actual modulation and coding scheme and channel model. The arctan capacity formula is selected over the standard Shannon capacity for the following reasons. The arctan formula takes into account the capacity saturation of discrete modulation schemes, as well as the performance of real error correction codes. The real performance of adaptive modulation and coding schemes in cellular networks is significantly different to the Shannon

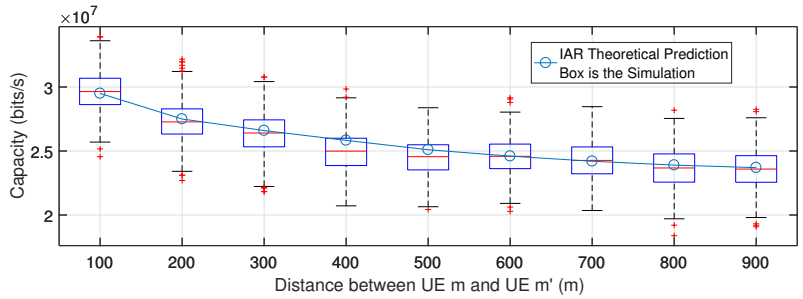

(a) The theoretical capacity for IAR compared with box plot simulation results.

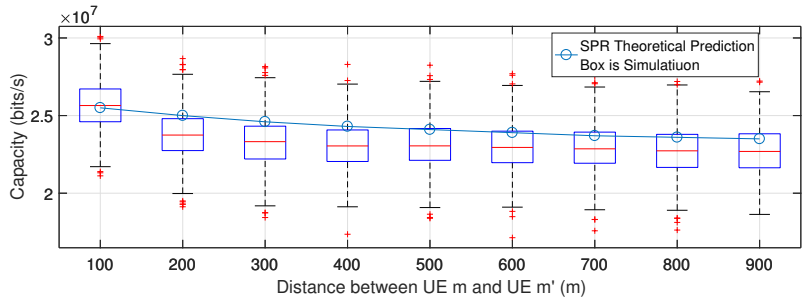

(b) The theoretical capacity for SPR compared with box plot simulation results.

Figure 5.8: The theoretical capacity for IAR and SPR routing schemes compared with the box plot of their simulation results.

capacity [126]. By using the SINR values found previously for SPR and IAR schemes, one can find the associated capacity values.

Figure 5.8 shows the theoretical predicted capacity of the D2D channel comparing with a boxplot of the simulation results. The results show that a single sequence of D2D multi-hop links can achieve the link capacity coexistence with CC interference from 19 Mbits/s to 33 Mbits/s depends on the different D2D UE location. The IAR is able to consistently achieve a superior throughput (10%) in comparison with SPR, because it attempts to reduce interference from the macro-BS when planning its longer route.

In terms of the capacity of the CC UEs, the CC capacity performance is dropped from 53.9 Mbits/s to 52.6 Mbits/s coexistence with SPR and dropped

to 52.9 Mbits/s with IAR. SPR and IAR D2D only degrade the CC capacity performances by 2.4% and 1.8% respectively. The capacity gain by offloading to D2D is approximately 43% for SPR and 51% for IAR. This is a significant improvement over cellular network and no significant increase in operational expenditures (i.e., backhaul infrastructure or rental costs) is incurred [127]. The sacrifice IAR makes to incur a longer route and involving more participating UEs, were now be examined.

5.5.3 Communication Success Probability

The communication success probability as a function of the minimum distance from BS to one of the source and destination UEs is now considered, and the effect of angle θ is also observed. The minimum distance concept is important when the distance from BS to UEs is considered, because it gives an idea of how close to the route path will get to the BS and hence to the level of cross-tier interference. Figure 5.9 shows the simulation results (symbols) and theory (lines), and there is good agreement of the theory and simulation results.

The first observation is that both the SPR and IAR can both achieve a high success probability ($\geq 70\%$) if certain spatial conditions are met. For SPR, the spatial conditions are: (1) the source or destination UE is far from the closest BS, and (2) there is a small incident angle θ in order to avoid the possibility of routing close to the closest interfering BS. For IAR, there is only one condition and that is the source or destination UE is far from the closest BS. If both of these scenarios are met, then the performance of SPR and IAR are approximately equal and that makes intuitive sense as the route is also similar. The angle θ between two UEs does not affect IAR communications,

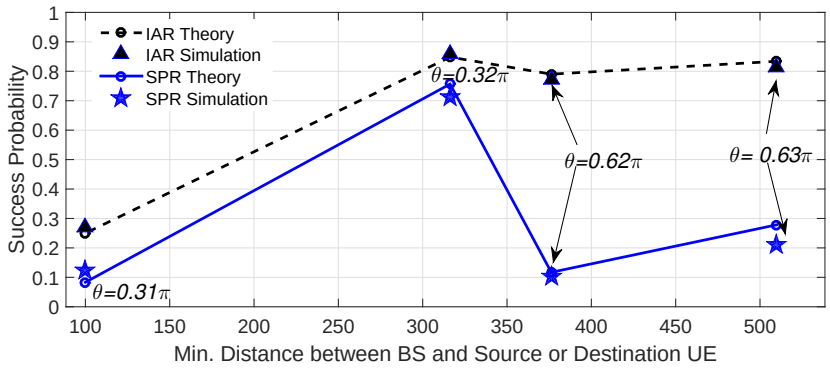

Figure 5.9: Compression of success probability with theory (line) and simulation (symbol) as a function of the minimum distance from BS to one of the source and destination UEs: $\min[r_{o,m}, r_{o,m'}]$.

as shown in Figure 5.9. There is less than 3% difference of the success probability between dramatically (up to 77%) different angles at any particular distance. Yet, for SPR, the angle can affect the success probability dramatically, as shown in Figure 5.9. This is consistent with results from earlier in this chapter (see Figure 5.4 and Figure 5.5). This is primarily because for SPR, the interference from the BS will be excessive, whereas for IAR, the routing path will always be at maximum distance from the BS, minimizing interference.

It was found that the IAR scheme can improve both the D2D transmission success probability by 14-18%, but will incur up more UEs to participate, which can incur privacy concerns. The privacy issue is beyond the scope of this chapter.

5.5.4 Operational Zones and Offloaded Traffic Volume

By considering the success probability for the D2D communications, and knowing the source and destination UEs' locations, the appropriate routing algorithm can be devised, Figure 5.10 is an operational zone. The operation zone

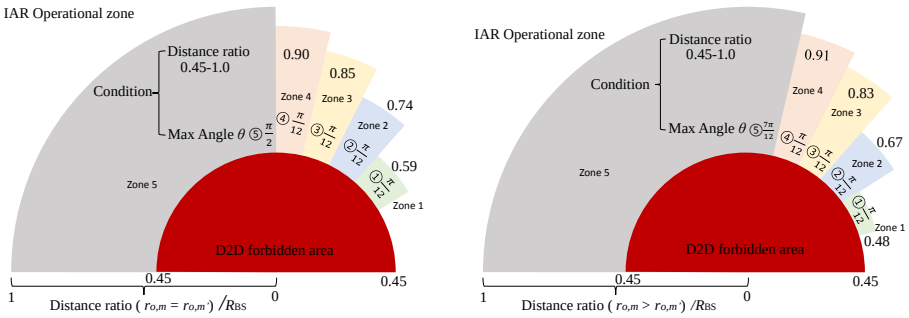

Figure 5.10: The interference routing algorithm in a cell set: the distance ratio scale of $r_{o,m}$ and $r_{o,m'}$ to R_{BS}.

is a location map, the sectors with the different angle of the $\angle mom'$ and the different distance ratio of the D2D UEs to the BS. If the distance of m and m' both bigger than the $0.45R_{\mathrm{BS}}$ and the $\angle mom' < \pi/2$, which this situation is in the zone 5 of the IAR operation. So the IAR is selected as a routing algorithm. For the operation zone 4, the conditions of operation are that $\pi/2 < \angle mom' < 7\pi/12$ and distance ration is between $0.45R_{\mathrm{BS}}$ and $0.9R_{\mathrm{BS}}$. And the rest of the semicircle with the radius ratio 1 is the operational zone of SPR. The full explanation is:

- **No D2D:** when the source or destination UEs are located within less than 45% of the cell radius from the BS, which is under the condition that the success probability is greater than 55% of IAR at angle θ is from 0 to π and of SPR angle θ is from 0 to $\pi/4$, no D2D routing should take place and all traffic should be handled by the BS as CC links.

- **IAR:** when the source and destination UEs are located far apart such that the angle is greater than $\pi/2$ with the distance ratio $r_{o,m}/R_{\mathrm{BS}} = r_{o,m'}/R_{\mathrm{BS}}$ for far from BS or the angle is greater than $5\pi/12$ with the distance ratio $r_{o,m}/R_{\mathrm{BS}} > r_{o,m'}/R_{\mathrm{BS}}$, and greater than $\pi/4$ for medium

distance from BS; IAR should be used as a priority algorithm. If the UEs are any closer then SPR become preferable.

- **SPR:** when the source and destination UEs are located in close proximity such that the angle $0 \leq \theta \leq \pi/6$; SPR should be used as a priority D2D routing algorithm. If the UEs are any further then IAR become to a preferable algorithm.

In summary, for the IAR, it is generally preferable if the source and destination UEs are far from the BS and the separation distance or angle is not less than $\pi/6$. The effect of the angle is not significant beyond this basic constraint. More than 70% of UEs in a cell fit this category. For SPR, the effect of angle is paramount, especially when the distance between the UEs is not small. Hence, SPR is only feasible for D2D communications between relatively nearby UEs, or those that already sit on the edge of the BS's coverage area.

By knowing the source and destination UEs' locations, the appropriate routing algorithm can be devised as an operational zone. The UEs are distributed as a Poisson distribution in the network, the total traffic rate offloaded from the cellular network is the ratio of the area of operation zone to the area of the BS. The maximum of the offload traffic from the BS is $O_{\mathrm{SPR}} = \frac{A_{\mathrm{SPR}}}{A_{\mathrm{BS}}}$ for SPR and $O_{\mathrm{IAR}} = \frac{A_{\mathrm{IAR}}}{A_{\mathrm{BS}}}$ for IAR. The parameter A_{IAR} is the operation area for the IAR and A_{SPR} is the operation area for the SPR, and A_{BS} is the area size of BS. Therefore, the maximum offload traffic ratio from BS is 79.75% and the ratio for IAR is 49.985% and for SPR is 29.765%.

5.6 Conclusions

In order to improve network capacity in a spectrum scarce environment, D2D communications has been investigated in a cellular context. Two contrasting multi-hop routing algorithms have been analyzed: SPR, and a newly proposed IAR. By dynamically selecting between the SPR and IAR algorithms, D2D can offload 79.75% of the traffic volume from BS. The IAR routing algorithm sacrifices a longer routing path for dramatically reduced mutual interference between the overlay macro-cells and the temporary underlay D2D channels. Several key discoveries have been presented in this chapter. Firstly, a longer routing path that minimizes cross-tier interference can achieve a superior performance compared to the intuitive shortest path route.

The second discovery is that there are clear geometric regions in the macro-cell coverage area that determine the D2D operations. In terms of performance metrics, it was found that the negative effect of D2D routing on regular cellular communications (CC) is negligible (1–2% degradation), and D2D communications can improve the CC network capacity by 44% for the SPR and 50% for the IAR routing scheme. When considering the D2D tier in isolation, the improvement of IAR over SPR is approximately 10% in capacity and 14% in outage probability. This demonstrates that careful cross-tier interference avoidance can yield productive improvements both within the D2D transmissions, but also for the conventional cellular links.

In this chapter, the main focus is the D2D performance and the interference from the cellular communications to D2D communications. The introduction of D2D communications cannot cause intolerable interference to cellular communications. So all our results for the conventional cellular (CC)

network users have considered the reciprocal D2D interference. However, how to optimal power control is used to guarantee a certain QoS in the CC network, which is a new problem required to be addressed.

Chapter 6

Collision Probability and Routing Strategy with Limited Location Information

6.1 Introduction

As studied in Chapter 5, there is a D2D forbidden zone around BS where the D2D communication cannot satisfy the required SINR of communication. In this chapter, the probability of D2D communication drop into the zone and relative routing strategy is addressed.

For D2D communications in co-existence with an overlay co-frequency CC network, one of the key challenges is interference management between the two tiers. Existing research has shown that a well-managed interference mitigation scheme can increase D2D communications reliability. One mechanism proposed in [128] found that the D2D receivers can exploit a retransmission of the interference signal from the BS to cancel the interference from prior CC

transmissions. Whilst this can improve the D2D outage probability, it does not consider the interference from the other D2D UEs. Furthermore, when a large number of UEs communicate at the same time, retransmission of the interference will cause significant resource overheads.

An alternative interference mitigation concept is the creation of an abstract interference zone, which is commonly defined as a circular area, centered on a point of interest (e.g. a macro- or femto-BS). The radius of the zone is directly related to a certain quality of service (QoS) requirement. For example in [129], the interference zone has been defined as the interference-limited coverage area (ILCA) for a femto-cell heterogeneous network to mitigate interference from femto- and macro-BSs. In this particular case, the ILCA of a femto-cell is an area within a circle centered by femto-BS, with a radius such that the edge of the circle has equal power levels from the nearest femto- and macro-BS. As a result, the channel allocation is based on the UE location with respect to the ILCA zone.

Currently, most routing and D2D papers assume synchronized accurate location knowledge among UEs and BSs. In reality, this level of location accuracy is difficult and power consuming in Universal Mobile Telecommunications System (UMTS). In pre-Release 9 and Release 10 of LTE, there is no location information from the cell besides range information from time measurements. In this chapter, it is assumed that each D2D UE only has knowledge of its relative distance to the nearest BS, and has no knowledge of its specific location or the location of other UEs. However, it does know the QoS targets required, as well as the final destination UE's distance to the nearest BS. On this basis, it must decide to use CC or D2D communications based on this.

In this chapter, a variable interference zone called the collision area

(CA) is defined, which is centred around BS. Inside the CA, the D2D receiver signal quality is less than a required Quality-of-Service (QoS) threshold. The probability that the D2D multi-hop routing path collides with the defined CA is addressed and an optimal switching strategy between CC and D2D communications according to the collision probability is presented in this chapter.

6.2 System model

6.2.1 D2D Routing Scenarios

The system considered in this chapter is a DL OFDMA based multiple-access network, the BSs' location are distributed as a Poisson distribution [86] with the density of Λ_{BS}. The network is modeled and analysed by the Stochastic Geometry as reviewed in Chapter 3 because this chapter aims to find the general probability of the D2D drop in the collision area. A CC communication exists as an umbrella over the D2D communication, both sharing the same spectrum due to resource scarcity and heavy traffic loads. The multi-hop communications are considered between two arbitrary located D2D UEs within one or more macro-BSs. For the SPR algorithm [130, 131], only the locations of the source m and destination m' UEs determine the multi-hop path. As shown in Figure 6.1, there are three scenarios:

1. *Intra-cell routing*: the D2D source and destination UEs are in the same cell.

2. *Intra-cell to cell boundary routing*: one of the source and destination UEs is on the cell boundary.

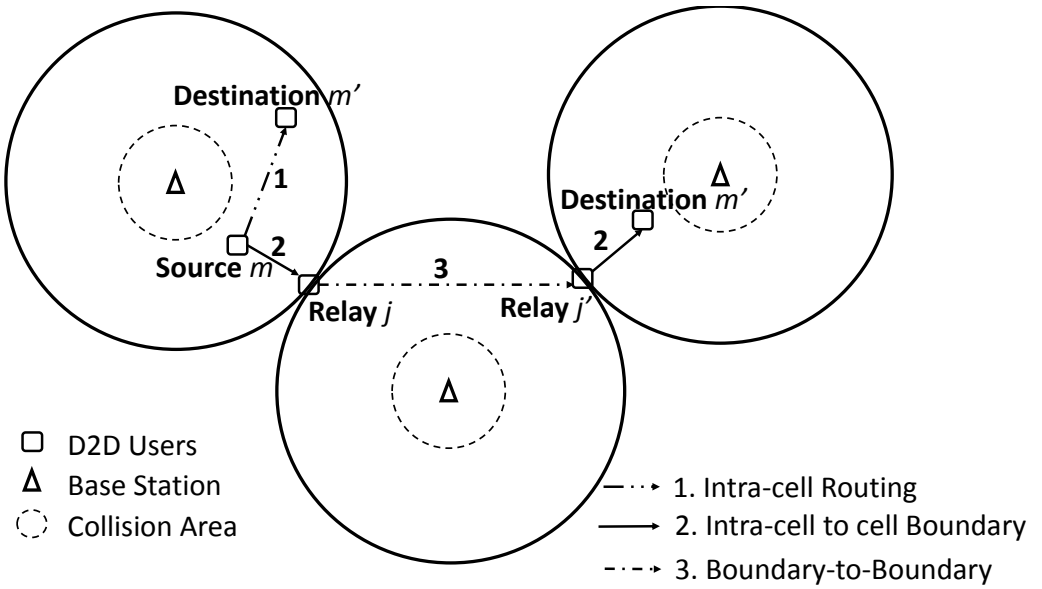

Figure 6.1: Illustration of three different routing paths: intra-cell; intra-cell to cell boundary; and cell boundary to cell boundary.

3. *Cell boundary to boundary routing*: both the source and destination UEs are on the cell boundary.

The assumptions in this chapter are as follows. The traffic model is assumed to be full buffer and the relaying protocol used is a non-cooperative DF protocol. The D2D UE density is sufficiently high that the SPR path can be approximately modelled by a straight line, and the average hop distance between D2D UEs is short. Furthermore, the interference received at each D2D UE is from two sources: (i) all the other co-channel D2D UEs, and (ii) the dominant interference from the nearest macro-BS.

Information is transmitted from a source m to a destination m' via a series of D2D relay UEs. For two random and adjacent relay UEs denoted j

and j', the instantaneous SINR from j to j' is:

$$\gamma\left(r_{o,j'}\right) = \frac{H_{j,j'} P_{\mathrm{D2D}} \lambda r_{j,j'}^{-\alpha}}{\sigma^2 + P_{\mathrm{BS}} \lambda r_{o,j'}^{-\alpha} + \sum\limits_{i \in \Phi, i \neq j'} H_{i,j'} P_{\mathrm{D2D}} \lambda r_{i,j'}^{-\alpha}}, \tag{6.1}$$

. Given that the aggregate interference power is typically significantly higher than noise power, it can be assumed that the AWGN power is negligible.

6.2.2 Collision Area (CA)

The CA is defined as an area centered around BS, where at the edge of the CA D2D UEs have an SINR equal to a threshold ζ. The value of ζ is typically chosen to satisfy some QoS constraint. For example, the minimum SINR for data throughput in LTE is approximate -6 dB. The radius of the CA is defined as r_{CA}. In order for the receiver's SINR $\gamma \geq \zeta$ (i.e., the receiver is outside the CA), it is that $r_{o,j'} = r_{\mathrm{CA}}$ in Eq. (6.1). Without considering instantaneous fading effects, r_{CA} can be found as:

$$\begin{aligned} r_{\mathrm{CA}} &= \arg\min \left\{ r_{\mathrm{CA}} | \gamma(r_{o,j'}) \geq \zeta \right\} \\ &= \arg\min \left\{ \frac{H_{j,j'} P_{\mathrm{D2D}} \lambda r_{j,j'}^{-\alpha}}{\sigma^2 + P_{\mathrm{BS}} \lambda r_{\mathrm{CA}}^{-\alpha} + \sum\limits_{i \in \Phi, i \neq j'} H_{i,j'} P_{\mathrm{D2D}} \lambda r_{i,j'}^{-\alpha}} \geq \zeta \right\} \\ &= \left[\frac{P_{\mathrm{D2D}}}{P_{\mathrm{BS}} \zeta} \left(r_{j,j'}^{-\alpha} - \zeta \sum_{i \in \Phi, i \neq j'} r_{i,j'}^{-\alpha} \right) \right]^{-1/\alpha} . \end{aligned} \tag{6.2}$$

For the case when the D2D interference is negligible ($r_{i,j'}$ is large), the CA zone can be said to be proportional to the QoS SINR threshold ζ with an exponent value of $1/\alpha$.

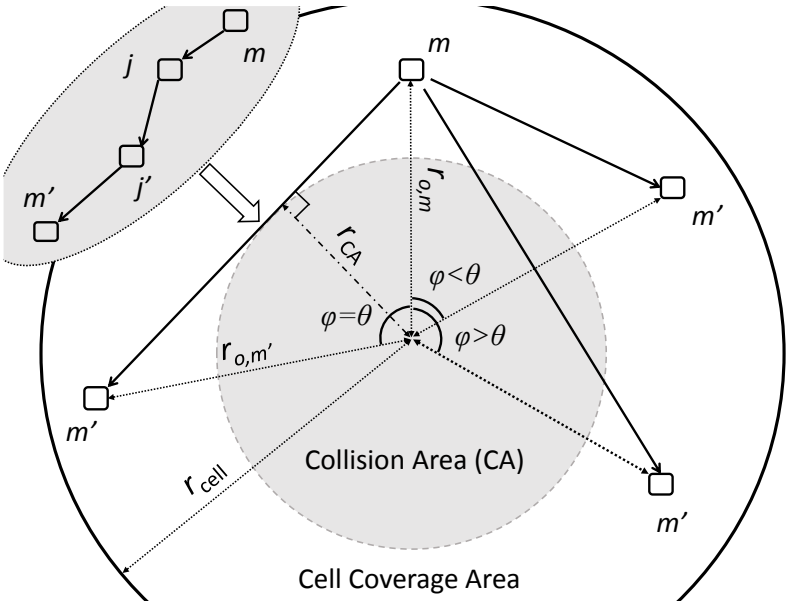

Figure 6.2: Illustration of multi-hop routing from a source m to destinations m' with three different possible m' locations (the distance $r_{o,m'}$ is constant).

6.3 Collision Probability

For a known CA radius in Eq. (6.2), the destination UE can detect whether it is located inside the CA via the pilot channel power from the nearest BS. When the destination UE is inside the CA, the collision probability is 100%. In which case, D2D communications is forbidden. If the destination UE is outside the CA, two possibilities for the collision between the D2D routing path and the CA exist, namely: (1) the source UE is located in the CA; (2) the source UE is located out of the CA but the routing path passes through the CA.

It is assumed that the source UE or any of the subsequent relay UEs have no knowledge of where the destination is or where any other UEs are. Each UE only know their own relative distance to the nearest BS. The collision probability in that context for the three routing paths is shown in Figure 6.1.

6.3.1 Intra-cell Routing

Figure 6.2 illustrates the intra-cell routing (scenario 1 in Figure 6.1), where $r_{o,m}$ is distance between the source m and nearest BS o, $r_{o,m'}$ is distance between the destination m' and BS o, φ is a variable presented the angle between $r_{o,m}$ and $r_{o,m'}$ $\angle mom'$, and θ is a particular value of φ when the routing path is a tangent to the CA.

Source UE Inside the CA

As mentioned previously, two possibilities exist for the multi-hop path to enter the CA when the destination UE is outside the CA. The first possibility, namely when the source UE is inside the CA. The pdf of finding one UE at a distance $r_{o,j'}$ from the nearest BS can be leveraged from Eq. (3.7):

$$g(r_{o,j'}) = 2\Lambda_{\mathrm{BS}} r_{o,j'} \pi e^{-\Lambda_{\mathrm{BS}} \pi r_{o,j'}^2}, \tag{6.3}$$

Therefore, the probability for finding this particular UE inside the CA area is:

$$\begin{aligned} \mathbb{P}_{\mathrm{CA}} &= \int_0^{r_{\mathrm{CA}}} 2\Lambda_{\mathrm{BS}} r_{o,j'} \pi e^{-\Lambda_{\mathrm{BS}} \pi r_{o,j'}^2} \mathrm{d}r_{o,j'} \\ &= 1 - e^{-\pi \Lambda_{\mathrm{BS}} r_{\mathrm{CA}}^2}. \end{aligned} \tag{6.4}$$

Collision Probability

When the source and destination UEs are both outside the CA, the collision probability is the probability of the multi-hop path colliding with the CA. Given that only the distance of the source and destination from the BS is known, there are a number of possibilities. As shown in Figure 6.2 when

$\theta < |\varphi| \leq \pi$, the routing path will pass through the CA. Given the uniform user distribution, the distribution of $|\varphi|$ is also uniform. Therefore, the probability of the routing path passing through the CA is:

$$\begin{aligned}\mathbb{P} &= \int_{\theta}^{\pi} \frac{1}{\pi}\,\mathrm{d}\varphi = \frac{\pi - \arccos\left(\frac{r_{\mathrm{CA}}}{r_{o,m}}\right) - \arccos\left(\frac{r_{\mathrm{CA}}}{r_{o,m'}}\right)}{\pi} \\ &= 1 - \frac{1}{\pi}\arccos\left[\frac{r_{\mathrm{CA}}}{r_{o,m}}\frac{r_{\mathrm{CA}}}{r_{o,m'}} - \sqrt{1-\left(\frac{r_{\mathrm{CA}}}{r_{o,m}}\right)^2}\sqrt{1-\left(\frac{r_{\mathrm{CA}}}{r_{o,m'}}\right)^2}\right] \\ &= 1 - \frac{1}{\pi}\arccos\left[\frac{r_{\mathrm{CA}}^2}{r_{o,m}r_{o,m'}} - \frac{\sqrt{\left(r_{o,m}^2 - r_{\mathrm{CA}}^2\right)\left(r_{o,m'}^2 - r_{\mathrm{CA}}^2\right)}}{r_{o,m}r_{o,m'}}\right]\end{aligned} \tag{6.5}$$

The value of r_{CA} is determined by the QoS target set out previously in Eq. (6.2). The collision probability for intra-cell routing is:

$$\mathbb{P}_{\mathrm{Collision}} = \begin{cases} 1 & 0 \leq r_{o,m'} \parallel r_{o,m} \leq r_{\mathrm{CA}} \\ \mathbb{P} \times (1 - \mathbb{P}_{\mathrm{CA}}) + \mathbb{P}_{\mathrm{CA}} & r_{\mathrm{CA}} < r_{o,m'} \& r_{o,m} \leq r_{\mathrm{cell}}, \end{cases} \tag{6.6}$$

From Eq. (6.4) and Eq. (6.5), the probability is:

$$\mathbb{P}_{\mathrm{Collision}} = \begin{cases} 1 & 0 \leq r_{o,m'} \leq r_{\mathrm{CA}} \\ 1 - \frac{1}{\pi}\arccos\left[\frac{r_{\mathrm{CA}}^2}{r_{o,m}r_{o,m'}} - \frac{\sqrt{\left(r_{o,m}^2 - r_{\mathrm{CA}}^2\right)\left(r_{o,m'}^2 - r_{\mathrm{CA}}^2\right)}}{r_{o,m}r_{o,m'}}\right] e^{-\pi\Lambda_{\mathrm{BS}}r_{\mathrm{CA}}^2} & r_{\mathrm{CA}} < r_{o,m'} \leq r_{\mathrm{cell}}. \end{cases} \tag{6.7}$$

6.3.2 Intra-cell to Cell Boundary Routing Path

Intra-cell to cell boundary routing (scenario 2 in Figure 6.1) is a special case of intra-cell routing. The collision probability for intra-cell to cell boundary routing is shown in Eq. (6.7) with the condition $r_{o,m'} = r_{\text{cell}}$.

$$\mathbb{P}_{\text{Collision}} = \begin{cases} 1 & 0 \leq r_{o,m} \leq r_{\text{CA}} \\ 1 - \frac{1}{\pi} \arccos \left[\frac{r_{\text{CA}}^2}{r_{o,m} r_{\text{cell}}} - \frac{\sqrt{\left(r_{\text{cell}}^2 - r_{\text{CA}}^2\right)\left(r_{\text{cell}}^2 - r_{\text{CA}}^2\right)}}{r_{o,m} r_{\text{cell}}} \right] e^{-\pi \Lambda_{\text{BS}} r_{\text{CA}}^2} & r_{\text{CA}} < r_{o,m} \leq r_{\text{cell}}. \end{cases} \tag{6.8}$$

6.3.3 Cell Boundary to Boundary Routing Path

For cell boundary to boundary routing (scenario 3 in Figure 6.1), both source and destination UEs are on the cell boundary which is a special case of intra-cell to cell boundary routing. The probability of a UE inside the CA is strictly zero. Thus, the collision probability is Eq. (6.7) with the conditions $r_{o,m} = r_{\text{cell}}$, $r_{o,m'} = r_{\text{cell}}$ and $\mathbb{P}_{\text{CA}} = 0$:

$$\mathbb{P}_{\text{Collision}} = 1 - 2 \frac{\arccos\left(\frac{r_{\text{CA}}}{r_{\text{cell}}}\right)}{\pi}. \tag{6.9}$$

In next section, the effect of different network parameters on the collision probability and how to dynamically select multi-hop routes is examined.

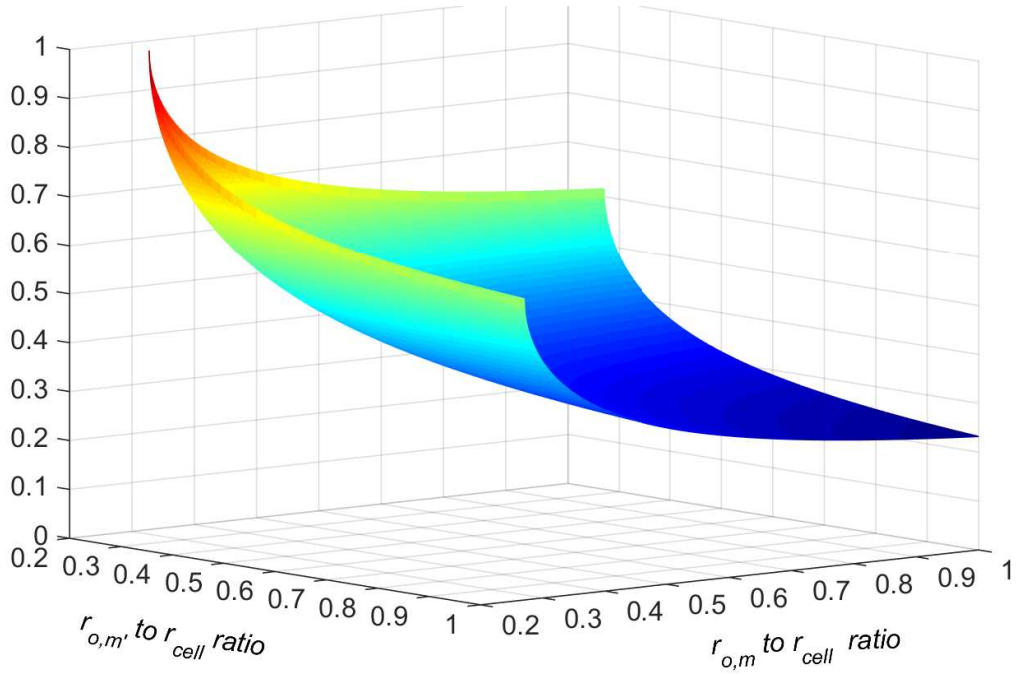

Figure 6.3: Collision probability for intra-cell and intra-cell to cell boundary routing paths with the distance scale of $r_{o,m'}$ and $r_{o,m}$, and CA radius ratio ($r_{\mathrm{CA}/r_{\mathrm{cell}}}$) is 27%.

6.4 Results and Analysis

6.4.1 Single-Cell and Multi-Cell Results

Figure 6.3 shows the collision probability for two routing path scenarios: (i) intra-cell routing, and (ii) intra-cell to cell boundary routing (when $r_{o,m'}/r_{\mathrm{cell}} = 1$). The CA's size is defined as a fraction of the BS's radius ($r_{\mathrm{CA}}/r_{\mathrm{cell}}$). In this particular case, the value is 27%, which is for typical QoS requirements of a minimum SINR ($\xi = -6$dB) and a pathloss distance exponent $\alpha = 4$ the parameters setting is in Table 3.2.

The first observation is that the collision probability is strictly convex, as a function of the distances from the BS to the source and destination UEs. This can be proven from Eq. (6.7), where the Hessian matrix is given by [132]:

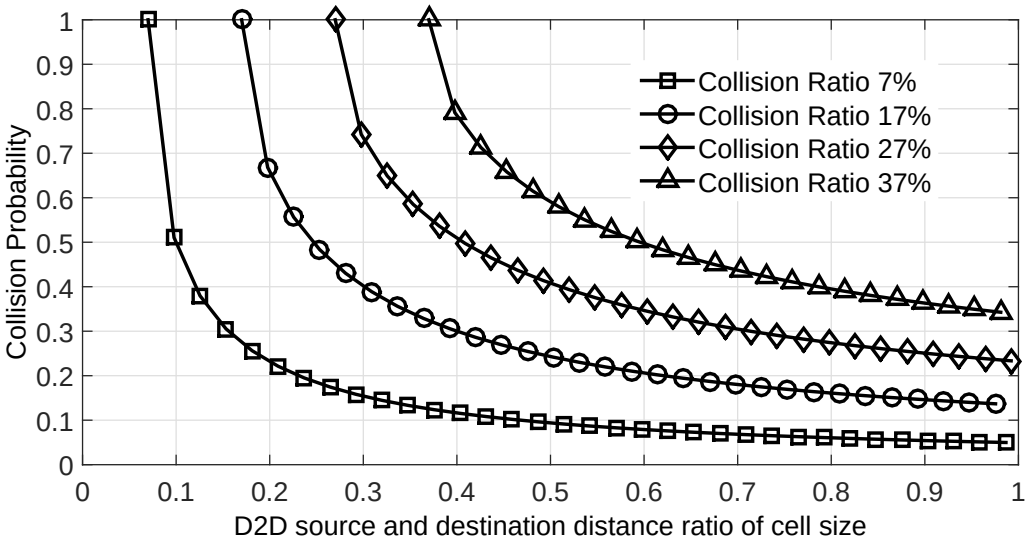

Figure 6.4: Collision probability (theory) for D2D intra-cell routing with different distances $r_{o,m'}$, $r_{o,m}$ (as a function of cell coverage radius $r_{o,m'} = r_{o,m}$).

$$\begin{bmatrix} \frac{2r_{\mathrm{CA}}(1-\mathbb{P}_{\mathrm{CA}})}{\pi r_{o,m}^2\sqrt{r_{o,m}^2-r_{\mathrm{CA}}^2}} & 0 \\ 0 & \frac{2r_{\mathrm{CA}}(1-\mathbb{P}_{\mathrm{CA}})}{\pi r_{o,m'}^2\sqrt{r_{o,m'}^2-r_{\mathrm{CA}}^2}} \end{bmatrix} \succeq 0, \tag{6.10}$$

for $r_{o,m} \geq r_{\mathrm{CA}}$, $r_{o,m'} \geq r_{\mathrm{CA}}$ and $0 \leq \mathbb{P}_{\mathrm{CA}} \leq 1$.

The second observation is that from the results and Eq. (6.7), a maximum collision probability of 100% is achieved when $r_{o,m} = r_{\mathrm{CA}}$ and $r_{o,m'} = r_{\mathrm{CA}}$. From Eq. (6.7), a third observation is that a minimum collision probability of

$$\min(\mathbb{P}_{\mathrm{Collision}}) = 1 - \frac{2}{\pi}\arccos\left(\frac{r_{\mathrm{CA}}}{r_{\mathrm{cell}}}\right). \tag{6.11}$$

can be achieved when $r_{o,m} = r_{\mathrm{cell}}$ and $r_{o,m'} = r_{\mathrm{cell}}$.

For D2D routing between the coverage area of multiple BSs, a combination of intra-cell to cell boundary routing and cell boundary to boundary

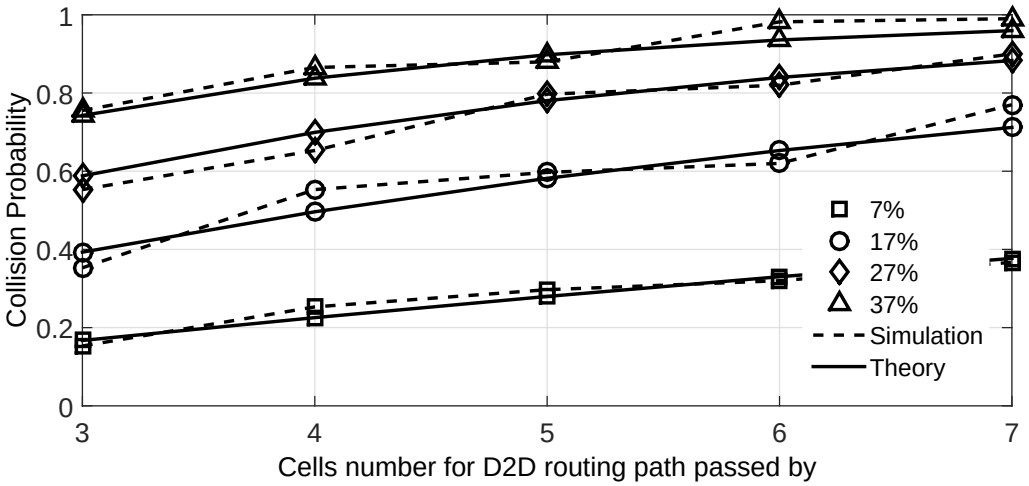

Figure 6.5: Collision probability of theory and simulation results for D2D multi-cell routing with different CA radius ratios.

routing is used.

The effecting of CA's size to collision probability is shown in Figure 6.4. The $r_{o,m}$ and $r_{o,m'}$ is set equally, the collision probability is increasing 15% in average when the collision ratio is bigger 10%. The collision probability is especially sensitive to the collision size. When the collision probability is 11% for the collision size is 7%r_{cell} and the collision probability is 79% for collision size is 37%r_{cell}, both with the distance ratio of 0.4 in Figure 6.4.. That means reducing collision area size can significant reduce decrease the probability.

The collision size contribute more compared with the distance to the collision probability. For example, when the distance of D2D source and destination is at 0.4 cell size, the collision probabilities are 11% and 79% respectively for the collision ratios are 7% and 37%; but collision probabilities are 7% and 42% when the distance is 0.7 cell size. The difference drops from 68% to 35% for the same distance difference.

Figure 6.5 shows the results of the collision probability as a function of the number of BSs passed through and different CA radius values ($r_{\text{CA}}/r_{\text{cell}}$).

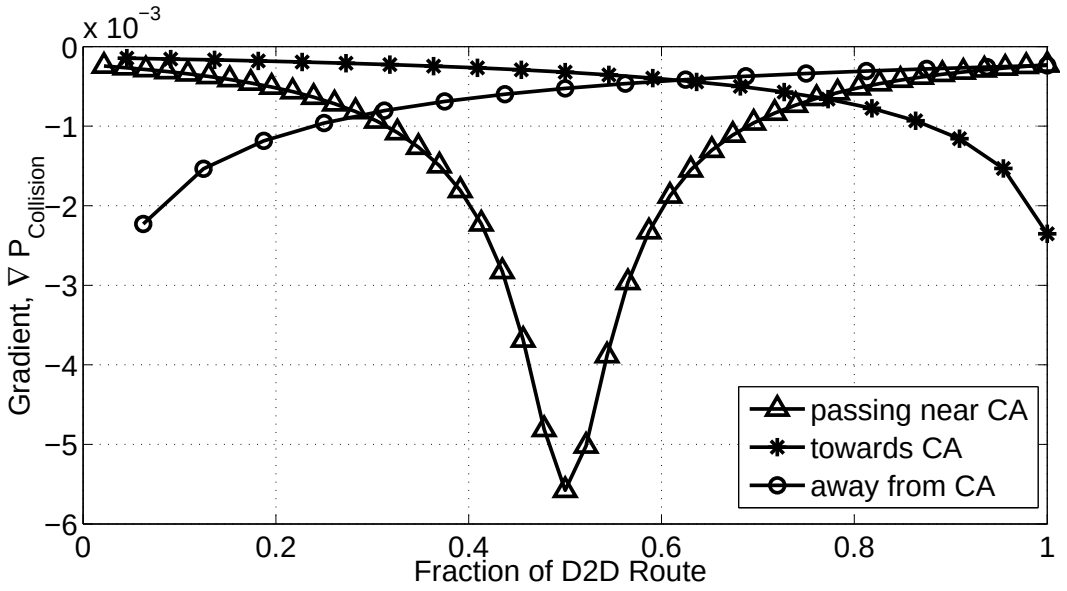

Figure 6.6: Gradient of the collision probability as a function of the normalized distance along the source-destination route.

The results show that the collision probability increases with the increasing number of BSs and bigger size of the CA, and the simulation and theoretical values agree.

More specifically, if with the 37% of CA size, the probability of collision is about 80% when routing passes through 3 BSs and it would be nearly 100% when the BSs number increases to 7. For the CA size is 7%, the collision probability is increasing from 20% to 40% with the cells number goes from 3 to 7.

6.4.2 Gradient Based Switch Strategy

Given the SPR multi-hop travels in a relatively straight line, each relay j can be interpreted as a temporary source m, and a fresh collision probability can be computed. As mentioned previously, the collision probability Eq. (6.7) is a convex function with respect to the UE-BS distances for the source and

destination. Therefore, the updated gradient descent at each relay UE j will reveal the increasing or decreasing probability of collision. The gradient with respect to the current relay UE's distance with BS ($r_{o,j}$) is given as:

$$\nabla \mathbb{P}_{\text{Collision}} = -r_{\text{CA}}(1 - \mathbb{P}_{\text{CA}})/(\pi r_{o,j}\sqrt{r_{o,j}^2 - r_{\text{CA}}^2}). \tag{6.12}$$

As the multi-hop path approaches the CA ($r_{o,j} \rightarrow r_{\text{CA}}$), the gradient will approach $\nabla \mathbb{P}_{\text{Collision}} \rightarrow -\infty$.

Figure 6.6 shows the gradient of the collision probability as a function of the normalized distance along the source-destination route. Three scenarios are considered: (i) when the path passes near the CA, (ii) when it moves towards the CA, and (iii) when it moves away from the CA. Hence, before the collision occurs, a certain gradient threshold β can be set whereby the D2D transmission will be forced to use CC channels in order to avoid colliding with the CA and cause unnecessary levels of interference. The detailed gradient based switching mechanism is given in Algorithm 2, and the impact on communication metrics is left for future research.

Algorithm 2 Switching algorithm

function SWITCH($r_{o,j}$, $r_{o,m'}$, r_{CA}, Λ_{BS})
  if ($r_{o,m'} \leq r_{\text{CA}}$) **then** *CC Communications*
  else($r_{o,m'} > r_{\text{CA}}$)
    D2D Communications Starts
    For each hop UE j, calculate $\nabla \mathbb{P}_{Collision}$
    if $|\nabla \mathbb{P}_{\text{Collision}}| > \beta$ **then**
      Switch to CC Communications
    else
      D2D Communications Resumes
    end if
  end if
end function

6.5 Conclusion

In this chapter, an interference zone (CA) is implemented to mitigate cross-tier interference between D2D and conventional cellular transmissions. Then investigated the routing algorithm for multi-hop D2D communications. Currently, most D2D routing algorithms assume synchronized accurate location knowledge among users and the base stations. In reality, this level of location accuracy is difficult and power consuming in UMTS. In current LTE, there is no location information from the cell besides range information from time measurements.

In the absence of perfect location information, the collision probability is able to derive as a function of the Quality-of-Service and other key network parameters. As a result, a simple gradient based switching mechanism between D2D and CC communications is devised. It can avoid collisions with the CA and requires only the distance information of the current transmission and final destination user.

Chapter 7

D2D in LTE-Unlicensed Heterogeneous Network

7.1 Introduction

In Chapter 4, 5 and 6, the performance of D2D UEs sharing CC spectrum is addressed [133]. However the D2D communication can utilize either the inband cellular spectrum or outband spectrum. The outband spectrum can be either unlicensed spectrum or allocated spectrum taken from the licensed band [31].

The concept of LTE-U (LTE for Unlicensed Spectrum), which suggests that LTE can operate in the unlicensed spectrum with significant modifications to its transmission protocols. LTE-U must adhere to unlicensed spectrum requirements, i.e., set transmit power limits and collision avoidance. By utilizing the considerable amount of unlicensed spectrum available, low power D2D transmissions can potentially avoid cross-tier interference with CC channels, at the cost of complicating the unlicensed spectrum usage [62].

Wi-Fi is a contention-based system with an appropriate mechanism taken to avoid interference, i.e., CSMA. However LTE is a demand-based system, so a critical element of LTE-U is to ensure fairness for Wi-Fi and other unlicensed users. In [63], an example of LTE-U channel access scheme is presented, where the femtocell base station (fBS) senses the unlicensed channel. If the channel is clear the link will access the unlicensed band, if not the fBS assigns the LTE licensed resource.

However, in Europe, Japan and India, there exist regulations for unlicensed spectrum that require equipment to periodically check for presence of other occupants in the channel (listen) before transmitting (talk) on a millisecond scale, also known as Listen Before Talk (LBT). In [134], a LBT algorithm is described for LTE-U D2D coexistence with Wi-Fi.

In this chapter, the technical problems are addressed as follows: (1) the waiting probability of D2D UEs with LBT, (2) the resulting expected time delay for the D2D UEs, and (3) the capacity of D2D UEs and Wi-Fi that share the same spectrum.

7.2 System Model

The system considered in this chapter is an OFDMA based 4G LTE multiple-access heterogeneous network. As analysed in Chapter 3, a Stochastic Geometry is used for modelling the network to get an overall performance of the D2D co-exist with Wi-Fi. Wi-Fi access points (APs) within the coverage of a CC base station, the D2D UEs communications are using unlicensed band as well. The scenario of D2D communications is a multi-hop relay system, with a greedy path algorithm named SPR [135].

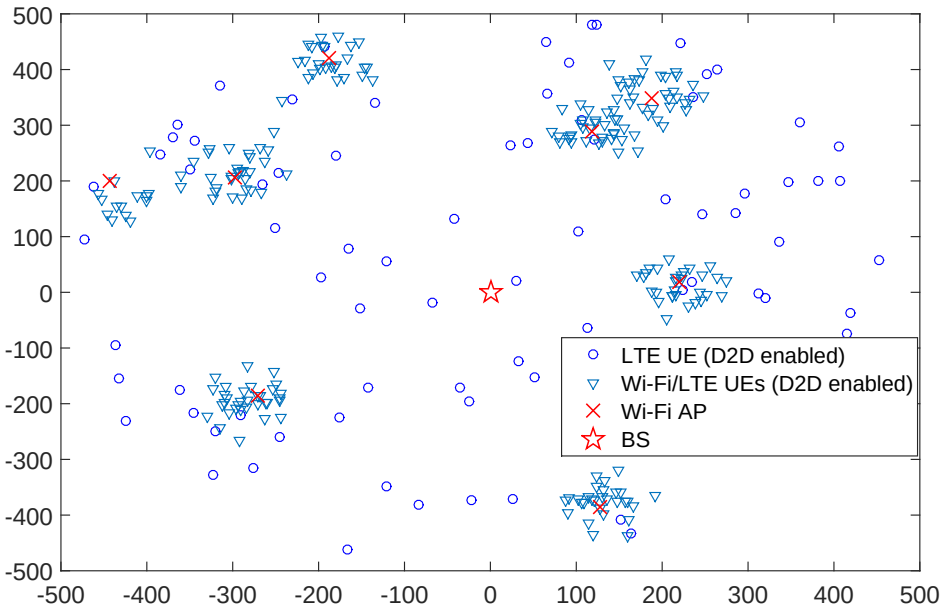

Figure 7.1: The UEs distribution in a macro-cell

7.2.1 UEs Distribution

The LTE (D2D enabled) locations of UEs are distributed as a PPP. The Wi-Fi APs are deployed from another independent PPP $\Phi_{\text{AP}} = \{x_1, x_2, ...\}$ of with density Λ_{AP}. The Wi-Fi (D2D enabled) UEs locations are generated by PCP, particularly a Matérn cluster process, which applies homogeneous independent clustering to an existing Wi-Fi AP process. The Wi-Fi UEs are uniformly scattered with the radius r_{AP} centred at each Wi-Fi AP, which is shown in Figure 7.1.

7.2.2 Wi-Fi Channel Capacity

The Wi-Fi is a collision avoidance system (e.g. CSMA), there is not channel interference. The received signal-to-noise-ratio (SNR) for a Wi-Fi UE i is

defined as

$$\gamma_i = \frac{H_i P \lambda r_i^{-\alpha}}{\sigma^2}, \tag{7.1}$$

where H_i is the multipath fading, P is the Wi-Fi AP transmit power, λ is the pathloss constant, r_i is the distance to the AP, σ^2 is the channel noise, and α is the pathloss distance exponent.

For the Shannon theory, the network capacity related to SNR is $C = B\log_2(1+\gamma_i)$. The expectation of a non-negative continuous random variable X is $\mathbb{E}[X] = \int_{t>0} \mathbb{P}(X > t)\mathrm{d}t$. Therefore, expectation capacity of any single Wi-Fi UE is:

$$\mathbb{E}(C_i) = \int_0^{+\infty} \mathbb{P}\left\{ B\log_2\left[1 + \frac{HP\lambda r^{-\alpha}}{\sigma^2}\right] > \zeta \right\} \mathrm{d}\zeta, \tag{7.2}$$

where B is the Wi-Fi bandwidth. The multipath fading has a pdf of $f_H(h) \sim \exp(\beta)$, where $\beta = 1/P\lambda$. So the capacity yields:

$$\mathbb{E}(C_i) = \int_0^{+\infty} e^{-\beta r^{-\alpha}\sigma^2(2^{\frac{\zeta}{B}}-1)} \mathrm{d}\zeta, \tag{7.3}$$

By a known spatial distribution of UEs relative to the APs in Eq. (3.7), the definition of the mean capacity of the Wi-Fi Channel is given by:

$$\begin{aligned} \overline{C} &= \int_0^{+\infty} \mathbb{E}(C_i) f_R(r)\mathrm{d}r \\ &= \int_0^{+\infty}\int_0^{+\infty} 2\Lambda_{\mathrm{AP}}\pi r e^{-\beta r^{-\alpha}\sigma^2(2^{\frac{\zeta}{B}}-1)} e^{-\Lambda_{\mathrm{AP}}\pi r^2} \mathrm{d}r\mathrm{d}\zeta \\ &= \int_0^{+\infty}\int_0^{+\infty} -e^{-\beta r^{-\alpha}\sigma^2(2^{\frac{\zeta}{B}}-1)} \mathrm{d}e^{-\Lambda_{\mathrm{AP}}\pi r^2} \mathrm{d}\zeta \end{aligned} \tag{7.4}$$

Let $e^{-\Lambda_{\mathrm{AP}}\pi r^2} = y$, so $r = \sqrt{\frac{\ln y}{-\Lambda_{\mathrm{AP}}\pi}}$

$$\begin{aligned}\overline{C} &= \int_0^{+\infty}\int_0^1 -e^{-\beta\left(\sqrt{\frac{\ln y}{-\Lambda_{\mathrm{AP}}\pi}}\right)^{-\alpha}\sigma^2(2^{\frac{\zeta}{B}}-1)}\mathrm{d}y\mathrm{d}\zeta \\ &= \int_0^1 -e^{\beta\left(\sqrt{\frac{\ln y}{-\Lambda_{\mathrm{AP}}\pi}}\right)^{-\alpha}\sigma^2} \\ &\times \int_0^{+\infty} e^{-\beta\left(\sqrt{\frac{\ln y}{-\Lambda_{\mathrm{AP}}\pi}}\right)^{-\alpha}\sigma^2 2^{\frac{\zeta}{B}}}\mathrm{d}\zeta\mathrm{d}y,\end{aligned} \tag{7.5}$$

Then let $\beta\left(\sqrt{\frac{\ln y}{-\Lambda_{\mathrm{AP}}\pi}}\right)^{-\alpha}\sigma^2 2^{\frac{\zeta}{B}} = m$, so

$$\begin{aligned}&\int_0^{+\infty} e^{-\beta\left(\sqrt{\frac{\ln y}{-\Lambda_{\mathrm{AP}}\pi}}\right)^{-\alpha}\sigma^2 2^{\frac{\zeta}{B}}}\mathrm{d}\zeta \\ &= \int_{\left[\beta\left(\sqrt{\frac{\ln y}{-\Lambda_{\mathrm{AP}}\pi}}\right)^{-\alpha}\sigma^2\right]}^{+\infty} \frac{B\times\frac{1}{m}\times e^{-m}}{\beta\left(\sqrt{\frac{\ln y}{-\Lambda_{\mathrm{AP}}\pi}}\right)^{-\alpha}\sigma^2\ln 2}\mathrm{d}\zeta \\ &= \frac{B\Gamma\left(0,\beta\left(\sqrt{\frac{\ln y}{-\Lambda_{\mathrm{AP}}\pi}}\right)^{-\alpha}\sigma^2\right)}{\beta\left(\sqrt{\frac{\ln y}{-\Lambda_{\mathrm{AP}}\pi}}\right)^{-\alpha}\sigma^2\ln 2},\end{aligned} \tag{7.6}$$

where $\Gamma(\cdot)$ is the gamma function.

So the average capacity is shown as:

$$\overline{C_{\text{Wi-Fi}}} = \int_0^1 -e^{\mathcal{A}(y,\alpha)\sigma^2}\frac{B}{\mathcal{A}(y,\alpha)\sigma^2\ln 2}\Gamma\big(0,\mathcal{A}(y,\alpha)\sigma^2\big)\mathrm{d}y. \tag{7.7}$$

Where $\mathcal{A}(y,\alpha)$ is given as:

$$\mathcal{A}(y,\alpha) = \beta\left(\sqrt{\frac{\ln y}{-\Lambda_{\mathrm{AP}}\pi}}\right)^{-\alpha}, \qquad 0\le y\le 1. \tag{7.8}$$

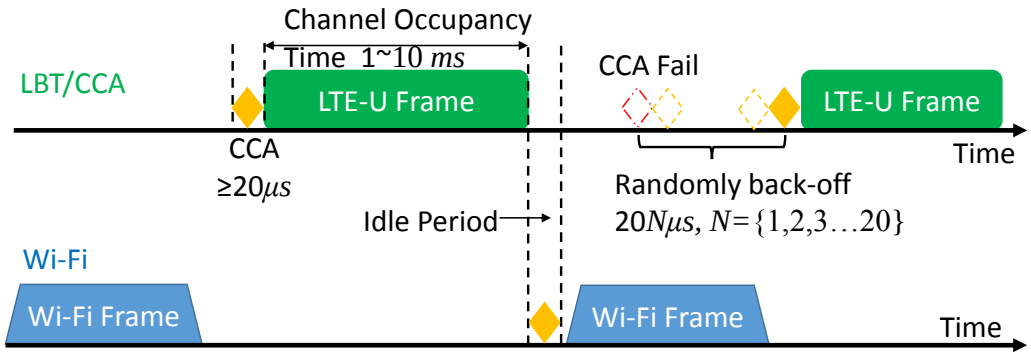

Figure 7.2: LBT specification for LET-U

Similarly, the capacity for any single hop between two D2D UEs can be found from Eq. (7.1) and Eq. (7.2). The capacity of each D2D hop link is shown in Eq. (5.20).

7.3 The D2D Routing Algorithm with LBT

7.3.1 Listen Before Talk (LBT)

Figure 7.2 shows the specification for frame based requirement[1]. When the D2D UEs want to transmit, it is required to detect the Wi-Fi energy level for a designed duration Clear Channel Assessment (CCA) period (typically 20 μs). If the energy level in the channel is below the CCA energy threshold, then the UE transmit for a Channel Occupancy Time (COT) (from 1 ms to 10 ms). If the energy level is over the CCA energy threshold, the D2D UEs will wait for a random period of $N \times 20$ μs, $N = \{1, 2, 3, ..., 20\}$ before it performs another CCA. After a COT, if the UE needs to continue, it has to repeat the CCA process.

[1]3GPP Response LS on Clarification of LBT Categories, Release 13, R1-152182, 24 April 2015.

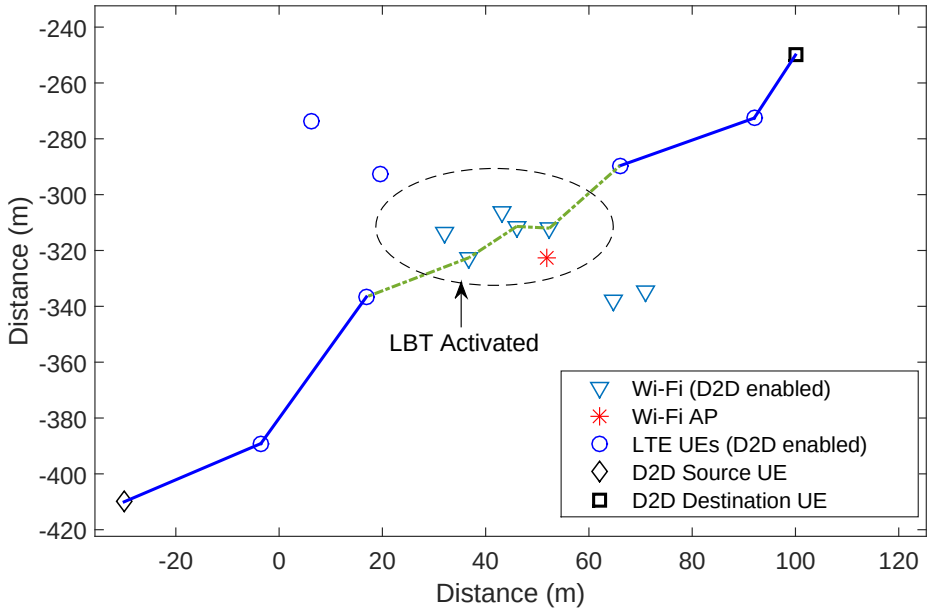

Figure 7.3: The Routing Paths for D2D LTE-U with SPR using LBT contention.

7.3.2 SPR Routing Algorithm with LBT

In SPR, each D2D UE knows its own location and that of the final destination UE. Furthermore, the relay UE can modify the routing path according to the periodically signal from the BS, in order to update the SPR path selection in the presence of mobility. At each hop, the Wi-Fi energy level is detected, if the detected energy lever is over the CCA energy level then LBT is activated. Figure 7.3 shows a LTE-enabled multi-hop D2D route based on SPR.

7.4 Traffic Model for D2D UEs with LBT

For the analysis of the traffic model, assumptions are: (1) the Wi-Fi UEs can only be attached to one Wi-Fi AP; (2) the probability of different Wi-Fi UEs launching the CCA at the same time is negligible; and (3) only one D2D UE

communication link for any Wi-Fi APs. The waiting time when CCA fails for next CCA is 2×20 μs, based on those assumptions the Wi-Fi communication traffic model is conceded as a Markov modulated Poisson process (MMPP). Specifically, in this chapter the $M/M/1/K$ queue-size process is chosen [136].

In this model, where the arrival process follows a Poisson process with the parameter τ and service times are assumed to be independent and identically distributed (i.i.d) and exponentially distributed with the parameter μ. The service processes are independent of the arrival process. From the Eq. (7.7), the mean service ratio μ is defined as:

$$\mu = \frac{\overline{C_{\text{Wi-Fi}}}}{S} = \frac{1}{S}\int_0^1 -e^{\mathcal{A}(y,\alpha)N}\frac{B}{\mathcal{A}(y,\alpha)N\ln 2}\Gamma\big(0,\mathcal{A}(y,\alpha)N\big)\mathrm{d}y, \tag{7.9}$$

where S is the average data package size. The mean arrival time is $\tau = \frac{N_{\text{Wi-Fi}}}{\sum_{i=0}^{N_{\text{Wi-Fi}}} T_i}$, where $N_{\text{Wi-Fi}}$ is the Wi-Fi UE in any AP and T_i is the Wi-Fi UE data demand duration.

7.4.1 D2D UEs Waiting Probability

The data service in a Wi-Fi channel is modeled as a continuous-time Markov-chain. The steady-state probabilities are defined as: $P_{k(k+1)}(t)$ is the probability: that given the process X is in state k at time t_0, then a time t later, it will be in state $k+1$. This process can be modeled as [137]:

$$P_{k(k+1)}(t) = P\left[X(t_0+t) = (k+1) | X(t_0) = k\right], \tag{7.10}$$

The steady-state probabilities are defined as, $\varphi_{k+1} = \lim_{t\to\infty} P_{k(k+1)}(t)$ where φ_{k+1} is the steady-state probability at state $k+1$. The global balance

steady-state equations for the $M/M/1/K$ is obtained [138]:

$\varphi_0\tau = \varphi_1\mu$

$\varphi_1\tau = \varphi_2\mu$

...

and in general for $K \geq 1$:

$$\varphi_k\tau = \varphi_{k+1}\mu \quad \text{for} \quad k = 0, 1, 2, 3, ..., K-1 \tag{7.11}$$

Figure 7.4 is the state transition diagram of $M/M/1/K$.

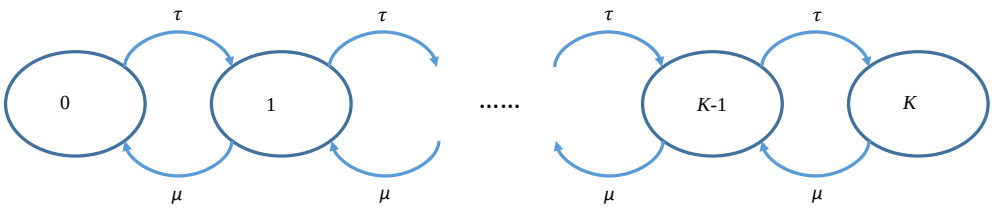

Figure 7.4: The balance equation

The normalizing equation is $\sum_{k=0}^{K} \varphi_k = 1$. Let the $\rho = \frac{\tau}{\mu}$, so the $\varphi_k = \rho^k\varphi_0$ for $k = 0, 1, 2, 3, ..., K$. Which is: $\sum_{k=0}^{K} \rho^k\varphi_0 = 1$. Therefore, the probability that no UE in the Wi-Fi system is,

$$\varphi_0 = \frac{1}{1 + \sum_{k=1}^{K} \left(\frac{SN_{\text{Wi-Fi}}}{\overline{C} \sum_{i=0}^{N_{\text{Wi-Fi}}} T_i} \right)^k} = \begin{cases} \frac{1-\rho^{K+1}}{1-\rho} & \rho \neq 1 \\ \frac{1}{K+1} & \rho = 1, \end{cases} \tag{7.12}$$

where $\rho = \frac{SN_{\text{Wi-Fi}}}{\overline{C} \sum_{i=0}^{N_{\text{Wi-Fi}}} T_i}$, and $\overline{C}$ can be found from Eq. (7.7). The Wi-Fi traffic collision probability is the probability that at least one Wi-Fi UE is communicating in the system.

$$\mathbb{P}_{\mathrm{c}} = \mathbb{P}\{\text{at least one UE}\} = \begin{cases} 1 - \frac{1-\rho^{K+1}}{1-\rho} & \rho \neq 1 \\ 1 - \frac{1}{K+1} & \rho = 1. \end{cases} \tag{7.13}$$

7.4.2 Average Time Delay for D2D UEs

When the unlicensed channel is occupied the D2D UEs have to wait for a clear channel slot. So the time delay for the D2D is:

$$\mathbb{E}(T_D) = \mathbb{E}(T_W) + \mathbb{E}(T_S) \tag{7.14}$$

where $\mathbb{E}(T_W)$ is the mean waiting time and $\mathbb{E}(T_S)$ is the mean severing time in the Wi-Fi system. The system limit is K so when K UEs are in the system there is no Wi-Fi access for the next UE therefore when $\rho \neq 1$, the mean number of waiting UEs is:

$$\begin{aligned} L_s &= \sum_{k=0}^{K} k\varphi_k = \varphi_0 \rho \sum_{k=1}^{K} k\rho^{k-1} \\ &= \frac{\varphi_0 \rho}{(1-\rho)^2} \left[1 - \rho^K - (1-\rho)K\rho^K\right] \\ &= \frac{\rho}{1-\rho} - \frac{(K+1)\rho^{K+1}}{1-\rho^{K+1}}, \end{aligned} \tag{7.15}$$

When $\rho = 1$:

$$L_s = \sum_{k=0}^{K} k\varphi_k = \sum_{k=1}^{K} k\rho^k \varphi_0 = \frac{1}{K+1} \sum_{k=1}^{K} k = \frac{K}{2}, \tag{7.16}$$

So,

$$\mathbb{E}(T_W) = \frac{L_s}{\tau} = \begin{cases} \left[\frac{\rho}{1-\rho} - \frac{(K+1)\rho^{K+1}}{1-\rho^{K+1}}\right] \frac{1}{\tau(1-\rho^K\varphi_0)} & \rho \neq 1 \\ \frac{K}{2\tau(1-\rho^K\varphi_0)} & \rho = 1. \end{cases} \tag{7.17}$$

And the mean severing time is $1/\mu$, so the $\mathbb{E}(T_D) = \mathbb{E}(T_W) + 1/\mu$, where $\mathbb{E}(T_D)$ can be found in Eq. (7.17).

7.5 Results and Analysis

In this section, the simulation results are presented to analyse the performance of LTE-U D2D with LBT protocols. The LTE-U is running at 5 GHz spectrum and Wi-Fi system is IEEE 802.11ac network, the bandwidth is 40 MHz, and LBT back-off duration is 40 μs. The macro-cell radius is 500 m with 8 Wi-Fi APs providing the Wi-Fi access. The Wi-Fi system limit K is 20. The three different Wi-Fi traffic volumes are selected to analyse the performance: light traffic with data package size 10 kbits and the Wi-Fi UEs communicating demand parameter is 1/20; for medium traffic data package size is 20 kbits and demand parameter is 1/6 ; and data package size is 30 kbits and demand parameter is 1/4 for heavy traffic.

7.5.1 Waiting Probability for D2D UEs with LBT

Figure 7.5 shows the D2D UE waiting probability inside a Wi-Fi AP's coverage area. The simulation results match the theoretical prediction well. The waiting probability increases when the Wi-Fi UE density grows. Specifically, the waiting probability is over 90% when more than 100 Wi-Fi are in the same AP's coverage area. From Eq. (7.13) it can be found that when the number of Wi-Fi UEs increases the traffic ratio ρ also increases, and so the waiting probability is greater.

Our analysis also found that the Wi-Fi traffic volume has a significant effect to the D2D UE waiting probability in Figure 7.5. Under heavy traffic

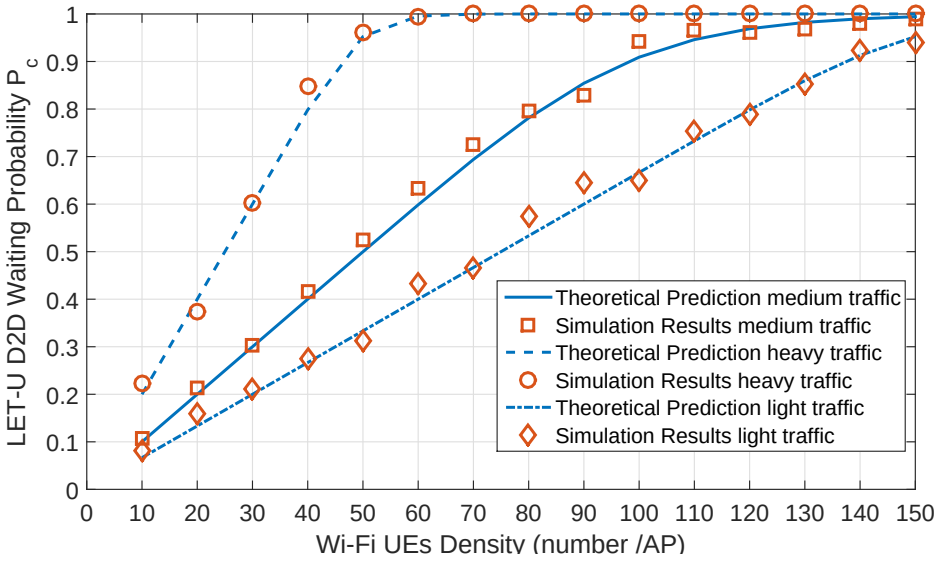

Figure 7.5: The theoretical prediction of D2D UE waiting probability under different traffic conditions with the Wi-Fi UEs density compared with simulation

loads, the waiting probability increases much more quickly as a function of UE density than the light and medium loads. This is due to the intuitive fact that the larger the traffic load, the more time is needed for the contention process in the channel, which in turn incurs a higher waiting probability for D2D UEs demanding LTE-U access.

7.5.2 Delay time for the D2D UEs with LBT

When the LBT protocol is utilized, the D2D UEs have to wait for a successful CCA. Figure 7.6 shows the correlation between D2D mean delay and Wi-Fi UEs density, and the delay rises with the UEs density from 0.1 s to 0.8 s when the number of Wi-Fi UEs in an AP increases from 10 to 150. This is because higher density means that need to wait a longer time for a successful CCA, which leads to a longer delay.

Generally, the delay is nearly the same for the light and medium traffic

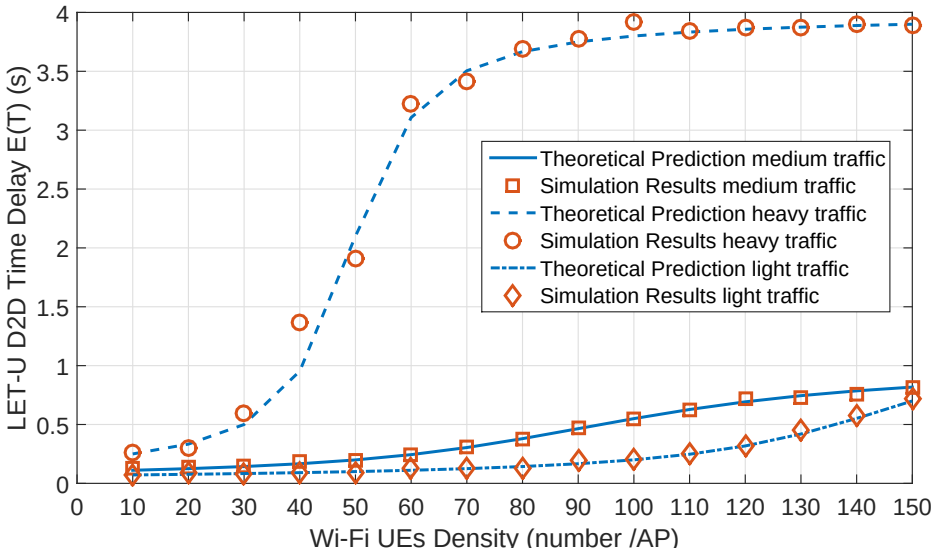

Figure 7.6: The theoretical prediction of D2D package delay under different traffic conditions with the Wi-Fi UEs density compared with simulation

Table 7.1: Simulation Average capacity

Capacity (Mbit/s)	Co-exist	Non co-exist
Wi-Fi	19.2	23.7
D2D	19.5	21.5
Total	38.7	23.7

load models (only 0.2 s difference). However, under the heavy traffic, the delay is 4 times stronger than the light and medium traffic loads.

7.5.3 Capacity for D2D and Wi-Fi Network

The network capacity during a time slot T is defined as: $\frac{T_{\text{active}} \times \overline{C}}{T}$, where T_{active} is the active communicating time, in this chapter T is 3,000 s. Without the Wi-Fi and LTE-U mutual interference, the capacity of D2D UEs is 23.7 Mbit/s and 21.5 Mbit/s for Wi-Fi UEs shown in Table 7.1 (with the Wi-Fi frame is 10ms and COT is 3 ms). Although the Wi-Fi capacity reduces to 19.2 Mbit/s

when in coexistence with LTE-U D2D UEs, the D2D UEs get a capacity of 19.5 Mbit/s. The benefit is that the total network capacity (licensed and unlicensed spectrum) increases 63.2% to 38.7 Mbit/s.

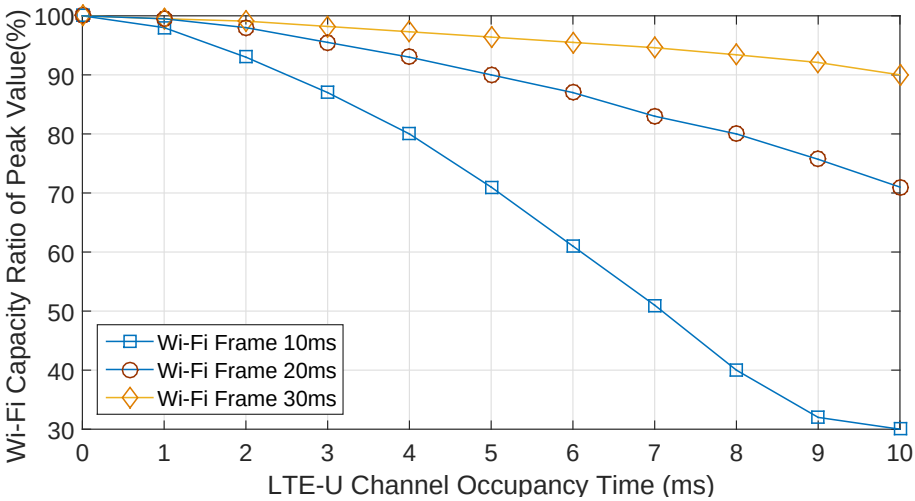

Figure 7.7: The Wi-Fi capacity attenuation with different LTE-U COT and Wi-Fi frame size

To analyse the effect of LTE-U D2D on the Wi-Fi capacity, the results in Figure 7.7, shows that the Wi-Fi capacity reduces with increased LTE-U COT values. The Wi-Fi capacity reduces to 30% when the LTE-U COT is the same size as the Wi-Fi frame value, 10 ms. As the COT value is reduced, the Wi-Fi capacity is 50% when the COT is 70% of the Wi-Fi frame.

When the Wi-Fi frame size is 30 ms, the Wi-Fi capacity only drops to 10% even when the D2D UEs reach their maximum COT. But the decline is 30% when the Wi-Fi frame size is 20 ms. So, when the Wi-Fi frame size is over 20 ms, the D2D share the same frequency with LBT could archive fair coexistence with the Wi-Fi UEs by only reduces less than 10% of Wi-Fi network capacity.

7.6 Conclusion

In this chapter, how the Device-to-Device (D2D) network can evolve to be more flexible by employing LTE-Unlicensed protocols and operating in the unlicensed spectrum with due care are examined. It was found that the D2D would take a longer delay when there is a high level of contention in the local unlicensed spectrum. Our results show that whilst D2D UEs reduce the Wi-Fi network capacity by sharing the unlicensed spectrum, it increased the overall network capacity (licensed and unlicensed) by 63%. In this way, D2D with LTE-U can be a friendly neighbour to the existing unlicensed spectrum users.

Chapter 8

Conclusion and Open Challenge

8.1 Conclusion

This thesis has mainly focused on the D2D multi-hop routing. As reviewed in Chapter 2, the traditional wireless routing algorithms are self-organised routing algorithms. They lack central control and need a complex self-organised mechanism to deal with routing environment changes such as UEs' movement and communication channel status changes. The traditional routing algorithms lack of the management of mutual interference between Device-to-device communication (D2D) and Conventional communication (CC).

In this thesis the base station (BS) assisted greedy routing namely Shortest Path Routing (SPR) and Interference Aware Routing for D2D communication are presented and analysed. D2D could be an emergency communication co-exist with the CC communications. In Chapter 4, it shows that in a co-existence and mutually interfering scenario, IAR is superior to the intuitive SPR and broadcasting routing when the UEs are close to the BS. Otherwise, for short distance D2D communications, the SPR and broadcasting algorithms

perform better. In general, there is a fundamental trade-off between D2D and CC outage performances, due to their mutual interference. For different CC outage constraints and D2D distances, it shows how different D2D routing strategies should be selected.

By utilising stochastic geometry framework to analyse the performance of SPR and IAR, it fundamentally proves that a longer routing path (IAR) that minimizes cross-tier interference can achieve a superior performance compared to the intuitive shortest path route (SPR). IAR on average achieves a 30% increase in hop distance, but can improve the overall network capacity by 50% whilst only incurring a minor 2% degradation to the CC capacity. In Chapter 5, the operation zone is defined that where IAR and SPR D2D algorithms should be utilized and where D2D should be avoided all together. This is our second discovery, there are clear geometric regions in the macro-cell coverage area that determine the D2D operations. The analysis framework and the results opens up new avenues of research in location-dependent optimization in wireless systems, which is particularly important for increasingly dense and semantic aware deployments. By dynamically selecting between the SPR and IAR algorithms, D2D can offload 79.75% of the traffic volume from BS.

According to the definition of the operation zone, there is an area that D2D communication is forbidden because of the interference from BSs. The probability of D2D routing path drop into the forbidden area is a function of the Quality-of-Service. As a result, a simple gradient based switching mechanism between D2D and CC communications is devised. It can avoid collisions in the forbidden area and requires only the distance information of the current transmission and final destination user.

The D2D network can evolve to be more flexible by employing LTE-

Unlicensed protocols and operating in the unlicensed spectrum with due care. A listen-before-talk (LBT) algorithm can efficiently manage the channel source fairness between D2D and Wi-Fi UEs. It was found that the D2D would take a longer delay when there is a high level of contention in the local unlicensed spectrum. Our results show that whilst D2D UEs reduce the Wi-Fi network capacity by sharing the unlicensed spectrum, it increased the overall network capacity (licensed and unlicensed) by 63%.

Overall, D2D can efficiently enhance the cellular network capacity, achieve high reliability of communication and can offload over half of the cellular traffic volume. D2D also can be a good neighbour to the Wi-Fi when operation on unlicensed band.

8.2 Open Challenge

Bearing in mind the summary of the findings for the research work conducted in this thesis, the research on D2D network routing performance evaluations does not stop here. There are still some research issues for the D2D communications.

Sensitivity Analysis: The results are based on some assumptions and simplifications. When the conditions change, how sensitive the analyses performed were to the variation of parameters used. Such as there only one D2D UEs pair in the same CC at the same time, if there is more than one D2D pair the interference distribution is more complicated.

Energy Efficiency: The ideal behind the IAR is routing a longer path for a smaller interference. The smaller interference would return a bigger network capacity, however, the longer routing path means more routing hops and more

transmission energy consumption. One of the potential advantages of D2D is network efficiency, moreover, the users are also interested in the battery life of their devices. Therefore how to balance between energy efficiency and network capacity needs investigation.

LBT Regulation: By applying LBT for the fairness with the Wi-Fi. When the number of D2D UEs number increasing, more UEs are likely to choose the same backoff time because the backoff range is limited and which is non-adaptive. Therefore, the collision (UEs want to use the channel at same time) is increased and the total network throughput is reduced. The challenge is that the EU LBT rules limit the backoff range within 20 μs and randomly choose the backoff time.

Bibliography

[1] Cisco, "http://www.cisco.com/en/US/netsol/ns827/networking_solutions_sub_solution.html," Technical Report, Technical Report, 2009.

[2] Habitat, "Planning and design for sustainable urban mobility global report on human settlements," United Nations, Technical Report, Tech. Rep., 2013.

[3] E. Pateromichelakis, M. Shariat, and R. Tafazolli, "On the evolution of multi-cell scheduling in 3GPP LTE/LTE-A," *IEEE Communications Surveys & Tutorials*, vol. 15, no. 2, pp. 701–717, 2013.

[4] M. B. Celebi and H. Arslan, "Theoretical analysis of the co-existence of lte-a signals and design of an ML-SIC receiver," *IEEE Transactions on Wireless Communications*, vol. 14, no. 8, pp. 4626–4639, 2015.

[5] R. Madan, J. Borran, A. Sampath, N. Bhushan, A. Khandekar, and T. Ji, "Cell association and interference coordination in heterogeneous LTE-A cellular networks," *IEEE Journal on Selected Areas in Communications*, vol. 28, no. 9, pp. 1479–1489, 2010.

[6] K. Truong and R. Heath, "Effects of channel aging in massive mimo systems," *Journal of Communications and Networks*, vol. 15, no. 4, pp. 338 – 351, August 2013.

[7] J.-C. Shen, J. Zhang, and K. Letaief, "Downlink user capacity of massive mimo under pilot contamination," *IEEE Transactions on Wireless Communications*, vol. 14, no. 6, pp. 3183 – 3193, June 2015.

[8] J. G. Andrews, S. Buzzi, W. Choi, S. V. Hanly, A. Lozano, A. C. K. Soong, and J. C. Zhang, "What will 5g be?" *IEEE Journal on Selected Areas in Communications*, vol. 32, no. 6, pp. 1065 – 1082, June 2014.

[9] E. Hossain and M. Hasan, "5g cellular: key enabling technologies and research challenges," *IEEE Instrumentation & Measurement Magazine,*, vol. 18, no. 3, pp. 11–21, 2015.

[10] K. Doppler, M. Rinne, C. Wijting, C. B. Ribeiro, and K. Hugl, "Device-to-device communication as an underlay to lte-advanced networks," *IEEE Communications Magazine,*, vol. 47, no. 12, pp. 42–49, 2009.

[11] L. Lei, Z. Zhong, C. Lin, and X. Shen, "Operator controlled device-to-device communications in lte-advanced networks," *IEEE Wireless Communications*, vol. 19, no. 3, p. 96, 2012.

[12] 3GPP, "Feasibility study for proximity services (prose), (release 12)," 3GPP TR 22.803 V0.2.0, Tech. Rep., Feb., 2012.

[13] ——, "Study on architecture enhancements to support proximity-based services (prose) (release 12)," 3GPP TR 23.703 V12.0.0, Tech. Rep., Feb., 2014.

[14] ——, "Proximity-based services (prose); stage 2 (release 12)," 3GPP TS 23.303 V12.1.0, Tech. Rep., Jun., 2014.

[15] ——, "Proximity-services (prose) user equipment (ue) to prose function protocol aspects; stage 3 (release 12)," 3GPP TS 24.334 V12.5.0, Tech. Rep., Dec., 2015.

[16] ——, "Study on security issues to support proximity services (prose) (release 12)," 3GPP TR 33.833 V1.0.0, Tech. Rep., May, 2014.

[17] ——, "Proximity-services (prose) management objects (mo)(release 13)," 3GPP TS 24.333 V13.1.0, Tech. Rep., Dec., 2015.

[18] Qualcomm, "Creating a digital 6th sense with lte direct," Qualcomm Technologies, Inc., Tech. Rep., September, 2015.

[19] T. I. GROUP, "Business opportunities beyond ultrabroadband: Proximity services and LTE direct," TELECOM ITALIA GROUP, Tech. Rep., March, 2015.

[20] Y. Li, T. Wu, P. Hui, D. Jin, and S. Chen, "Social-aware d2d communications: qualitative insights and quantitative analysis," *IEEE Communications Magazine,*, vol. 52, no. 6, pp. 150–158, 2014.

[21] X. Chen, B. Proulx, X. Gong, and J. Zhang, "Exploiting social ties for cooperative D2D communications: A mobile social networking case," *IEEE/ACM Transactions on Networking*, vol. 23, no. 5, pp. 1471 – 1484, Oct. 2015.

[22] G. Fodor, S. Parkall, S. Sorrentino, P. Wallentin, Q. Lu, and N. Brahmi, "Device-to-device communications for national security and public

safety," *IEEE Access:5G Wireless Technologies*, vol. 2, pp. 2169–3536, January 2015.

[23] A. Prasad, A. Kunz, G. Velev, K. Samdanis, and J. Song, "Energy-efficient D2D discovery for proximity services in 3GPP LTE-Advanced networks: Prose discovery mechanisms," *IEEE Vehicular Technology Magazine*, vol. 9, no. 4, pp. 40 – 50, January 2015.

[24] A. Bhorkar, M. Naghshvar, T. Javidi, and B. Rao, "Adaptive opportunistic routing for wireless Ad Hoc networks," *IEEE/ACM Transactions on Networking*, vol. 20, no. 1, pp. 243–256, Feb. 2012.

[25] Z. Chang and T. Ristaniemi, "Efficient use of multicast and unicast in collaborative OFDMA mobile cluster," in *IEEE Vehicular Technology Conference*, Dresden, Jun. 2013, pp. 1–5.

[26] Y. Li, P. Wang, D. Niyato, and W. Zhuang, "A dynamic relay selection scheme for mobile users in wireless relay networks," in *IEEE Conference on Computer Communications (INFOCOM)*, Shanghai, Apr. 2011, pp. 256–260.

[27] W. Guo and I. J. Wassell, "Capacity-Outage-Tradeoff for cooperative networks," *IEEE Journal on Selected Areas in Communications (JSAC)*, vol. 30, no. 9, pp. 1641–1648, Oct. 2012.

[28] D. Feng, L. Lu, Y. Yi, G. Li, G. Feng, and S. Li, "Device-to-Device communications underlaying cellular networks," *IEEE Transactions on Communications*, vol. 61, no. 8, pp. 3541–3551, Aug. 2013.

[29] P. Phunchongharn, E. Hossain, and D. I. Kim, "Resource allocation for Device-to-Device communications underlaying lte-advanced networks," *IEEE Wireless Communications*, vol. 20, no. 4, pp. 91–100, Aug. 2013.

[30] J. Sachs, I. Maric, and A. Goldsmith, "Cognitive Cellular Systems within the TV Spectrum," in *IEEE New Frontiers in Dynamic Spectrum (DYSPAN)*, Singapore, 2010, pp. 1–12.

[31] A. Asadi, Q. Wang, and V. Mancuso, "A Survey on Device-to-Device Communication in Cellular Networks," *IEEE Communications Surveys & Tutorials*, vol. 16, no. 4, pp. 1801 – 1819, 2014.

[32] 3GPP, "RP-140808: Review of Regulatory Requirements for Unlicensed Spectrum," Alcatel-Lucent, Alcatel-Lucent Shanghai Bell, Ericsson, Huawei, HiSilicon, IAESI, LG, Nokia, NSN, Qualcomm, NTT Docomo, Tech. Rep., June 2014.

[33] ——, "Study on lte device to device proximity services; radio aspects (release 12)," 3GPP TR 36.843 V12.0.1, Tech. Rep., Mar. , 2014.

[34] D. Feng, L. Lu, Y.-W. Yi, G. Li, S. Li, and G. Feng, "Device-to-device communications in cellular networks," *IEEE Communications Magazine*, vol. 52, no. 4, pp. 49 – 55, 2014.

[35] X. Lin, J. Andrews, A. Ghosh, and R. Ratasuk, "An overview of 3GPP Device-to-Device proximity services," *IEEE Communications Magazine*, vol. 52, no. 4, pp. 40–48, May 2014.

[36] D. Feng, L. Lu, Y. Yuan-Wu, G. Y. Li, G. Feng, and S. Li, "Device-to-device communications underlaying cellular networks," *IEEE Transactions on Communications,*, vol. 61, no. 8, pp. 3541–3551, 2013.

[37] M. Simsek, A. Merwaday, N. Correal, and I. Guvenc, "Device-to-device discovery based on 3gpp system level simulations," in *IEEE Globecom Workshops (GC Wkshps),*, 2013, pp. 555–560.

[38] Z. Zhou, M. Dong, K. Ota, J. Wu, and T. Sato, "Energy efficiency and spectral efficiency tradeoff in device-to-device (d2d) communications," *IEEE Wireless Communications Letters,*, vol. 3, no. 5, pp. 485–488, 2014.

[39] Y. A. Sambo, M. Z. Shakir, K. A. Qaraqe, E. Serpedin, and M. A. Imran, "Expanding cellular coverage via cell-edge deployment in heterogeneous networks: Spectral efficiency and backhaul power consumption perspectives," *IEEE Communications Magazine,*, vol. 52, no. 6, pp. 140–149, 2014.

[40] Y. Pei and Y.-C. Liang, "Resource allocation for device-to-device communications overlaying two-way cellular networks," *IEEE Transactions on Wireless Communications*, vol. 12, no. 7, pp. 3611–3621, 2013.

[41] S. Shalmashi and S. Ben Slimane, "Cooperative device-to-device communications in the downlink of cellular networks," in *IEEE Wireless Communications and Networking Conference (WCNC),*, 2014, pp. 2265–2270.

[42] Y. Li, D. Jin, F. Gao, and L. Zeng, "Joint optimization for resource allocation and mode selection in device-to-device communication under-

laying cellular networks," in *IEEE International Conference on Communications (ICC)*, Sydney, 2014, pp. 2245–2250.

[43] S. Choi and S. S. Pradhan, "A graph-based framework for transmission of correlated sources over broadcast channels," *IEEE Transactions on Information Theory*, vol. 54, no. 7, pp. 2841–2856, 2008.

[44] P. Patel and J. Holtzman, "Analysis of a simple successive interference cancellation scheme in a DS/CDMA system," *IEEE journal on selected areas in communications*, vol. 12, no. 5, pp. 796–807, 1994.

[45] J. Zander, S.-L. Kim, M. Almgren, and O. Queseth, *Radio resource management for wireless networks*. Artech House, Inc., 2001.

[46] S. Haykin, "Cognitive radio: brain-empowered wireless communications," *IEEE journal on selected areas in communications*, vol. 23, no. 2, pp. 201–220, 2005.

[47] M. Sheng, J. Liu, Y. Zhang, H. Sun, and J. Li, "On transmission capacity region of d2d integrated cellular networks with interference management," *Communications, IEEE Transactions on*, vol. 63, no. 4, pp. 1383–1399, 2015.

[48] X. Wu, Y. Chen, X. Yuan, and M. E. Mkiramweni, "Joint resource allocation and power control for cellular and device-to-device multicast based on cognitive radio," *IET Communications,*, vol. 8, no. 16, pp. 2805–2813, 2014.

[49] L. Qianxi, M. Qingyu, G. Fodor, and N. Brahmi, "Clustering schemes for d2d communications under partial/no network coverage," in *IEEE Vehicular Technology Conference (VTC Spring)*, 2014, pp. 1–5.

[50] J. Jiang, S. Zhang, B. Li, and B. Li, "Maximized cellular traffic offloading via device-to-device content sharing," *IEEE Journal on Selected Areas in Communications*, vol. 34, no. 1, pp. 82–91, 2016.

[51] E. Yaacoub, "Achieving green lte-a hetnets with d2d traffic offload and renewable energy powered small cell bss," in *IEEE Online Conference on Green Communications (OnlineGreencomm)*, 2014, pp. 1–6.

[52] Y. Bao, G. Miao, S. Zhou, and Z. Niu, "Base station sleeping control and power matching for energy-delay tradeoffs with bursty traffic," *IEEE Transactions on Vehicular Technology*, no. 1, 2015.

[53] A. H. Sakr, H. Tabassum, E. Hossain, and D. I. Kim, "Cognitive spectrum access in device-to-device-enabled cellular networks," *IEEE Communications Magazine*, vol. 53, no. 7, pp. 126–133, 2015.

[54] A. Asadi, Q. Wang, and V. Mancuso, "A survey on Device-to-Device communication in cellular networks," *IEEE Communication Surveys & Tutorials*, vol. 16, no. 4, pp. 1801–1819, Dec. 2014.

[55] Y. Cao, T. Jiang, and C. Wang, "Cooperative Device-to-Device communications in cellular networks," *IEEE Wireless Communications*, vol. 22, no. 3, pp. 124 – 129, June 2015.

[56] B. Zhou, H. Hu, S.-Q. Huang, and H.-H. Chen, "Intracluster device-to-device relay algorithm with optimal resource utilization," *IEEE Transactions on Vehicular Technology*, vol. 62, no. 5, pp. 2315–2326, 2013.

[57] J. C. Li, M. Lei, and F. Gao, "Device-to-device (d2d) communication in mu-mimo cellular networks," in *IEEE Global Communications Conference (GLOBECOM)*, 2012, pp. 3583–3587.

[58] G. Fodor, E. Dahlman, G. Mildh, S. Parkvall, N. Reider, G. Miklós, and Z. Turányi, "Design aspects of network assisted device-to-device communications," *IEEE Communications Magazine,*, vol. 50, no. 3, pp. 170–177, 2012.

[59] S. Zhang, J. Liu, N. Kato, H. Ujikawa, and K. Suzuki, "Average rate analysis for a d2d overlaying two-tier downlink cellular network," in *IEEE International Conference on Communications (ICC),*, 2015, pp. 3376–3381.

[60] J. Liu, S. Zhang, H. Nishiyama, N. Kato, and J. Guo, "A stochastic geometry analysis of d2d overlaying multi-channel downlink cellular networks," in *IEEE Conference on Computer Communications (INFOCOM),*, 2015, pp. 46–54.

[61] B. Zhou, S. Ma, J. Xu, and Z. Li, "Group-wise channel sensing and resource pre-allocation for LTE D2D on ISM band," in *IEEE Wireless Communications and Networking Conference*, Shanghai, April 2013, pp. 118 – 122.

[62] R. Zhang, M. Wang, L. Cai, Z. Zheng, and X. Shen, "LTE-unlicensed: the future of spectrum aggregation for cellular networks," *IEEE Communications Magazine*, vol. 22, no. 3, pp. 150 – 159, June 2015.

[63] F. Liu, E. Bala, E. Erkip, M. C. Beluri, and R. Yang, "Small-cell traffic balancing over licensed and unlicensed bands," *IEEE Transactions on Vehicular Technology*, vol. 64, no. 12, pp. 5850 – 5865, December 2015.

[64] E. Ferro and F. Potorti, "Bluetooth and wi-fi wireless protocols: a survey and a comparison," *IEEE Wireless Communications,*, vol. 12, no. 1, pp. 12–26, 2005.

[65] H. Song and X. Fang, "A spectrum etiquette protocol and interference coordination for LTE in unlicensed bands (LTE-U)," in *IEEE International Conference on Communication Workshop (ICC)*, London, June 2015, pp. 2338 – 2343.

[66] I. Qualcomm Technologies, "Lte in unlicensed spectrum: Harmonious coexistence with wi-fi," Qualcomm Technologies, Inc., Whitepaper, 2014.

[67] C. Cano and D. J. Leith, "Unlicensed lte/wifi coexistence: Is lbt inherently fairer than csat?" *arXiv preprint arXiv:1511.06244*, 2015.

[68] M.-S. Chen, K. G. Shin, and D. D. Kandlur, "Addressing, routing, and broadcasting in hexagonal mesh multiprocessors," *IEEE Transactions on Computers*, vol. 39, no. 1, pp. 10–18, 1990.

[69] M. Xie, W. Zhang, and K.-K. Wong, "A geometric approach to improve spectrum efficiency for cognitive relay networks," *IEEE Transactions on Wireless Communications*, vol. 9, no. 1, pp. 268 – 281, 2010.

[70] S. Giordano and I. Stojmenovic, "Position based routing algorithms for ad hoc networks: A taxonomy," in *Ad hoc wireless networking*. Springer, 2004, pp. 103–136.

[71] C.-H. Lin, S.-A. Yuan, S.-W. Chiu, and M.-J. Tsai, "Progressface: An algorithm to improve routing efficiency of GPSR-like routing protocols in wireless Ad hoc networks," *IEEE Transactions on Computers*, vol. 59, no. 6, pp. 822–834, Jun. 2010.

[72] X. Wu, S. Tavildar, S. Shakkottai, T. Richardson, J. Li, R. Laroia, and A. Jovicic, "FlashLinQ: A synchronous distributed scheduler for peer-to-peer ad hoc networks," *IEEE/ACM Transactions on Networking (TON)*, vol. 21, no. 4, pp. 1215–1228, 2013.

[73] H. Min, J. Lee, S. Park, and D. Hong, "Capacity enhancement using an interference limited area for device-to-device uplink underlaying cellular networks," *IEEE Transactions on Wireless Communication*, vol. 10, no. 12, pp. 3995–4000, 2011.

[74] S. E. Deering and D. R. Cheriton, "Multicast routing in datagram internetworks and extended lans," *ACM Transactions on Computer Systems (TOCS)*, vol. 8, no. 2, pp. 85–110, 1990.

[75] H. Takagi and L. Kleinrock, "Optimal transmission ranges for randomly distributed packet radio terminals," *IEEE Transactions on Communications,*, vol. 32, no. 3, pp. 246–257, 1984.

[76] E. Kaplan and C. Hegarty, *Understanding GPS: principles and applications*. Artech house, 2005.

[77] J. Li, J. Jannotti, D. S. De Couto, D. R. Karger, and R. Morris, "A scalable location service for geographic ad hoc routing," in *ACM Proceedings of the 6th annual international conference on Mobile computing and networking*, 2000, pp. 120–130.

[78] E. Schiller, P. Starzetz, F. Rousseau, and A. Duda, "Binary waypoint geographical routing in wireless mesh networks," in *ACM Proceedings of the 11th international symposium on Modeling, analysis and simulation of wireless and mobile systems*, 2008, pp. 252–259.

[79] Y.-J. Kim, R. Govindan, B. Karp, and S. Shenker, "On the pitfalls of geographic face routing," in *ACM Proceedings of the 2005 joint workshop on Foundations of mobile computing*, 2005, pp. 34–43.

[80] F. Kuhn, R. Wattenhofer, and A. Zollinger, "An algorithmic approach to geographic routing in ad hoc and sensor networks," *IEEE/ACM Transactions on Networking (TON)*, vol. 16, no. 1, pp. 51–62, 2008.

[81] P. Bose, P. Morin, I. Stojmenović, and J. Urrutia, "Routing with guaranteed delivery in ad hoc wireless networks," *Wireless networks*, vol. 7, no. 6, pp. 609–616, 2001.

[82] S. J. Bae, J. Gu, and M. Y. Chung, "Two-hop communication scheme for FlashLinQ device-to-device communication system," in *IEEE International Conference on Information Networking (ICOIN),*, 2014, pp. 85–90.

[83] K. J. Zou, M. Wang, K. W.Yang, J. Zhang, W. Sheng, Q. Chen, and X. You, "Proximity discovery for Device-to-Device communications over

a cellular network," *IEEE Communications Magazine*, vol. 52, no. 6, pp. 98 – 107, 2014.

[84] G. Parissidis, M. Karaliopoulos, T. Spyropoulos, and B. Plattner, "Interference-aware routing in wirless multihop networks," *IEEE Transactions on Mobile Computing*, vol. 10, no. 5, pp. 716–734, May. 2011.

[85] M. O. Hasna and M.-S. Alouini, "End-to-end performance of transmission systems with relays over rayleigh-fading channels," *IEEE Transactions on Wireless Communications*, vol. 2, no. 6, pp. 1126–1131, 2003.

[86] F. Baccelli and B. Blaszczyszyn, "Stochastic geometry and wireless networks, volume ii-applications," 2009.

[87] D. P. Kroese, T. Brereton, T. Taimre, and Z. I. Botev, "Why the monte carlo method is so important today," *Wiley Interdisciplinary Reviews: Computational Statistics*, vol. 6, no. 6, pp. 386–392, 2014.

[88] A. Baggio and K. Langendoen, "Monte carlo localization for mobile wireless sensor networks," *Ad Hoc Networks*, vol. 6, no. 5, pp. 718–733, 2008.

[89] J. Schuster and R. Luebbers, "Hybrid SBR/GTD radio propagation model for site specific predictions in an urban environment," in *12th Annual Review of Progress in Applied Computational Electromagnetics*, Monterey, Mar. 1996, pp. 84–92.

[90] J. Schuter and R. Luebers, "Comparison of Site-Specific radio propagation path loss predictions to measurements in an urban area," in *IEEE AP-S International Symposium and URSI Radio Science Meeting*, Baltimore, MD, July 1996, pp. 21–26.

[91] 3GPP, "Further advancements for E-UTRA physical layer aspects (rel.9)," 3GPP TR36.814v9, Technical Report, Mar. 2010.

[92] S. Musa and W. Wasylkiwskyj, "Co-channel interference of spread spectrum systems in a multiple user environment," *IEEE Transactions on Communications*, vol. 26, no. 10, pp. 1405–1413, 1978.

[93] C. C. Chan and S. V. Hanly, "Calculating the outage probability in a cdma network with spatial poisson traffic," *IEEE Transactions on Vehicular Technology*, vol. 50, no. 1, pp. 183–204, 2001.

[94] X. Yang and A. P. Petropulu, "Co-channel interference modeling and analysis in a poisson field of interferers in wireless communications," *IEEE Transactions on Signal Processing*, vol. 51, no. 1, pp. 64–76, 2003.

[95] P. C. Pinto, A. Giorgetti, M. Z. Win, and M. Chiani, "A stochastic geometry approach to coexistence in heterogeneous wireless networks," *IEEE Journal on Selected Areas in Communications*, vol. 27, no. 7, pp. 1268–1282, 2009.

[96] W. Ren, Q. Zhao, and A. Swami, "Power control in cognitive radio networks: how to cross a multi-lane highway," *IEEE Journal on Selected Areas in Communications*, vol. 27, no. 7, pp. 1283–1296, 2009.

[97] A. Ghasemi and E. S. Sousa, "Interference aggregation in spectrum-sensing cognitive wireless networks," *IEEE Journal of Selected Topics in Signal Processing*, vol. 2, no. 1, pp. 41–56, 2008.

[98] V. Chandrasekhar and J. G. Andrews, "Uplink capacity and interference avoidance for two-tier femtocell networks," *IEEE Transactions on Wireless Communications*, vol. 8, no. 7, pp. 3498–3509, 2009.

[99] O. Dousse, M. Franceschetti, and P. Thiran, "On the throughput scaling of wireless relay networks," *IEEE Transactions on Information Theory*, vol. 52, no. 6, pp. 2756–2761, 2006.

[100] J. G. Andrews, F. Baccelli, and R. K. Ganti, "A tractable approach to coverage and rate in cellular networks," *IEEE Transactions on Communications*, vol. 59, no. 11, pp. 3122–3134, 2011.

[101] A. Guo and M. Haenggi, "Spatial stochastic models and metrics for the structure of base stations in cellular networks," *IEEE Transactions on Wireless Communications*, vol. 12, no. 11, pp. 5800–5812, 2013.

[102] J. Moller and R. P. Waagepetersen, *Statistical inference and simulation for spatial point processes*. CRC Press, 2003.

[103] M. Haenggi, J. G. Andrews, F. Baccelli, O. Dousse, and M. Franceschetti, "Stochastic geometry and random graphs for the analysis and design of wireless networks," *IEEE Journal on Selected Areas in Communications*, vol. 27, no. 7, pp. 1029–1046, 2009.

[104] J. Illian, A. Penttinen, H. Stoyan, and D. Stoyan, *Statistical analysis and modelling of spatial point patterns*. John Wiley & Sons, 2008, vol. 70.

[105] A. Okabe, B. Boots, K. Sugihara, and S. N. Chiu, *Spatial tessellations: concepts and applications of Voronoi diagrams*. John Wiley & Sons, 2009, vol. 501.

[106] C.-H. Lee, C.-Y. Shih, and Y.-S. Chen, "Stochastic geometry based models for modeling cellular networks in urban areas," *Wireless networks*, vol. 19, no. 6, pp. 1063–1072, 2013.

[107] Y. J. Chun, M. O. Hasna, and A. Ghrayeb, "Modeling heterogeneous cellular networks interference using poisson cluster processes," *IEEE Journal on Selected Areas in Communications*, vol. 33, no. 10, pp. 2182–2195, 2015.

[108] R. W. Heath, M. Kountouris, and T. Bai, "Modeling heterogeneous network interference using poisson point processes," *IEEE Transactions on Signal Processing*, vol. 61, no. 16, pp. 4114–4126, 2013.

[109] H. S. Dhillon, R. K. Ganti, F. Baccelli, and J. G. Andrews, "Modeling and analysis of k-tier downlink heterogeneous cellular networks," *IEEE Journal on Selected Areas in Communications*, vol. 30, no. 3, pp. 550–560, 2012.

[110] C.-h. Lee and M. Haenggi, "Interference and outage in poisson cognitive networks," *IEEE Transactions on Wireless Communications*, vol. 11, no. 4, pp. 1392–1401, 2012.

[111] S. N. Chiu, D. Stoyan, W. S. Kendall, and J. Mecke, *Stochastic Geometry and its Applications, 3rd Edition*. Wiley, 2013.

[112] S. Wang, W. Guo, and M. D. McDonnell, "Downlink interference estimation without feedback for heterogeneous network interference avoidance," in *IEEE International Conference on Telecommunications (ICT)*, Lisbon, May 2014, pp. 82–87.

[113] L. Lovász, "On the shannon capacity of a graph," *IEEE Transactions on Information Theory,*, vol. 25, no. 1, pp. 1–7, 1979.

[114] S. Wang and W. Guo, "Energy and cost implications of a traffic aware and quality-of-service constrained sleep mode mechanism." *IET Communications*, vol. 7, no. 18, pp. 2092–2101, 2013.

[115] G. Fodor, S. Parkvall, S. Sorrentino, P. Wallentin, Q. Lu, and N. Brahmi, "Device-to-device communications for national security and public safety," *IEEE Access,*, vol. 2, pp. 1510–1520, 2014.

[116] B. Raghothaman, E. Deng, R. Pragada, G. Sternberg, T. Deng, and K. Vanganuru, "Architecture and protocols for lte-based device to device communication," in *IEEE International Conference on Computing, Networking and Communications (ICNC),*, 2013, pp. 895–899.

[117] L. Goratti, G. Steri, K. M. Gomez, and G. Baldini, "Connectivity and security in a d2d communication protocol for public safety applications," in *IEEE International Symposium on Wireless Communications Systems (ISWCS),*, 2014, pp. 548–552.

[118] Y. Duan, C. Borgiattino, C. Casetti, C. F. Chiasserini, P. Giaccone, M. Ricca, F. Malabocchia, and M. Turolla, "Wi-fi direct multi-group data dissemination for public safety," in *World Telecommunications Congress (WTC)*, 2014, pp. 1–6.

[119] S. P. Hyunkee Min, Jemin Lee and D. Hong, "Capacity enhancement using an interference limited area for Device-to-Device uplink underlaying cellular networks," *IEEE Transactions on Wireless Communications*, vol. 10, no. 12, pp. 3395–4000, Dec. 2011.

[120] S. P. Weber, X. Yang, J. G. Andrews, and G. de Veciana, "Transmission capacity of wireless Ad Hoc networks with outage constraints," *IEEE Transactions on Information Theory*, vol. 51, no. 12, pp. 4091–4102, Dec. 2005.

[121] H. ElSawy, E. Hossain, and M. Haenggi, "Stochastic geometry for modeling analysis and design of Multi-Tier and cognitive cellular wireless networks a survey," *IEEE Communication Surveys & Tutorials*, vol. 15, no. 3, pp. 996–1019, Sep. 2013.

[122] M. Haenggi, J. G. Andrews, F. Baccelli, O. Dousse, and M. Franceschetti, "Stochastic geometry and random graphs for the analysis and design of wireless networks," *IEEE Journal on Selected Areas in Communications*, vol. 27, no. 7, pp. 1029 – 1046, September 2009.

[123] X. Lin, J. G. Andrews, and A. Ghosh, "Spectrum sharing for Device-to-Device communication in cellular networks," *IEEE Transaction on Wireless Communications*, vol. 13, no. 12, pp. 6727 – 6740, Dec 2014.

[124] W. Wang, F. Zhang, and V. K. N. Lau, "Dynamic power control for delay-aware Device-to-Device communications," *IEEE Journal on Selected Areas in Communications*, vol. 33, no. 1, pp. 14 – 27, January 2015.

[125] S. De, "On hop count and euclidean distance in greedy forwarding in wireless ad hoc networks," *IEEE Communications Letters*, vol. 9, no. 11, pp. 1000–1002, Nov. 2005.

[126] S. Wang, W. Guo, and X. Chu, "Capacity expression and power allocation for arbitrary modulation and coding rates," in *IEEE Wireless Com-*

munications and Networking Conference (WCNC),, Shanghai, China, Apr. 2013.

[127] S. Andreev, A. Pyattaev, K. Johnsson, O. Galinina, and Y. Koucheryavy, "Cellular traffic offloading onto network-assisted device-to-Device connections," *IEEE Communications Magazine*, vol. 52, no. 4, pp. 20–31, Apr. 2014.

[128] L. Wei, R. Hu, Y. Qian, and G. Wu, "Enable Device-to-Device communications underlaying cellular networks: Challenges and research aspects," *IEEE Communications Magazine*, vol. 52, no. 6, pp. 90–96, June 2014.

[129] I. Güvenç, M.-R. Jeong, F. Watanabe, and H. Inamura, "A hybrid frequency assignment for femtocells and coverage area analysis for co-channel operation," *IEEE Communications Letters*, vol. 12, no. 12, pp. 413–418, Dec. 2008.

[130] H. Yuan, W. Guo, and S. Wang, "Emergency route selection for D2D cellular communications during an urban terrorist attack," in *IEEE International Conference on Communications Workshops (ICC)*, Sydney, June 2014, pp. 237 – 242.

[131] H. Yuan, W. Guo, Y. Jin, S. Wang, and M. Ni, "Interference-aware multi-hop path selection for device-to-device communications in a cellular interference environment," *IET Communications*, pp. 1–13, 2016.

[132] S. Boyd, *Convex Optimization*. Cambridge Uni. Press, 2004.

[133] H. Yuan, W. Guo, and S. Wang, "D2d multi-hop routing: collision probability and routing strategy with limited location information," in *IEEE*

International Conference on Communication Workshop (ICC). London: IEEE, 2015, pp. 670–674.

[134] ——, "Device-to-device communications in lte-unlicensed heterogeneous network," in *IEEE International Workshop on Signal Processing Advances in Wireless Communications (SPAWC)*. Edinburgh: IEEE, 2016, pp. 1–5.

[135] Y. Wu, W. Guo, H. Yuan, L. Li, S. Wang, X. Chu, and J. Zhang, "Device-to-device meets lte-unlicensed," *IEEE Communications Magazine*, vol. 54, no. 5, pp. 154–159, 2016.

[136] O. Gurewitz, M. Sidi, and I. Cidon, "The ballot theorem strikes again: Packet loss process distribution," *IEEE Transactions on Information Theory*, vol. 46, no. 7, pp. 2588–2595, 2000.

[137] S. K. Bose, *An introduction to queueing systems*. Springer Science & Business Media, 2013.

[138] Y. Koh and K. Kim, "Loss probability behavior of pareto/m/1/k queue," *IEEE communications letters*, vol. 7, no. 1, pp. 39–41, 2003.